New findings of ancient Greek silver sources

Markos Vaxevanopoulos, Janne Blichert-Toft, Gillan Davis, Francis Albarède

New findings of ancient Greek silver sources

Markos Vaxevanopoulos[1*], Janne Blichert-Toft[1], Gillan Davis[2], Francis Albarède[1]

[1] *Ecole Normale Supérieure de Lyon, CNRS, and Université de Lyon, France*

[2] *Australian Catholic University, Sydney, Australia*

**Corresponding author:* Markos Vaxevanopoulos (Markos.vaxevanopoulos@ens-lyon.fr)

Abstract

Over the last 60 years, much analytical research has sought to determine the ore sources of ancient Greek silver artefacts. Lead isotopic analysis has played a key role in this endeavor. While most studies so far have limited their search to places mentioned in historical sources, the present study takes a different approach by first identifying Ag-bearing ore sources in the Aegean world based on their geological characteristics and then using Pb isotopes to determine whether they were exploited in antiquity. To this end, we have geolocated, sampled, and measured high-precision Pb isotopic compositions of 17 Ag-bearing mineralizations in Greece for which we have evidence of ancient mining activity, and a further 10 exhibiting minor Ag occurrences that may also have been exploited in ancient times. We found that Pb model ages provide better discrimination of ore sources than the more conventional plots of raw Pb isotope data.

Our study establishes Lavrion, northeast Chalkidiki, Pangaeon, Thasos, Siphnos, Palaea Kavala, Angistron, and south Euboea as the most important ancient silver mining districts in Greece. Two previously undiscovered ancient mining areas in Pelion and in the Kroussia mountain range are also documented. The latter may be identified with ancient Mount Dysoron, from which King Alexander I of Macedon reportedly extracted the fabulous sum of a talent of silver per day. For the first time, we isotopically differentiate some of the mining districts in Thraco-Macedonia, and show that the mines of Thasos include geologically different silver-bearing ore sources. We further identify the hitherto unrealized importance of Euboean silver mines and demonstrate that they isotopically overlap those of Siphnos, with major implications for our understanding of ancient Greek history.

1. Introduction

Understanding metal production and circulation in antiquity is directly related to our knowledge of ore sources, but, for the most part, these are uncertain. The main reasons for these uncertainties directly related to the primary tool used to track ore sources, namely Pb isotopes. First and foremost, similar Pb isotopic compositions can be found in more than one locality, especially if provenance is determined exclusively with the help of two-dimensional Pb isotope plots. Coincidence in full-fledged three-dimensional space is required to robustly establish a source (Albarède *et al.*, 2020). Other reasons are the analytical quality of the Pb isotope data, the mineralogy of the ore in question (e.g. galena, chalcopyrite), and the nature

of the object (e.g. artefact, slag) used to represent a given locality. Lead isotopic analysis (LIA) has long been widely used for Pb-Cu-Ag-bearing ore deposits to assign provenances to copper/lead/silver artefacts as it has proved to be the most reliable analytical technique for providing coherent provenance signatures, especially in coin provenance studies (Gentner *et al.*, 1978; Gale, 1979; Chamberlain and Gale, 1980; Gale *et al.*, 1980; Wagner *et al.*, 1980; Wagner and Weisgerber, 1985; Artioli *et al.*, 2020; Killick *et al.*, 2020). During the 1960s, sampling and Pb isotopic measurement established Pb isotopic signatures for some major ancient mining districts including Lavrion (in Attica, Greece), Asia Minor, southern Iberia (Spain), and Roman Britain (Brill and Wampler, 1965; 1967; Grögler *et al.*, 1966). A major study of Greek ore deposits published by Gale *et al.* (1980) for Lavrion, the Cyclades, and northern Greece, as well as many silver coinages, using different Pb isotopic ratios has underpinned most subsequent historical understandings of silver extraction and usage in archaic Greek coin production.

The identification of ancient metal sources is based on the study of ancient mining territories and sampling of the related mineralizations combined with the study of the archeometallurgical remains and applied metallurgical processes. Provenance studies using LIA may encounter problems such as mixing during smelting, cupellation, or refining (though unlikely for small operations), as well as isotopic overlap between different ore deposits. Nevertheless, LIA is a powerful tool for *excluding* a given ore district as a raw silver-lead provider (Stos-Gale and Gale, 2009). To help avoid erroneous source assignments using LIA, complementary archeological evidence obtained from mining/metallurgical operations and artefacts should be taken into consideration as well. However, the exact periods of ancient exploitation may be difficult to establish as it is not always possible to find archeologically datable material in a mine. Additionally, long-lasting exploitation poses interpretative difficulties because subsequent mining activity has often superimposed and hence obliterated earlier mining phases - an acute problem especially for Lavrion and Siphnos.

In this study, we first geolocated the Ag occurrences in Greece and obtained samples from those areas where the archaeological and geological features indicate the existence or likelihood of ancient mining (Fig. 1). Our approach relies on understanding the geological processes that determine where silver ores could have formed, rather than reckoning with largely anecdotal information provided by ancient writers that has happened to survive. The geological context of Greece can be described as the subduction of the African (tectonic) plate under continental Europe over the last 200 million years. During this period, convergence, obduction, collision, and subduction of geotectonic units, nappe stacking, slab retreats, and tearing processes constituted the main compounds of the geotectonic processes in the Aegean (Pe-Piper and Piper, 2002; Schmid *et al.*, 2008; Jolivet and Brun, 2010; Jolivet *et al.*, 2013; Menant *et al.*, 2016; Schmid *et al.*, 2020). Numerous Ag-bearing mineralizations in Greece are associated with intrusion-related veins, skarns, carbonate replacements, and epithermal systems (Melfos and Voudouris, 2017; Voudouris *et al.*, 2019, Ross *et al.*, 2020). The different types of Ag occurrences located mainly in the Rhodope massif, the Serbo-Macedonian zone, the Circum-Rhodope Belt, and the Attic-Cycladic crystalline complex are listed in Table 1 and shown in Fig. 2. Further information on the geotectonic evolution of Greece and its relationship with mineralizations found in ancient mining areas, as well as detailed descriptions of the archaeological settings, are included in the supplementary material (Appendix I-II).

Following this first step which underpins our sample selection, we undertook a broad, high-precision, Pb isotopic survey of the ores found at ancient mining localities in Greece with the

expectation that improved state-of-the-art analytical quality would help associate Ag-bearing ores with metal use. The acquired high-precision Pb isotope data were used to calculate 'Pb model ages' using the parameters of Albarède and Juteau (1984) and the equations of Albarède *et al.* (2012). The advantage of Pb model ages is that they define ore provenance better than conventional two-dimensional plots of unprocessed (raw) Pb isotopic ratios by supplying additional information and clarity. Lead model ages establish the geological age of initial Pb segregation from the crustal source to form the ore precursor. The U/Pb (μ) and Th/U (κ) ratios, also deduced from the measured Pb isotopic abundances of the ores, constitute two additional sensitive parameters characteristic of their crustal source (Albarède *et al*., 2012; 2021). Lead model ages tend to be distributed in well-defined frequency peaks which represent a useful and strongly visual tool (Milot *et al.*, in press). By contrast, plots of conventional raw Pb isotopic ratios normalized to ^{204}Pb show strong correlations which obscure the true data relationships. This correlation is due to the much larger statistical noise on the small ^{204}Pb peak with respect to the peaks of the other more abundant Pb isotopes. Correlation coefficients were calculated by Albarède *et al*. (2004) and are approximately 0.94 in ^{207}Pb/^{204}Pb versus ^{206}Pb/^{204}Pb plots and 0.96 in ^{208}Pb/^{204}Pb versus ^{206}Pb/^{204}Pb plots, which are statistically highly significant. Slanted, narrow elliptic error surfaces in two-dimensional space (such as those commonly used for U-Pb dating) and ellipsoidal volumes in three-dimensional space therefore are more appropriate than the simple 'error boxes' often used in LIA. To give an example (e.g. Artioli *et al.*, 2020; Wind *et al.*, 2020), in a plot of ^{207}Pb/^{204}Pb versus ^{206}Pb/^{204}Pb, or, as would be the case in another plot also widely used in archaeometry, ^{208}Pb/^{206}Pb versus ^{207}Pb/^{206}Pb, different groups of points overlap to some extent. In addition to better error treatment as outlined above, improving the overall analytical quality of Pb isotopic data will be certain to enhance provenance resolution. Moreover, as will be shown in this paper, a one-dimensional T_{mod} histogram based on the new high-precision Pb isotope data from this study shows several well-defined peaks, which, when compared to the broader peaks based on older, often less precise literature data, confirms the necessity of focusing on data collected with modern quality standards, in particular those acquired by MC-ICP-MS for which analytical mass bias is well controlled.

2. Materials and Methods

We have identified 44 Ag-rich mineralizations in Greece (Table 1). Of these, we obtained samples from 17 for which we could find evidence of ancient mining activity (Fig. 1). We sampled another 10 districts with minor Ag occurrences where no proven ancient mining activity, but for which, based on the local geology, it seems a reasonable possibility that future archeological research may uncover such evidence. These areas present sparse and unidentified mining traces, such as from chisel and pick, that might date to antiquity, but pottery or organic material that could provide reliable dating are absent. In some cases, modern exploitation has obliterated probable ancient mining phases. The remaining 17 minor Ag ore deposits with no evidence or geological likelihood of ancient mining were not sampled and are not described in the present study. The field investigations were conducted from March to July 2019, and from June to July 2020.

Silver and Pb concentrations and Pb isotopic compositions of 149 samples from the above mentioned mineralizations were analyzed by, respectively, quadrupole inductively-coupled plasma mass spectrometry (Q-ICP-MS) and multiple-collector inductively-coupled plasma mass spectrometry (MC-ICP-MS) at the Ecole Normale Supérieure in Lyon (ENS Lyon).

Further information on sample preparation, analytical techniques, and accuracy and precision can be found in the supplementary material (Appendix III). The geological characteristics, latitude and longitude, Ag and Pb concentrations, Pb isotopic compositions, Pb model ages T_{mod}, and apparent $^{238}U/^{204}Pb$ (μ) and $^{232}Th/^{238}U$ (κ) values are listed in Table 2.

Lead model ages (T_{mod}) (Table 2) were calculated from the measured Pb isotopic compositions according to Albarède and Juteau (1984) and would differ by 30 Ma at most from those calculated from the parameters of Stacey and Kramer (1975) but have the advantage of eliminating most negative values. The values of μ ($^{238}U/^{204}Pb$) and κ ($^{232}Th/^{238}U$) also were computed (Table 2) from the measured Pb isotopic compositions. Table 3 lists Pb isotopic data from previous studies of Greek Pb-Zn mineralizations, which have been used in this paper though they are, in general, less precise that the Pb isotopic data acquired in the present study. Data on slags, litharge, and copper mineralizations were not included.

3. Results and discussion

3.1 On-site investigation and Ag grades of ancient Aegean mining districts

Field observations of ancient mining territories allow (i) the documentation of the extent of mining activity, (ii) to distinguish between different exploitation phases, (iii) to record the extent of the metallurgical processes, and (iv) to evaluate the relative importance of each mining area (Table 4). In the following, the investigated mining districts are described according to their geological context and their archeological importance. Silver yields are also summarized in Table 2.

3.1.1 Attic-Cycladic Core Complex (central Greece and southern Aegean)

Lavrion. Mining galleries span kilometers of underground workings with >2km in the Esperanza mine in east Kamareza (Fig. 3a). The exploitation is extensive at the numerous mantos (horizontal) Ag occurrences mainly in the Kamaresa, Souresa, Botsari, and Ari areas. The Plaka area presents numerous modern exploitation adits, but only scarce remains of ancient mines are found at the surface. The ancient mining areas closest to the Plaka granodiorite are at Ari and Dimoliaki with numerous adits and shafts that explore the contact between the Lavrion schists and Pounta marble (Fig. 3b). The Sounion area has shafts and ancient mines at the south edge of the Lavreotiki. The consistently high Ag yields reveal the importance of Lavrion with Ag concentrations varying from 1673 ppm in Kamareza to 5872 ppm in the modern mines of Plaka. A galena sample (L-17) found at the metallurgical area of Poundazeza (southeast coast of Lavrion) has a Ag concentration of 4220 ppm, which is representative of the ores being processed at the metallurgical areas.

Mount Hymettus. Situated to the east of Athens, the mountain hosts argentiferous galena veins (Stouraiti *et al.*, 2019) exploited by three modern adits and a shaft in Agios Ioannis Kynigos and two adits in the Kamini area. No ancient mining has been recorded in the underground exploitations. Concentrations of Ag are low (0 to 6.3 ppm), whereas Stouraiti *et al.* (2019) mentions Ag concentrations from 6 to >1500 ppm.

South Euboea. There are three Ag-bearing ore districts: the Kallianou valley, the Schinodavli site escarpment in the Agios Dimitrios gorge, and the Gialpides gorge. Mining activity and prospecting are recorded at the Kallianou valley with 11 modern adits and two ancient workings. The Ag concentration in a galena sample from the ancient Moskies mine in Kallianoi is 730 ppm. The most significant mine of the Gialpides gorge is located near the

shore with almost 500 m of underground galleries (Fig. 3c). Pottery from the Classical period is found in the inner part of the mine. An extensive, but poorly investigated, metallurgical area at the Archampolis settlement in south Euboea (Keller, 1984) suggests that south Euboea should be considered an important ancient mining area which has been largely, if not totally, ignored in discussions of ancient Greek silver sources.

Central Euboea. There is one minor Ag occurrence in the Almyropotamos mining district comprising three modern shafts and two horizontal galleries with scarce traces of ancient mining. Supergene alteration of the mineralization is major at its higher levels. The supergene mineralization contains 75-91 ppm Ag.

Siphnos. The central part of the island has five mining subdistricts with ancient galleries at Agios Sostis, Agios Sylvestros, Voreini, Kapsalos-Frase, and Xero-Xylo (Fig. 3d, e) exploiting the Ag-rich mineralization pods from the carbonate replacement bodies in marbles. Other mines in the southern part of the island contain very low-grade Ag ore. Wagner and Weisgerber (1985) documented prehistoric (3rd mil. BC), Archaic-Classical (5-4th cent. BC), and modern mining (19-20th cent. AD) in Siphnos. Roman and Byzantine pottery was found at the surface of the mining areas of Kapsalos-Frase and Xero-Xylo. Iron-manganese exploitation during the 19th and 20th centuries has obliterated most ancient traces at Agios Sylvestros, Kapsalos, Frase, and Xero-Xylo, while Voreini has been converted to a landfill. The mineralization from the ancient district of Agios Sylvestros contains high concentrations of Ag up to 4983 ppm.

Seriphos. Nine modern adits with parts testifying to ancient exploitation exist in the Moutoula area in the northern part of the island (Fig. 3f). The mines explore the Ag-rich vein system in the schist-marble intercalations. The mineralization contains 161-470 ppm Ag.

Melos. Two ancient open works were discovered on the island in Triades and one ancient adit at Katsimouti beach. In Triades, Ag concentrations in the galena reach 2473 ppm.

Syros. Silver-rich sulphides are found as disseminations and massive sulfide bodies along the marbles and schists with the most representative ore district being Rozos, an ancient mine with prehistoric rock tools in its interior with high Pb-Zn-Cu-Ag contents. The Ag concentrations in galena vary from 1 to 26 ppm. Ores with higher grades (25 to >100 ppm) are documented in Azolimnos (Voudouris *et al.*, 2014).

Kythnos. In Agios Dimitrios, at the southern edge of the island, Pb mineralization takes place mainly as galena. Ancient galleries of limited length in low-grade (0.2-16.2 ppm) Ag-bearing veins were discovered near the shore of Agios Dimitrios and near the acropolis of Kastellas (Fig. 3g).

Antiparos. Quartz veins in the gneisses and schists at the central and western parts of the island host Ag-bearing mineralizations (2-386 ppm). In the inner parts of modern mines in the Monastiria area, undatable older mining phases have been recorded.

Polyaigos. Modern mining activity was recorded in Ba-rich veins, but ancient traces are absent. The veins contain Ag up to 116 ppm.

Anaphi. Modern mining is located at the central-south part of Anaphi. The Ag concentration is 81 ppm.

Pelion. Ancient mines with Ag-bearing mineralizations are documented here for the first time. Numerous mineralized veins occur at the Pelion tectonic window (Attic-Cycladic Massif) from Zagora to Ksourichti village. Two ancient mines were discovered in Tsagarada and Ksourichti villages, respectively (Fig. 3h). They exploited low-grade Ag veins (3-13 ppm).

3.1.2 Rhodope Massif-Serbo-Macedonian Zone-Circum Rhodope Belt (northern Greece and northern Aegean islands)

Northeast Chalkidiki. The Olympiada mining subdistrict of northeast Chalkidiki comprises several ancient mining shafts and horizontal mines which were used to exploit Ag-rich veins (14.2-2879.6 ppm) (Fig. 3i). At the Madem Lakkos, Mavres Petres, and Stratoni areas, modern mining activity may have obliterated older phases of exploitation.

Thasos. The Acropolis mine, next to the ancient fortification of Thasos, constitutes the island's most significant ancient exploitation of Ag-bearing veins (Fig. 3j) The mine has 1226 m of underground galleries. The mineralizations are rich in Pb, Zn, and Cu and contain Ag up to 945 ppm and Au up to 60.9 ppm. Modern exploitation of Fe-Mn-Zn-rich mineralizations has presumably destroyed ancient mining traces at areas such as Vouves and Mavrolakas.

Kroussia. This ancient mining district was discovered during the present study. At Koulachli in the northeast, a number of ancient mines were investigated which exploited Ag ore hosted in veins that crosscut the schist (Fig. 3k). The Ag-bearing mineralization at the Agios Markos area contains up to 1364 ppm Ag. Field observations such as the existence of several ancient mines together with the high Ag concentrations point to the importance of the Kroussia mining area. Its location plausibly allows it to be identified as ancient Dysoron, situated on the eastern borders of the kingdom of Macedon under Alexander I (Xydopoulos, 2016). It was mentioned by Herodotus (5.17) as providing the king with the huge sum of a talent of silver per day.

Angistron. Two extended mines in the Lechovo subdistrict were recorded. The exploitation followed the carbonate replacement voids and the veins in the marbles filled with oxidized mineralization. Pottery found in the inner parts of the ancient mines dates to the Hellenistic and Roman periods. The ore contains up to 182 ppm Ag.

Pangaeon. Asimotrypes is the most extended mining system on Mount Pangaeon and comprises eight ancient galleries (Fig. 3l). The concentration of Ag is higher than any other ancient Greek mining district (up to 9906 ppm).

Palaea Kavala. An extensive mining area with horizontal adits and vertical shafts (Fig. 3m) mentioned in the literature (Koukouli-Chrysanthaki, 1990; Vavelidis *et al.,* 1996) as the ancient "Scapti Yli". Roman pottery is abundant at the surface of most galleries. The analyzed samples from Palaea Kavala contain from 57 to 213 ppm Ag. The extent of the underground works suggests it was a very important mining area for gold and silver which has so far been underestimated.

Lesbos. Modern adits are found at the northern part of Lesbos in the Megala Therma area close to Argenos village. Ancient narrow galleries and shafts have been recorded in the inner part of the modern adits (Pernicka *et al.,* 2003), but during the present study only modern mining activity was documented. The Ag concentration is 154 ppm.

Rhodope mountain range. Thermes, Sappes, Neda, Aisymi, and Pefkos have low-grade concentrations of Ag except for the Kirki ore deposit. The epithermal deposits of Sappes, Neda, Aisymi, and Pefkos contain up to 66 ppm Ag The carbonate replacement system in Thermes is characterized by similarly low Ag concentrations (4-52 ppm). Although the Kirki area has Ag-rich mineralizations (97-1044 ppm), no signs of ancient mining activity have been found there or in the neighboring areas. Modern mining has taken place in Kirki, and modern prospection trenches and adits exist in Aisymi, Sappes, and Neda. One sample from the epithermal vein system in south Samothrace island contains 471 ppm Ag. Modern prospecting galleries are found in the island.

3.2 Lead isotope analysis

The Pb isotopic compositions of the 149 galena, cerussite, and anglesite samples from the 27 Ag-bearing mineralizations in Greece investigated here are listed in Table 2. Table 3 lists the relevant literature data (Barnes *et al.*, 1975; Gale and Stos-Gale, 1981a; Wagner and Weisgerber, 1985; Wagner *et al.*, 1986; Kalogeropoulos *et al.*, 1989; Nebel *et al.*, 1991; Frei, 1992; Stos-Gale *et al.*, 1996; Gale, 1998; Asderaki *et al.*, 2017; OXALID and IGME unpublished data). Comments on the existence of ancient mining activity for each Ag-bearing mineralization based on field investigations and literature also are provided.

We first focus on the results of the present work. Figure 4 shows the standard plots of $^{207}Pb/^{204}Pb$ (a) and $^{208}Pb/^{204}Pb$ (b) versus $^{206}Pb/^{204}Pb$, and $^{208}Pb/^{206}Pb$ versus $^{207}Pb/^{206}Pb$ (c). T_{mod} (Pb model age) is plotted versus μ ($^{238}U/^{204}Pb$) and κ ($^{232}Th/^{238}U$) in Fig. 4d and 4e, respectively. Figure 5 also displays the raw Pb isotope ratios but in map view: $^{206}Pb/^{204}Pb$ (a), $^{207}Pb/^{204}Pb$ (b), $^{208}Pb/^{204}Pb$ (c), $^{207}Pb/^{206}Pb$ (d), and $^{208}Pb/^{206}Pb$ (e). The data from the southern Aegean and northern Greece are better separated in Fig. 5a-c (^{204}Pb-normalized) than in Fig. 5d-e (^{206}Pb-normalized).

Figure 6 shows maps of T_{mod} (Pb model age) (a), μ ($^{238}U/^{204}Pb$) (b), and κ ($^{232}Th/^{238}U$) (c) for the new data of the present study. Except for a few Upper Devonian ages, the Pb model ages calculated for Aegean localities cluster in groups from the Jurassic to the present as observed on the map of Fig. 6a. Although overall regional consistency is observed, the Pb model ages of some ores from the same island, such as Thasos, Kythnos, and Euboea show a broad range of values. The Pb model ages define different domains in the Aegean. The oldest Pb model ages are recorded in Hymettus (367-345 Ma), Samothrace (360 Ma), and Myriophyto-Kroussia (343 Ma), representing the oldest Ag-bearing mineralization group (Fig. 6a, Table 2). The most recent Pb model ages (15-3 Ma) are recorded at Agios Dimitrios on the island of Kythnos. The μ values of the southern Aegean are higher than those of northern Greece (Fig. 6b). The highest κ values are more frequent in the eastern Cyclades and, in general, μ seems to have a strong potential to discriminate different mining districts (Fig. 6b, c). The crust systematically has high U/Pb and Th/U in the eastern relative to the western Cyclades and even more so relative to northern Greece. This difference clearly is due to subduction bringing together terranes with very different tectonic histories.

The isotopic field for Lavrion is compact (Fig. 4b, c) and easily distinguished from the fields of other ancient mining areas of Pangaeon, Thasos, Chalkidiki, Euboea, and Siphnos. Samples from the Lavrion mining subdistricts of Kamaresa, Soureza, Botsari, and Ari, and even the modern Plaka and Filoni-80 mines have similar isotopic signatures that fall within a well-defined field. Chalkidiki, Pangaeon, and Thasos overlap in most LIA plots not involving ^{204}Pb (Fig. 4c, 5e). The geographical proximity and relative similarities in the geological setting of

these mining districts (Rhodope Massif) lead to difficulties in distinguishing between ore clusters.

The partial overlapping of the Siphnos, Euboea, Pangaeon, Thasos, and Chalkidiki fields poses a problem for determination of provenance (Fig. 4c). The Palaea Kavala and Angistron mining districts, which here have been measured for their Pb isotopic compositions for the first time, overlap with Chalkidiki, Euboea, Thasos, Rhodope, and Pangaeon (Fig. 4). The Pb isotopic signature of the Acropolis mine in northeast Thasos is significantly different from that of the southwest Thasos Pb-Zn ores (Fig. 4). Analogous segmentation is observed for the fields of Kythnos and Euboea (Fig. 4). The present work also presents the Pb isotopic composition for the Kroussia mining area for the first time. Its isotopic field is close to those of Lavrion, Chalkidiki, and Thasos (Fig. 4). The ore sample D-10 was collected in the northwest part of Kroussia, deriving from a different mineralization where no mining traces have been found so far in the adjacent area. This difference is depicted in the diagrams as well as observed for the Hymettus and Samothrace samples (Fig. 4a-c). The Pb isotopic signatures of south Euboea mineralizations from Kallianoi, Gialpides, and Schinodavli are different from those of Almyropotamos situated in the center of the island (Fig. 4a-c), as a probable expression of the local tectonic complexity (Jolivet et al., 2013; Melfos and Voudouris, 2017).

3.3 Lead model ages and other geologically informative parameters

Although Fig. 5 shows regional differences in raw Pb isotope ratios (in particular for ^{204}Pb-normalized ratios), the differences are regionally more coherent in T_{mod}-μ-κ space, in which northern Greece and the eastern and western Cyclades form well-delineated provinces consistent with local tectonics. In most, if not all, cases, Pb model ages are significantly older than the corresponding emplacement ages (Tables 1 and 2) (see Milot *et al.*, in press). Lead model ages, therefore, cannot be used to date ore deposits or their country rocks. The significance of the multiple but well-defined peaks present in the model age histogram of Fig. 7 thus must be clarified. If the peaks corresponded to different mixtures of Pb from the country rocks, the outcome would be much broader peaks than those observed or even no peaks at all. We will therefore adopt the straightforward model proposed by Milot *et al.* (in press) which states that, regardless of ore type, ore genesis involves two independent steps: (1) formation of the original Pb stock followed by (2) transport of this stock to its current location. Lead model ages correspond to the last U/Pb fractionation event that formed the current Pb(-Zn-Ag) stock. Whether the current deposit is magmatic, hydrothermal, epigenetic, or other is irrelevant to radiogenic Pb ingrowth. The petrogenesis of Pb ores is in many aspects reminiscent of the petrogenesis of oil fields, which has been pointed out a number of times in the literature.

We calculated Gaussian Mixture Models using the *fitgmdist* function of Matlab™. This function implements the iterative technique called 'Expectation Maximization' which assumes that each cluster has an independent Gaussian distribution, each with its own mean and covariance matrix. We found that a Gaussian mixture of five components provides an adequate description of the present data set. Table 5 shows the results in the T_{mod}, μ, and κ space for the galena samples analyzed in this work with and without literature data included. Comparison with the groups identified by Milot *et al.* (in press) for the Iberian Peninsula shows that the very strong Cenozoic peak (35±9 Ma) is absent from Iberia, where late Devonian (395±40 Ma) prevails. The T_{mod}, μ, and κ space therefore offers a potential provenance tool allowing a distinction to be made between the Aegean and the Iberian provinces on the condition that three rather than two, not even pair by pair, isotopic variables

are used. The Early to Mid-Cretaceous Pb model age peak is present in both the Aegean realm (107±39 Ma) and the Iberian Pb-Zn ores (90±34 Ma, Milot et al., submitted). The Cretaceous peaks are strong in both provinces, whereas the Early to Mid-Jurassic peak (190±13 Ma) is subdued in both provinces.

It has long been known that Pb must be derived from the upper crust, such as the Cycladic basement and Cycladic Blueschist in the southern Aegean, and not from the mantle (Doe and Delevaux, 1972; Heyl *et al.*, 1974; Leach *et al.*, 2005; Wilkinson, 2013; Arribas and Tosdal, 1994; Wind *et al.*, 2020). Explaining the existence of well-defined peaks of Pb model ages under such conditions remains a challenge. Milot *et al.* (in press) suggested that Pb was originally concentrated in marine sediments during anoxic events, whether global or more local, with sulfur being derived from volcanic activity. Because hydrothermal sulfides are quickly oxidized as sulfate in seawater, the concentration step of massive deposits is unlikely to be possible under normal oxic conditions. As for the second step, hydrothermal activity associated with magmatism or convection of basinal fluids constitute the most probable mechanisms leading to the transportation of Pb(-Zn-Ag) to their current position in the crust.

The arguments presented by Milot et *al.* (in press) for the Iberian Peninsula to support the initial segregation of large amounts of Pb in sediments during anoxic events are also valid for the Cretaceous Pb model ages in the Aegean. The prominent peak of Cenozoic Pb model ages (35±9 Ma; Fig. 7) is consistent with the ubiquitous accumulation of carbon-rich sediments in the Paratethys during the Oligocene in a broadly east-west trending zone extending from the Panonian Basin to the Carpathian, all the way to Azerbaidjan to a rock formation locally known as the Maikopian group (Pawlewicz, 2007; Hudson *et al.*, 2008; Sachsenhofer *et al.*, 2018; Shnyukov and Yanko-Hombach, 2020). The abundant Cretaceous Pb model ages are reflected by some geological evidence from northwestern Greece (Tsikos *et al.*, 2004). In contrast, the Early to Mid-Jurassic peak (190±13 Ma; Fig. 7) expected from stratigraphic studies (e.g. Kafousia *et al.*, 2018) is subdued.

3.4 A remark on overlapping fields

Possible ambiguities created by fields overlapping in two-dimensional plots, such as $^{207}Pb/^{204}Pb$ versus $^{206}Pb/^{204}Pb$, and sometimes in two of such paired plots at the same time, should not be overemphasized. Cases for which groups of data plotted in the three-dimensional $^{206}Pb/^{204}Pb$-$^{207}Pb/^{204}Pb$-$^{208}Pb/^{204}Pb$ space overlap on their projections onto two 'faces' of the coordinate system, while defining separate volumes in three dimensions, are easy to conceive and visualize. The same situation is also conceivable in the three-dimensional T_{mod}-μ-κ space. Use of three-dimensional plots to represent Pb isotope data is unfortunately uncommon in archeometry (Albarède et al., 2020). In practice, such ambiguities rarely arise in three dimensions as three-dimensional fields, or volumes, rarely overlap. An efficient 'convex hull' technique to assess provenance issues in three-dimensional Pb isotope space is described by Gentelli *et al*. (submitted).

4. Conclusions

Field observations made during this study have led to the conclusion that the most significant ancient Ag mining territories in the Aegean were Lavrion, northeast Chalkidiki, Pangaeon mountain, the islands of Siphnos, Thasos and Euboea, Palaea Kavala, Kroussia, and the Angistron district. This significantly broadens the mining areas from which ancient peoples

extracted silver beyond those specifically attested to in ancient sources and deduced from numismatic considerations. High Ag concentrations in samples from Lavrion (5872 ppm), Chalkidiki (2880 ppm), Pangaeon (9906 ppm) and Siphnos (4983 ppm) are indicative of the importance of these deposits, while the galena sample found at the Poundazeza metallurgical area in Lavrion with 4220 ppm Ag provides information about what was considered to be profitable yields, though mines with lower yields were also exploited possibly as extraction techniques improved in Hellenistic and Roman times.

We have provided new high-precision Pb isotopic data from samples obtained from the known ancient mining territories in Greece with the intention of providing a useful tool for silver artefact provenance studies. A clear distinction in Pb isotopic composition is observed between the major silver mining territories in the Aegean, such as Lavrion and Siphnos-Pangaeon-Thasos-Chalkidiki. Samples originating from proximate and geologically relevant areas, such as Pangaeon, Thasos, and Chalkidiki, overlap to some extent in lead isotopic plots. We further demonstrate that combining plots of raw Pb isotope ratios with calculated Pb model ages provides more reliable provenance assessment**.**

An important finding is that the measured Pb isotopic variations and calculated Pb model ages from some closely neighboring mining areas, especially on islands such as Thasos, Kythnos, and Euboea, may sometimes reveal different Pb sources. Thus, northeast Thasos differs from southwest Thasos, north-central Kythnos differs from southwest Kythnos, and south Euboea differs from Almyropotamos (central Euboea).

In contrast to the older, generally more noisy literature data, the Pb model age histogram of the new high-precision Pb isotope data of this study shows well-defined peaks which further enhance the resolution of provenance assignment. This observation is consistent with that of Milot *et al*. (in press) for Iberian ores. Lead model ages do not date the formation of the present ore deposits as the two sets of ages are distinctly different, with Pb model ages being systematically older than ore emplacement ages. Regardless of ore type, the isotopic data can be accounted for by a two-stage evolution model, much reminiscent of that of oil-field formation. The first stage accounts for Pb accumulation in sediments during global or local anoxic events, while the second stage corresponds to the remobilization of the original Pb stocks by basinal and metamorphic fluids.

Another important finding is that, until now, ores from Euboea have been neglected in provenance studies but may have contributed more substantially to coinage production than currently realized, especially in the late Archaic period for the island of Aegina, considered to be the earliest Greek minter outside of Asia Minor (Stos-Gale and Davis, 2020).

Likewise, evidence of extensive ancient exploitation from Palea Kavala and exceptionally high Ag yields from Pangaeon (Asimotrypes) in northern Greece suggest that these districts have been underestimated as mining sources, while low yields from the Rhodope mountain range suggest it has been overestimated.

Finally, field investigations combined with Pb isotopic data have revealed two so-far undiscovered ancient mining areas in the Mounts Pelion and Kroussia. The geographic location of the mining district in Kroussia and the characteristics of the Ag-bearing mineralization allow it to be plausibly identified with Mount Dysoron described as a silver-rich area during Alexander's I reign *(*Hdt. 5.17).

Acknowledgements

This work was funded by the European Research Council H2020 Advanced Grant 741454-SILVER-ERC-2016-ADG 'Silver isotopes and the rise of Money' awarded to Francis Albarède. The Archaeological Ephorates of the East Attica Cyclades, Euboea, Magnesia, Chalkidiki, Kilkis, Serres, Kavala, and Thasos (Greek Ministry of Culture) kindly gave permission to conduct the fieldwork and ore sampling carried out during this study. Pavlos Tsitsanis, exploration manager of Eldorado Gold Corporation, is gratefully acknowledged for providing galena samples. We thank Philippe Télouk, Jean Milot, and Chloé Malod-Dognin for help with the mass spectrometers and Vasilis Melfos, Panagiotis Voudouris, and James Ross for facilitating sampling by sharing their knowledge and experience. Fieldwork assistance by Zacharoula Papadopoulou, Anna Aslanoglou, Kyriaki Fellachidou, and numerous local people in the ancient mining areas of Greece is also gratefully acknowledged.

References

Albarède, F., Juteau, M., 1984. Unscrambling the lead model ages. Geochim. Cosmochim. Acta 48,207–212. https://doi.org/10.1016/0016-7037(84)90364-8

Albarède, F., Telouk, P., Blichert-Toft, J., Boyet, M., Agranier, A., Nelson, B., 2004. Precise and accurate isotopic measurements using multiple-collector ICPMS, Geochim. Cosmochim. Acta 68, 2725-2744.

Albarede, F., Desaulty, A.M., Blichert-Toft, J., 2012. A geological perspective on the use of Pb isotopes in Archaeometry, Archaeometry 54, 853-867.

Albarède, F., Blichert-Toft, J., Gentelli, L., Milot, J., Vaxevanopoulos, M., Klein, S., Westner, K., Birch, T., Davis, G., de Callataÿ, F., 2020. A miner's perspective on Pb isotope provenances in the Western and Central Mediterranean, Journal of Archaeological Science 121, 105194.

Albarède, F., Blichert-Toft, J., de Callataÿ, F., Davis, G., Debernardi, P., Gentelli, L., Kemmers, F., Klein, S., Malod-Dognin, C., Milot, J., Telouk, P., Vaxevanopoulos, M., Westner, K. 2021. From commodity to money: The rise of silver coinage around the Ancient Mediterranean (sixth–first centuries bce). Archaeometry, 63(1), 142-155. https://doi.org/10.1111/arcm.12615

Alfieris, D., Voudouris, P., Spry, P. G. 2013. Shallow submarine epithermal Pb–Zn–Cu–Au–Ag–Te mineralization on western Milos Island, Aegean Volcanic Arc, Greece: Mineralogical, geological and geochemical constraints. Ore Geology Reviews, 53, 159-180.

Arribas, A., Tosdal, R.M. 1994. Isotopic composition of Pb in ore-deposits of the Betic Cordillera, Spain - Origin and relationship to other European deposits. Economic Geology 89, 1074-1093.

Artioli, G., Canovaro, C., Nimis, P., Angelini, I. 2020. LIA of prehistoric metals in the central mediterranean area: A review. Archaeometry, 62, 53-85.

Asderaki-Tzoumerkioti, E., Rehren, T., Skafida, E., Vaxevanopoulos, M., Connolly, P.J., 2017. Kastro Palaia settlement, Volos, Greece: a diachronical technological approach to

bronze metalwork. STAR: Science & Technology of Archaeological Research, 3(2), pp.179-193.

Barnes, I. L., Shields, W. R., Murphy, T. J., Brill, R. H. 1975. Isotopic analysis of Laurion lead ores.

Bassiakos, Y., Philaniotou, O. 2007. Early copper production on Kythnos: archaeological evidence and analytical approaches to the reconstruction of metallurgical process. Metallurgy in the early bronze age Aegean, 7, 19.

Brill, R.H., Wampler, J.M. 1965. September. Isotope ratios in archaeological objects of lead. In Application of science in examination of works of art. Proceedings of the seminar: September 7-16, 1965 (pp. 155-166).

Brill, R.H., Wampler, J.M. 1967. Isotope studies of ancient lead. American Journal of Archaeology, 71(1), pp.63-77.

Bonsall, T.A., Spry, P.G., Voudouris, P.C., Tombros, S., Seymour, K.S., Melfos, V. 2011. The geochemistry of carbonate-replacement Pb-Zn-Ag mineralization in the Lavrion district, Attica, Greece: Fluid inclusion, stable isotope, and rare earth element studies. Economic Geology, 106(4), pp.619-651.

Chamberlain, V, Gale N. H. 1980. The isotopic composition of lead in Greek coins and in galena from Greece and Turkey. In: Slater EA, Tate JO (eds) Proceedings of the 16th International Symposium on Archaeometry and Archaeological Prosepection, Edinburgh 1976. The National Museum of Antiquities of Scotland, pp 139-155.

Chiotis, E., Koukouzas, C., Papadimitriou, G. 1996. Old mining and metallurgical activities in Angistron-Serres-Macedonia. In Proceedings of the 2nd Symposium of the Hellenic Archaeometric Society (pp. 77-89). Hellenic Archaeometric Society Thessaloniki.

Conophagos, C.E. 1980. Le Laurium antique: et la technique Grecque de la production de l'argent (Athens).

Doe, B.R., Delevaux, M.I.-I. 1972. Source of Lead in Southeast Missouri Galena Ores'. Econ. Geol. 67, 409-425.

Ducoux, M., Branquet, Y., Jolivet, L., Arbaret, L., Grasemann, B., Rabillard, A., Gumiaux, C., Drufin, S. 2017. Synkinematic skarns and fluid drainage along detachments: The West Cycladic Detachment System on Serifos Island (Cyclades, Greece) and its related mineralization. Tectonophysics, 695, pp.1-26.

Fornadel, A. P., Spry, P. G., Melfos, V., Vavelidis, M., Voudouris, P. C. 2011. Is the Palea Kavala Bi–Te–Pb–Sb±Au district, northeastern Greece, an intrusion-related system?. Ore Geology Reviews, 39(3), 119-133.

Frei, R. 1992. Isotope (Pb, Rb-Sr, S, O, C, U-Pb) geochemical investigations on Tertiary intrusives and related mineralizations in the Serbomacedonian Pb-Zn, Sb+ Cu-Mo metallogenetic province in Northern Greece. Unpublished Doctoral dissertation, ETH Zurich.

Fytikas, M., Vougioukalakis, G. 1992. Volcanic Structure and evolution of Kimolos and Polyaigos Isl.,(Milos Island Complex). In 6th Congress of the Greek Geologic Society (pp. 221-237).

Gale, N. H. 1979. Lead isotopes and Archaic Greek silver coins. Archaeophysica 10. Rheinisches Landesmuseum Bonn, pp 194-208.

Gale, N. H. 1998. The role of Kea in metal production and trade in the Late Bronze Age. Kea-Kythnos: History and Archaeology, 737-58.

Gale, N. H, Stos-Gale, Z. A. 1981a. Lead and silver in the ancient Aegean. Scientific American 244(6):176–192.

Gale, N. H, Stos-Gale, Z. A. 1981b. Cycladic lead and silver metallurgy. Annual of the British School at Athens 76:169–224.

Gale, N. H., Gentner, W., Wagner, G. A. 1980. Mineralogical and geographical silver sources of archaic Greek coinage. Metallurgy in numismatics, 1, 3-49.

Gialoglou, G., Drymniotis, D. 1983. Northeastern Greece: mining activities, mineral exploration and future developments. Trans. Inst. Min. Metall., Sect. A 92, A180–183.

Gentelli, L. Blichert-Toft, J., Davis, G., Gitler, H., and Albarède, F. (submitted) Metal provenance of Iron Age *Hacksilber* hoards in the southern Levant. Journal of Archaelogical Sciences.

Gentner, W., Müller, O., Wagner, G. A., Gale, N. H., 1978. Silver sources of archaic Greek coinage. Naturwissenschaften, 65(6), 273-284.

Grögler N, Geiss J, Grünenfelder, M, Houtermans, FG. 1966. Isotopenuntersuchungen zur Bestimmung der Herkunft römischer Bleirohre und Bleibarren. ZeitschriftfürNaturforschung 21a:1167–72.

Grossou-Valta, M., Adam, K., Constantinides, D.C., Prevosteau, J.M., Dimou, E. 1990. Mineralogy of and potential beneficiation process for the Molai complex sulphide orebody, Greece. In Sulphide deposits—their origin and processing (pp. 119-133). Springer, Dordrecht.

Heyl, A.V., Landis, G.P., Zartman, R.E. 1974. Isotopic evidence for the origin of Mississippi valley-type mineral deposits: a review. Economic Geology 69, 992-1006.

Hudson, S.M., Johnson, C.L., Efendiyeva, M.A., Rowe, H.D., Feyzullayev, A.A., Aliyev, C.S. 2008. Stratigraphy and geochemical characterization of the Oligocene–Miocene Maikop series: implications for the paleogeography of Eastern Azerbaijan. Tectonophysics 451, 40-55.

Institute of Geological and Mineral Exploration (IGME) 1965 Metallogenetic Map of Greece. Athens.

Jolivet, L., Brun, J. P., 2010. Cenozoic geodynamic evolution of the Aegean. International Journal of Earth Sciences, 99(1), 109-138.

Jolivet, L., Faccenna, C., Huet, B., Labrousse, L., Le Pourhiet, L., Lacombe, O., Lecomte, E., Burov, E., Denèle, Y., Brun, J.-P., Philippon, M., Paul, A., Salaün, G., Karabulut, H.,

Piromallo, C., Monié, P., Gueydan, F., Okay, A.I., Oberhänsli, R., Pourteau, A., Augier, R., Gadenne, L., Driussi, O., 2013. Aegean tectonics: strain localization, slab tearing and trench retreat. Tectonophysics 597, 1–33.

Kafousia, N., Karakitsios, V., Jenkyns, H., Mattioli, E. 2011. A global event with a regional character: the Early Toarcian Oceanic Anoxic Event in the Pindos Ocean (northern Peloponnese, Greece). Geological Magazine 148, 619-631.

Kalogeropoulos, S.I., Kilias, S.P., Bitzios, D.C., Nicolaou, M., Both, R.A. 1989. Genesis of the Olympias carbonate-hosted Pb-Zn (Au, Ag) sulfide ore deposit, easternChalkidiki Peninsula, northern Greece. Econ. Geol. 84, 1210–1234.

Kanellopoulos, C., Voudouris, P., Moritz, R. 2014. Detachment-related Sb-Pb-Zn-Ag-Au-Te mineralization in Kallintiri area, northeastern Greece: mineralogical and geochemical constraints. In Proc. 20th CBGA Congress, Tirana (pp. 162-165).

Keller, D. R. 1984. Archampolis, an early iron-age settlement and sanctuary in Southern Euboea. In American Journal of Archaeology (vol. 88, no. 2, pp. 249-249). 135 William St, New York, NY 10038-3805: Archaeological inst.

Killick, D., Stephens, J., Fenn, T., 2020. Geological constraints on the use of lead isotopes for provenance in archaeometallurgy, Archaeometry 62, 86-105.

Kontis, E., Kelepertsis, A. E., Skounakis, S. 1994. Geochemistry and alteration facies associated with epithermal precious metal mineralization in an active geothermal system, northern Lesbos, Greece. Mineralium Deposita, 29(5), 430-433.

Koukouli-Chrysanthaki, C. 1990. The mines of the Thasians' coast, Mélanges D. Lazaridis: cité et territoireenMacédoine et Thrace antiques, Recherches Franco-Helléniques, 1, Greek Ministry of Culture, École francaise d' Athénes, Athens (in Greek).

Leach, D.L., Sangster, D.F., Kelley, K.D., Large, R.R., Garven, G., Allen, C.R., Gutzmer, J., Walters, S. 2005. Sediment-hosted lead-zinc deposits: A global perspective, in: Hedenquist, J.W., Thompson, J.F.H., Goldfarb, R.J., Richards, J.P. (Eds.), Economic Geology 100th Annversary Volume. Society of Economic Geologists, Littleton, pp. 561-607.

Maratos, G. 1956. Brief report on the Taygetos mineralogical research. IGEY. Unpublished internal report. Athens. (in Greek).

Marinos, G., Petrascheck, W.E. 1956. Lavrion: geological and geophysical research. Institute for Geology and Subsurface Research 4, 1–246.

Melfos, V., Voudouris, P. 2016. Fluid evolution in Tertiary magmatic-hydrothermal ore systems at the Rhodope metallogenic province, NE Greece. A review. Geologia Croatica, 69(1), 157-167.

Melfos, V., Voudouris, P. 2017. Cenozoic metallogeny of Greece and potential for precious, critical and rare metals exploration. Ore Geology Reviews, 89, 1030-1057.

Melidonis, N., Constantinides, D. 1983. The stratabound sulphide Mineralisation of Syros (Cyclades, Greece). Z. dt. geol. Ges. 134, 555-575.

Menant, A., Jolivet, L., Vrielynck, B. 2016. Kinematic reconstructions and magmatic evolution illuminating crustal and mantle dynamics of the eastern Mediterranean region since the late Cretaceous. Tectonophysics, 675, 103-140.

Milot, J., Blichert-Toft, J., Ayarzagüena Sanz, M., Fetter, N., Télouk, P., Albarède, F. (in press). The significance of galena Pb model ages and the formation of large Pb-Zn sedimentary deposits. Chemical Geology.

Nebel, M.L., Hutchinson, R.W., Zartman, R.E. 1991. Metamorphism and polygenesis of the Madem Lakkos polymetallic sulfide deposit, Chalkidiki, Greece. Economic Geology, 86(1), pp.81-105.

Nesbitt, R. W., Billett, M. F., Ashworth, K. L., Deniel, C., Constantinides, D., Demetriades, A., Katirtzoglou, C., Michael, C., Mposkos, E., Zachos, S., Sanderson, D. 1988. The geological setting of base metal mineralisation in the Rhodope Region, northern Greece. In Mineral deposits within the European Community (pp. 499-514). Springer, Berlin, Heidelberg.

Pawlewicz, M. 2007. Total petroleum systems of the Carpathian-Balkanian basin province of Romania and Bulgaria. US Geological Survey.

Pe-Piper, G., Piper, D.J.W, 2002. The igneous rocks of Greece. The anatomyof an orogen, Beiträge der regionalen Geologie der Erde 30. Berlin-Stuttgart. 573 p.

Perlikos, P. 1989. Some new aspects on the geology and metallogeny of southern Euboea. Bull Geol Soc Greece 23:327–344 (in Greek).

Pernicka, E., Eibner, C., Öztunalı, O., Wagner, G. A. 2003. Early Bronze Age metallurgy in the north-east Aegean. In Troia and the Troad (pp. 143-172). Springer, Berlin, Heidelberg.

Ross, J. R., Voudouris, P., Melfos, V., Vaxevanopoulos, M. 2020. Mines, Metals and Money in Attica and the Ancient World: The Geological Context. In: Sheedy, K. A., Davis, G. 2020. Metallurgy in Numismatics 6: Mines, Metals and Money: Ancient World Studies in Science, Archaeology and History.

Sachsenhofer, R., Popov, S., Coric, S., Mayer, J., Misch, D., Morton, M., Pupp, M., Rauball, J., Tari, G. 2018 Paratethyan petroleum source rocks: an overview. Journal of Petroleum Geology 41, 219-245.

Salemink, J. 1985. Skarn and ore formation at Seriphos, Greece as a consequence ofgranodiorite intrusion. GeologicaUntrajectina 40, 231 p.

Schmid, S. M., Fügenschuh, B., Kounov, A., Maţenco, L., Nievergelt, P., Oberhänsli, R., Pleuger, J., Schefer, S., Schuster, R. Tomljenovic, B., Ustaszewski, K., van Hinsbergen, D. J. 2020. Tectonic units of the Alpine collision zone between Eastern Alps and western Turkey. Gondwana Research, 78, 308-374.

Schmid, S.M., Bernoulli, D., Fügenschuh, B., Matenco, L., Schefer, S., Schuster, R., Tischler, M., Ustaszewski, K. 2008. The Alpine-Carpathian-Dinaridic orogenic system: correlation and evolution of tectonic units. Swiss J. Geosci. 101, 139–183.

Shnyukov, E., Yanko-Hombach, V. 2020. Mud Volcanoes of the Black Sea Region and Their Environmental Significance. Springer Nature.

Siron, C.R. 2018. Magmatic, structural, and metallogenic framework of the Kassandra mining district, Chalkidiki peninsula, Northern Greece. Unpublished PhD Thesis.

Skarpelis, N. S. 1999. Epithermal type ores in the Aegean. The hot spring mineralization of northern Chios island, Greece. BGSG, 33, 61-68.

Skarpelis, N. 2020. Setting, sulfur isotope variations, and metamorphism of Jurassic massive Zn- Pb- Ag sulfide mineralization associated with arc- type volcanism (Skra, Vardar zone, Northern Greece). Resource Geology, 70(4), 311-335.

Stacey, J. S. & Kramer, J. D. 1975. Approximation of terrestrial lead isotope evolution by a two-stage model. Earth Planet. Sci. Lett. 26, 207-221.

Stergiou, C., Melfos, V., Voudouris, P., Michailidis, K., Spry, P., Chatzipetros A. 2016. Hydrothermal alteration and structural control of the Vathi porphyry Cu-Au-Mo-U ore system, Kilkis district, N. Greece. Scientific Annals of the School of Geology, Aristotle University of Thessaloniki (Honorary Publication in Memory of Professor A. Kasoli-Fournaraki) 105, 69–74.

Stos-Gale, Z.A. 1998. The role of Kythnos and other Cycladic islands in the origins of Early Minoan metallurgy. Meletimata, 27, pp.717-736.

Stos-Gale, Z. A., Davis, G. 2020. The minting/mining nexus: new understandings of Archaic Greek silver coinage from lead isotope analysis. In Sheedy, K.A., Davis, G. (eds) Metallurgy in Numismatics 6: Mines, Metals and Money: Ancient World Studies in Science, Archaeology and History, Royal Numismatic Society Special Publications vol. 56, London, 87-100.

Stos-Gale, Z. A., Gale, N. H. 2009. Metal provenancing using isotopes and the Oxford archaeological lead isotope database (OXALID). Archaeological and Anthropological Sciences, 1(3), 195-213.

Stos- Gale, Z. A., Gale, N. H., Annetts, N. 1996. Lead isotope data from the Isotrace Laboratory, Oxford: archaeometry data base 3, ores from the Aegean, part 1. Archaeometry, 38(2), 381-390.

Stouraiti, C., Soukis, K., Voudouris, P., Mavrogonatos, C., Lozios, S., Lekkas, S., Beard, A., Strauss, H., Palles, D., Baziotis, I. Soulamidis, G. 2019. Silver-rich sulfide mineralization in the northwestern termination of the Western Cycladic Detachment System, at Agios Ioannis Kynigos, Hymettus Mt. (Attica, Greece): A mineralogical, geochemical and stable isotope study. Ore Geology Reviews, 111, 102992.

Tataris, A. 1960. Ai flevikai ekrixigeneis emfaniseis kai imetallogenesieis to Anat. Pilion. [In Greek] I.G.E.Y. Athens, VI, 4, 207–303.

Tombros, S., St. Seymour, K., Spry, P.G., Williams-Jones, A. 2007. The genesis of epithermal Au-Ag-Te mineralization, Panormos Bay, Tinos Island, Cyclades, Greece. Econ. Geol. 102, 1269–1294.

Tsikos, H., Karakitsios, V., van Breugel, Y., Walsworth-Bell, B., Bombardiere, L., Petrizzo, M.R., Damsté, J.S.S., Schouten, S., Erba, E. Silva, I.P. 2004. Organic-carbon deposition in the Cretaceous of the Ionian Basin, NW Greece: the Paquier Event (OAE 1b) revisited. Geological Magazine 141, 401-416.

Vavelidis, M. 1988. Geochemistry of trace elements in galenas from Ag-containing lead-zinc ore deposits in Sifnos (Greece). Bull. Geol. Soc., 329-341.

Vavelidis, M., Amstutz, G.C. 1983. New genetic investigations on the Pb-Zn deposits of Thasos (Greece). In Mineral Deposits of the Alps and of the Alpine Epoch in Europe (pp. 359-365). Springer, Berlin, Heidelberg.

Vavelidis, M., Gialoglou, G., Melfos, V., Wagner, G.A. 1996. 'Goldgrube in Palaea Kavala Griechenland: Entdeckung von Skaptehyle', Erzmetall 49, 547–54.

Vaxevanopoulos, M. 2017. Recording and study of ancient mining activity on Mount Pangaeon, E. Macedonia, Greece. Unpublished Doctoral dissertation, Thessaloniki, Greece, Aristotle University of Thessaloniki. 337 (in Greek).

Vaxevanopoulos, M., Vavelidis, M., Melfos, V., Malamidou, D., Pavlides, S. 2018. Ancient Mining in Gold-Silver-Copper Deposits and Metallurgical Activity in Mavrokofi Area, Pangaeon Mount (NE Greece). In: Ben-Yosef, E. (ed.), Mining for Ancient Copper: Essays in Memory of Beno Rothenberg. Tel Aviv: The Institute of Archaeology of Tel Aviv University.

Veranis, N., Tsamantouridis, P., 1991. Using panning method to the exploration of auriferous mineralizations of Krousia metallogenic province. Institute of Geology and Mineral Exploration Internal Report (in Greek).

Voudouris, P. 2006. Comparative mineralogical study of Tertiary Te-rich epithermal and porphyry systems in northeastern Greece. Mineral. Petrol. 87, 241–275.

Voudouris, P., Alfieris, D. 2005. New porphyry—Cu±Mo occurrences in the north-eastern Aegean, Greece: Ore mineralogy and epithermal relationships. In Mineral deposit research: Meeting the global challenge (pp. 473-476). Springer, Berlin, Heidelberg.

Voudouris, P., Manoukian, E., Veligrakis, Th., Sakellaris, G.A., Koutsovitis, P., Falalakis, G., 2014. Carbonate-replacement and vein-type Pb-Zn-Ag-Au mineralization at Syros Island, Cyclades: Mineralogical and geochemical constraints. In: Proceedings 20th CBGA Congress, Tirana, Albania, Buletinii Shkencave Gjeologjike Special Issue 1, 183–186.

Voudouris, P., Mavrogonatos, C., Spry, P. G., Baker, T., Melfos, V., Klemd, R., Haase, K., Repstock, A., Djiba, A., Bismayer, U., Tarantola, A., Scheffer, C., Moritz, R., Kouzmanov, K., Alfieris, D., Papavassiliou, K., Schaarschmidt, A., Galanopoulos, E., Galanos, E., Kolodziejczyk, J., Stergiou, C., Melfou, M. 2019. Porphyry and epithermal deposits in Greece: An overview, new discoveries, and mineralogical constraints on their genesis. Ore Geology Reviews, 107, 654-691.

Voudouris, P., Melfos, V., Mavrogonatos, C., Photiades, A., Moraiti, E., Rieck, B., Kolitsch, U., Tarantola, A., Scheffer, C., Morin, D.,Vanderhaeghe, O., Spry, P., Ross, J., Soukis, K., Vaxevanopoulos, M., Pekov, I., Chykanov, N., Magganas, A., Kati, M.,

Katerinopoulos, A., Zaimis, S. 2021. The Lavrion Mines: A Unique Site of Geological and Mineralogical Heritage. Minerals, 11(1), p.76.

Voudouris, P., Melfos, V., Spry, P.G., Bonsall, T., Tarkian, M., Economou-Eliopoulos, M., 2008a. Mineralogical and fluid inclusion constraints on the evolution of the Plaka intrusion-related ore system, Lavrion, Greece. Mineralogy and Petrology, 93(1-2), pp.79-110.

Voudouris, P., Melfos, V., Spry, P.G., Bonsall, T.A., Tarkian, M. and Solomos, C., 2008b. Carbonate-replacement Pb–Zn–Ag±Aumineralization in the Kamariza area, Lavrion, Greece: Mineralogy and thermochemical conditions of formation. Mineralogy and Petrology, 94(1-2), p.85.

Voudouris, P., Spry, P.G., Sakellaris, G.A., Mavrogonatos, C. 2011. A cervelleite-like mineral and other Ag-Cu-Te-S minerals [Ag2CuTeS and (Ag, Cu)2TeS] in gold bearing veins in metamorphic rocks of the Cycladic Blueschist Unit, Kallianou, Evia Island, Greece. Mineral. Petrol. 101, 169–183.

Voudouris P, Skarpelis N. 1998. Epithermal gold-silver mineralization at Perama (Thrace) and Lemnos Island. Geol Soc Greece Bull 32:125–135.

Vryniotis, D. 1978. Έκθεση προκαταρκτικών εργασιών για την σκοπιμότητα πραγματοποίσης γεωχημικής έρευνας στην περιοχή Αλμυροποτάμου Ν. Εύβοιας. I.G.M.E. Athens. (In Greek).

Wagner, G. A, Gentner, W., Gropengiesser H., Gale, N. H. 1980. Early bronze age lead–silver mining and metallurgy in the Aegean. In: Craddock PT (ed) Scientific studies in early mining and extractive metallurgy. British Museum Occasional Paper 20:63-86.

Wagner, G. A, Weisgerber, G., 1985. Silber, Blei und Gold auf Sifnos, prähistorische und antike Metallproduktion, Der Anschnitt, Beiheft 3. Deutsches Bergbau-Museum, Bochum.

Wagner, G. A., Weisgerber, G., (eds). 1988. "Antike Edel- und Buntmetallgewinnung auf Thasos." Der Anschnitt: Beiheft 6 (Veröffentlichung aus dem Deutschen Bergbau-Museum Nr. 42). Bochum 1988.

Wagner, G.A., Pernicka, E., Vavelidis, M., Baranyi, I., Bassiakos, I. 1986. Archaeometallurgische Untersuchungen auf Chalkidiki. Anschnitt, 38, H5-6, 166-186.

Wilkinson, J. 2013. Sediment-Hosted Zinc-Lead Mineralization: Processes and Perspectives: Processes and Perspectives, Treatise on Geochemistry. Elsevier Ltd.

Wind, S. C., Schneider, D. A., Hannington, M. D., McFarlane, C. R. 2020. Regional similarities in lead isotopes and trace elements in galena of the Cyclades Mineral District, Greece with implications for the underlying basement. Lithos, 366, 105559.

Xydopoulos, I. 2016. The Eastern Macedonian border in Alexander I's reign. In: ΗΧΑΔΙΝ. *Τιμητικός τόμος για τη Στέλλα Δρούγου*. Athens. (In Greek).

FIGURE CAPTIONS

Figure 1. Geographic map depicting the Ag-bearing mineralizations of Greece (base map modified after SRTM worldwide elevation data 3-arc-second resolution).

Figure 2. Simplified geotectonic map of the Aegean region showing the main tectonic zones within the Hellenide orogen (modified after Schmid et al., 2008; 2020). Silver-bearing mineralizations are shown (Tables 1 and 3 and references therein). The North Cycladic Detachment System (NCDS) and the West Cycladic Detachment System (WCDS) are also depicted.

Figure 3. Selected representative photos from the mining areas where samples were obtained. (a) Esperanza-1 horizontal mine in Lavrion. (b) Dimoliaki mine supergene alteration close to the Plaka granodiorite intrusion. (c) Gialpides-1 mine in the Euboea mining district. (d) Ancient adits in the modern trench of Agios Silvestros mining area in Siphnos. (e) Agios Sostis-1 ancient mine in Siphnos. (f) Modern mine intersected by ancient gallery in Moutoula mining area in Seriphos. (g) Ancient mine entrance at the shore of Kastellas area in Kythnos island. (h) Ksourichti mine in Pelion mining area. (i) Horizontal mine OLY-12 in Olympiada Chalkidiki mining district. (j) Acropolis mine in the northeast part of Thasos island. (k) Koulachli-1 ancient mine in Kroussia mountain. (l) Koryfis-1 mine in Pangaeon mountain. (m) Lazaros ancient mine in Palaea Kavala.

Figure 4. Measured Pb isotopic compositions of galena, cerussite, and anglesite from ancient Greek mining territories and selected Ag-bearing occurrences in Greece. (a) $^{207}Pb/^{204}Pb$ versus $^{206}Pb/^{204}Pb$, (b) $^{208}Pb/^{204}Pb$ versus $^{206}Pb/^{204}Pb$, (c) $^{208}Pb/^{206}Pb$ versus $^{207}Pb/^{206}Pb$, (d) T_{mod} (Pb model age) versus μ ($^{238}U/^{204}Pb$), (e) T_{mod} (Pb model age) versus κ ($^{232}Th/^{238}U$). Literature data (Barnes et al., 1975; Gale and Stos-Gale, 1981a; Wagner and Weisgerber, 1985; Wagner et al., 1986; Kalogeropoulos et al., 1989; Nebel et al., 1991; Frei, 1992; Stos-Gale et al., 1996; Gale, 1998; Asderaki et al., 2017; OXALID and IGME unpublished data) provided in Table 3 is depicted with crosses. Lead model ages calculated according to Albarède and Juteau (1984).

Figure 5. Maps of (a) $^{206}Pb/^{204}Pb$, (b) $^{207}Pb/^{204}Pb$, (c) $^{208}Pb/^{204}Pb$, (d) $^{207}Pb/^{206}Pb$, and (e) $^{208}Pb/^{206}Pb$. Data from this study only.

Figure 6. Maps of (a) T_{mod} (Pb model age), (b) μ ($^{238}U/^{204}Pb$), and (c) κ ($^{232}Th/^{238}U$). Data from this study and literature data (Tables 2 and 3).

Figure 7. One-dimensional histogram of Pb model ages from Greek Ag-bearing mineralizations (data from this study and literature data; Tables 2 and 3). Lead model ages were calculated with the assumption of a mixture of five normal populations.

TABLE CAPTIONS

Table 1. Characteristics of Ag-bearing mineralizations in Greece.

Table 2. High-precision Pb isotopic compositions of Ag-bearing localities in Greece.

Table 3. Lead isotope data from the literature (Barnes et al., 1975; Gale and Stos-Gale, 1981a; Wagner and Weisgerber, 1985; Wagner et al.*, 1986; Kalogeropoulos* et al.*, 1989; Nebel* et al.*, 1991; Frei, 1992; Stos-Gale* et al.*, 1996; Gale, 1998; Asderaki* et al.*, 2017; OXALID and IGME unpublished data).*

Table 4. Characteristics of the recorded mining and metallurgical activity based on field observations. Extended mining areas are separated in subdistricts.

Table 5. Mean and standard-deviation of T_{mod}, μ, and κ inferred from a 5-group mixing model found in the galena samples analyzed in this work. N stands for the number of samples in each group and s for standard deviation. Note the differences between the results when literature data are included, which reflects the smaller number and much broader peaks observed in the histogram of Fig. 7. The present groups are compared with the groups identified by Milot et al. *(in press) for the Iberian Peninsula. Groups 1 (N=42), 2 (79), and 3 (N=22) are the most populated. Note that the very strong Cenozoic peak (35±9 Ma) is absent from Iberia, where late Devonian (395±40 Ma) prevails. The Cretaceous peaks are strong in both provinces, whereas the Early to Mid-Jurassic peak (190±13 Ma) is subdued in both provinces.*

Table 1

Click here to access/download;Table;TABLE 1. Silver Deposits of Greece Revised 17-8-2021.xlsx

	Ore District	Geotectonic Unit	Other Major Met. Compounds	Host Geology	Deposit Type/Style	Mineralization Age	Indicative References
1	Lavrion	Attic-Cycladic Massif	Pb, Zn, Fe, Cu, As, Sn, Au	Marble, schist, granodiorite	Carbonate replacement, veins, intrusion related	Upper Miocene	Marinos and Petracheck, 1956; Conophagos, 1980; Voudouris et al, 2008a; b; Bonsall et al, 2011; Voudouris et al, 2021
2	South Euboea	Attic-Cycladic Massif	Pb, Zn, Cu, Fe, As, Au	Schist, gneiss, marble	Detachment fault	Miocene	Perlikos, 1989; Voudouris et al, 2011
3	Central Euboea (Almyropotamos)	Attic-Cycladic Massif	Fe, Pb, Zn, As	Marble, schist	Fault controled, veins		Vryniotis, 1978; this study
4	Siphnos	Attic-Cycladic Massif	Fe, Mn, Cu, Pb, Zn, Au	Marble, gneiss, schist	Detachment fault/ Carbonate replacement	Miocene	Wagner and Weisgerber, 1985; Vavelidis, 1988; this study
5	Seriphos	Attic-Cycladic Massif	Fe, Pb, Zn, As, Cu	Schist, marble	Detachment fault/ Carbonate replacement	Upper Miocene	Gale and Stos-Gale, 1981b; Ducoux et al, 2017
6	Melos	Attic-Cycladic Massif	Pb, Zn, Cu, Au	Rhyolite, dacite, andesites, pyroclastic rocks	Epithermal	Pliocene to Pleistocene	Alfieris et al, 2013
7	Syros	Attic-Cycladic Massif	Fe, Pb, Zn, Cu, Sn, Au	Marble, schist	Detachment fault/ Carbonate replacement, veins	Upper Miocene	Melidonis and Konstantinidis, 1983; Voudouris et al, 2014
8	Kythnos	Attic-Cycladic Massif	Fe, Pb, Zn, Cu, Au	Marble, schist	Detachment fault/Carbonate replacement		Stos-Gale, 1998; Bassiakos and Philaniotou, 2007; this study
9	Antiparos	Attic-Cycladic Massif	Pb, Zn, Fe, Cu	Marble, schist	Epithermal	Miocene	Gale and Stos-Gale, 1981b; Voudouris et al, 2019
10	Polyaigos	Attic-Cycladic Massif	Pb, Zn	Ignimbrite, andesite	Epithermal		Fytikas and Vougioukalakis, 1992; this study
11	Thera	Attic-Cycladic Massif	Pb, Fe, Cu, Zn	Phyllitic schist	Epithermal		Gale, 1998
12	Anaphi	Attic-Cycladic Massif	Pb, Zn	Marble, granodiorite	Epithermal		Voudouris et al, 2019; this study
13	Kos	Pelagonic zone	Pb, Zn	Marble breccia	Veins		IGME, 1965
14	Samos	Attic-Cycladic Massif	Pb, Fe, Au	Pyroclastics, conglomerates and carbonates	Epithermal	Miocene	IGME, 1965; Voudouris et al, 2019
15	Mykonos	Attic-Cycladic Massif	Fe, Pb, Zn, Cu, Au	Monzogranite, schist	Veins	Miocene	IGME, 1965; Voudouris et al, 2019
16	Tinos	Attic-Cycladic Massif	Pb, Zn, Au	Marble, schist	Epithermal	Miocene	Tombros et al, 2007; Voudouris et al, 2019
17	Kea	Attic-Cycladic Massif	Pb, Fe	Marble	Veins		Gale, 1998
18	Tyros	Gavrovo Unit	Pb, Zn	Marble	VMS	Triassic	IGME, 1965; Skarpelis, 2020
19	Molaoi	Gavrovo Unit	Pb, Zn	Tuffs, tuffites lavas and pyroclastics	VMS	Triassic	Grossou-Valta et al, 1990
20	Taygetus	Ionian Zone	Pb, Zn, Fe, Cu, Au	Schist	Veins/VMS?		Maratos, 1956
21	Hymettus	Attic-Cycladic Massif	Fe, Pb, As, Cu	Schist, marble	Carbonate Replacement	Upper Miocene	IGME; 1965; Stouraiti et al, 2019
22	Chios	Sakarya Block	Pb, Zn, Au	Clastic sediments	Epithermal	Mid-Miocene	Skarpelis, 1999
23	Pelion	Pelagonic zone	Fe, Pb, Zn, Cu	Schist, Marble	Veins / Carbonate replacement		Tataris, 1960; this study
24	Lesbos (Argenos)	Rhodope Massif-Sakarya	Fe, Pb, Zn, Cu, Au	Dacite, trachyandesite	Epithermal	Upper Miocene	Kontis et al, 1994; Pernicka et al, 2003; Voudouris et al, 2019
25	Limnos (Fakos)	Rhodope Massif	Pb, Zn, Cu, As, Au	Sandstone, monzodiorite	Epithermal	Lower Miocene	Voudouris and Skarpelis, 1998; Voudouris and Alfieris, 2005; Voudouris et al, 2019

26	Samothrace	Circum Rhodope Belt	Pb, Fe, Cu	Granite	Epithermal	Miocene	Voudouris et al, 2019
27	Sykia Chalkidiki	Circum Rhodope Belt	Pb, Cu, Zn, Fe	Granodiorite	Veins		IGME, 1965; Wagner et al, 1986
28	NE Chalkidiki (Olympiada, Madem Lakkos, Mavres Petres)	Rhodope Massif	Pb, Zn, Cu, As, Au	Marble, gneiss, amphibolite	Carbonate replacement, intrusion related	Oligocene	Wagner et al, 1986; Kalogeropoulos et al, 1989; Siron et al, 2016
29	Thasos	Rhodope Massif	Fe, Mn, Pb, Zn, Cu, As, Au	Marble, gneiss, schist	Carbonate replacement, intrusion related	Miocene	Vavelidis and Amstutz, 1983; Wagner and Weisgerber, 1988
30	Kilkis (Drakontio, Stefania, Koronouda)	Vertiskos Unit	Pb, Zn, Cu. Au	Gneiss, schist, amphibolite	Intrusion related	Oligocene-Miocene	Melfos and Voudouris, 2017
31	Kroussia	Vertiskos Unit	Pb, Zn, Cu. Au	Schist, gneiss, marble	Carbonate replacement / Porphyry		IGME, 1965; Veranis and Tsamantouridis, 1991; Stergiou et al, 2016
32	Skra	Circum Rhodope Belt	Pb, Zn	Rhyodacitic lavas, pyroclastics, porphyries and cherty tuffs	VMS	Upper Jurassic	Skarpelis, 2020
33	Angistron	Rhodope Massif	Fe, Mn, Pb, Zn, Cu, Au	Marble	Veins/ Carbonate replacement		Chiotis et al, 1996; this study
34	Pangaeon	Rhodope Massif Serbomacedonian Zone	Pb, Zn, Cu, Fe, Mn, Au	Marble, schist, gneiss, amphibolite	Intrusion related/ Carbonate replacement	Miocene	Vaxevanopoulos, 2017; 2018
35	Palaea Kavala	Rhodope Massif	Fe, Mn, Pb, Zn, Cu, Au	Marble, gneiss, schist, granodiorite	Intrusion related/ Carbonate replacement	Miocene	Vavelidis et al, 1996; Fornadel et al, 2011
36	Thermes	Rhodope Massif	Fe, Pb, Zn, Cu, Au	Marble, gneiss, amphibolite	Carbonate replacemement	Oligocene	Gialoglou and Drymniotis, 1983; Kalogeropoulos et al, 1996; Nesbitt et al, 1998
37	Perama Hill	Circum Rhodope Belt	Cu, Pb, Au	Andesite, breccia, sandstone	Epithermal	Oligocene	Voudouris and Skarpelis, 1998
38	Kallintiri	Circum Rhodope Belt	Pb, Zn, Au	Marble, schist	Pollymetalic	Oligocene	Kanellopoulos, 2014; Melfos and Voudouris, 2017
39	Sappes	Circum Rhodope Belt	Fe, Cu, Pb, Zn, Au	Monzodiorite	Epithermal	Oligocene	Voudouris et al, 2006
40	Kirki	Circum Rhodope Belt	Fe, Cu, Pb, Zn, As, Sn, Au	Andesite	Epithermal	Oligocene	Nesbitt et al, 1988; Melfos and Voudouris, 2017
41	Aisymi	Circum Rhodope Belt	Fe, Pb, Zn, Cu,	Granodiorite	Epithermal	Oligocene	Voudouris et al, 2006
42	Neda (King Arthour)	Rhodope Massif	Fe, Pb, Cu, Zn	Andesite-Gneiss	Epithermal	Oligocene	Nesbitt et al, 1988; Voudouris et al, 2019
43	Pefka	Circum Rhodope Belt	Pb, Cu, Zn, As, Bi, Sn, Au	Rhyodacitic lavas and pyroclastics	Epithermal	Oligocene	Voudouris, 2006; Melfos and Voudouris, 2017
44	Loutros	Circum Rhodope Belt	Fe, Pb, As	Rhyolite	Epithermal	Miocene	Melfos and Voudouris, 2016; 2017

Table 2

Click here to access/download;Table;TABLE 2. LIA results Revised 17-8-2021.xlsx

Sample	Region	District / Mine	Mining Phase	Mineralization	Host Rock	Ag (ppm)	Pb (wt %)	$^{206}Pb/^{204}Pb$
L-01	Lavrion	Hilarion	Ancient	Gal, Conich, Goeth	Marble	320.844	19.599	18.8401
L-02A	Lavrion	Porto-09	Modern-Ancient	Gal	Schist	124.200	18.090	18.8591
L-02B	Lavrion	Porto-09	Modern-Ancient	Gal	Schist	107.184	12.862	18.8593
L-03	Lavrion	Ari	Ancient	Gal	Marble	294.591	15.730	18.8635
L-04	Lavrion	Esperanza	Ancient	Cer, Angl	Marble	182.346	1.142	18.8688
L-05	Lavrion	Dimoliaki	Ancient	Goeth, Gal	Marble	20.856	3.491	18.8744
L-06	Lavrion	Jean Vaptiste	Modern-Ancient	Gal, Cer, Mal, Con	Marble	1673.407	70.729	18.8599
L-07	Lavrion	Esperanza	Modern-Ancient	Gal, Cer	Marble	1977.548	67.949	18.8607
L-08	Lavrion	Plaka-80	Modern	Gal, Spha	Marble	1656.376	51.957	18.8906
L-09	Lavrion	Plaka-80	Modern	Gal, Spha	Marble	3029.485	65.682	18.8845
L-10	Lavrion	Dimoliaki	Ancient	Cer, Gal, Goeth	Marble	1181.700	32.512	18.8741
L-11	Lavrion	Plaka-145	Modern	Gal	Marble	5872.432	65.728	18.8762
L-12	Lavrion	Esperanza	Ancient	Gal, Spha	Marble	1959.088	79.339	18.8649
L-13	Lavrion	Esperanza	Ancient	Gal, Spha	Marble	2005.232	69.751	18.8670
L-14	Lavrion	Esperanza	Ancient	Spha, Gal	Marble	329.663	0.972	18.8594
L-15	Lavrion	Esperanza	Ancient	Spha, Gal	Marble	332.786	0.982	18.8625
L-16	Lavrion	HIL-24	Ancient	Gal, Cer	Marble	17.637	0.023	18.8220
L-17	Lavrion	Poundazeza	Ancient	Gal	Marble	4219.914	55.620	18.8764
L-26	Lavrion	Sounio-06	Modern-Ancient	Cer	Marble	2.407	0.289	18.8238
L-32	Lavrion	Elafos	Modern-Ancient	Goeth, Cer	Marble	0.000	0.717	18.8515
L-34	Lavrion	Dimoliaki	Ancient	Cer, Gal, Goeth, Smith	Marble	2463.710	22.195	18.8637
L-40	Lavrion	Sykia	Ancient	Gal, Cer	Marble	1036.609	42.923	18.8602
L-41	Lavrion	Mpotsari	Ancient	Gal, Cer	Marble	3669.772	70.541	18.8504
L-42	Lavrion	Christiana	Modern-Ancient	Gal, Cer	Marble	3951.002	70.371	18.8642
L-43	Lavrion	MAN-HOR-1	Ancient	Cer, Goeth	Marble	40.223	10.804	18.8792
L-47	Lavrion	Thorikos Mine	Ancient	Goeth, Cer	Marble	0.000	3.643	18.8727
E-01	Euboea	Kordelas	Modern	Gal	Marble	19.897	2.243	18.6864
E-02	Euboea	St Barbara	Modern	Gal	Marble	583.086	1.620	18.6935
E-03	Euboea	St Barbara	Modern	Gal	Marble	86.947	0.879	18.7024
E-05	Euboea	Moskies	Ancient	Gal	Marble	730.871	40.775	18.6893
E-06	Euboea	Moskies	Ancient	Gal, Py,	Marble	509.115	29.896	18.6869
GIA-02A	Euboea	Gialpides	Ancient	Cpy, Cer	Marble	10.946	0.020	18.7279
GIA-02B	Euboea	Gialpides	Ancient	Cpy, Cer	Marble	48.824	0.023	18.6715
SCHI-01A	Euboea	Schinodavli Mine	Ancient	Goeth, Cer	Schist	0.000	0.041	18.6742
SCHI-01B	Euboea	Schinodavli Mine	Ancient	Goeth, Cer	Schist	0.919	0.042	18.7249
AL-01	Euboea	Almyropotamos Mine-01	Modern-Ancient	Cer, Goeth	Marble	91.447	6.968	18.7987
AL-02	Euboea	Almyropotamos Mine-02	Modern-Ancient	Cer, Goeth	Marble	65.291	14.076	18.7802
AL-03	Euboea	Almyropotamos Mine-07	Modern-Ancient	Cer, Goeth	Marble	74.679	10.301	18.7929
SI-02	Siphnos	Ai Sostis	Ancient	Goeth, Cer, Hem, Pyrol	Marble	13.244	6.438	18.7367
SI-03	Siphnos	Ai Sostis	Ancient	Goeth, Hem, Pyrol, Cer	Marble	1.710	2.660	18.7291
SI-10	Siphnos	Agios Silvestros	Ancient	Goeth, Hem, Pyrol, Gal, Cer	Marble	4983.329	7.107	18.7361
SI-11	Siphnos	Xero Xylo	Ancient	Cer, Goet, Hem	Marble	126.393	0.430	18.7298
SI-13	Siphnos	Kapsalos-Frase	Ancient-Modern	Cer, Goet, Hem	Marble	20.985	2.287	18.7273
SI-14	Siphnos	Ai Sostis	Ancient	Cer, Goet, Hem	Marble	3.199	0.761	18.7344
SI-15	Siphnos	Xero Xylo	Ancient-Modern	Cer, Goet, Hem	Marble	40.233	0.478	18.7265
SE-02	Seriphos	Moutoula-07	Ancient	Gal	Marble	161.506	69.965	18.9000
SE-03	Seriphos	Moutoula-08	Ancient	Gal	Marble	470.289	85.248	18.9024
M-01A	Melos	Agios Nikolaos	Modern-Ancient	Gal	Tuff	2388.673	66.390	18.8601
M-01B	Melos	Agios Nikolaos	Modern-Ancient	Gal	Tuff	2473.074	28.166	18.8619
M-03A	Melos	Triades	Modern-Ancient	Goeth, Cer	Tuff	1.475	0.014	18.8205
M-03B	Melos	Triades	Modern-Ancient	Goeth, Cer	Tuff	6.018	0.003	18.8200
SYR-04	Syros	Azolimnos	Modern	Gal, Cer	Marble	0.971	0.171	18.8401
SYR-06	Syros	Rozos	Ancient	Gal, Cer	Marble	1.181	0.001	18.8178
SYR-07	Syros	Rozos	Ancient	Gal, Cer	Marble	26.091	0.821	18.8296
SYR-08	Syros	Rozos	Ancient	Gal, Cer	Marble	0.781	0.128	18.8208
SYR-09	Syros	Rozos	Ancient	Gal, Cer	Marble	23.202	0.418	18.8202
SYR10	Syros	Rozos	Modern	Gal, Cer	Marble	1.343	0.366	18.8376
KY-01	Kythnos	Agios Dimitrios Mine	Ancient	Goeth, cer	Marble	0.000	0.187	18.9374
KY-02	Kythnos	Agios Dimitrios	Modern	Goeth, cer	Marble	12.986	0.595	18.9225
KY-05	Kythnos	Katafyki Mine	Modern	Goeth, cer	Marble	0.772	0.003	18.8357
KY-08	Kythnos	Kastellas	Ancient	Goeth, cer	Marble	0.231	0.956	18.9053
KY-10	Kythnos	Tourkala	Modern	Goeth, cer	Marble	16.189	0.035	18.8271
AN-02	Antiparos	Monastiria Mine 1	Modern-Ancient	Cer, Gal	Gneiss	339.640	55.828	18.8392
AN-03	Antiparos	Chatzovounia Mine 1	Modern	Cer, Goeth	Marble	2.300	0.126	18.8412
AN-04A	Antiparos	Agios Georgios Mine 3	Modern	Gal	Marble	386.406	66.982	18.8238
AN-04B	Antiparos	Agios Georgios Mine 4	Modern	Gal	Marble	237.798	61.638	18.8229
PO-01A	Polyaigos	Modern Mine	Modern	Gal, Bar	Marble	80.570	33.227	18.8771
PO-01B	Polyaigos	Modern Mine	Modern	Gal, Bar	Marble	67.629	54.612	18.8726
PO-01C	Polyaigos	Modern Mine	Modern	Gal, Bar	Marble	116.004	89.208	18.8779
ANA-01	Anaphi	Ntoumparia	Modern	Gal, Spha	Marble	81.189	36.854	18.8946
HYM-01	Hymettus	Kynigos-1 Mine	Modern	Goeth, Cer	Marble	1.855	1.162	18.4301
HYM-02	Hymettus	Hymittos-2 (kamini)	Modern	Goeth, Cer	Marble	0.000	0.191	18.4053
HYM-03	Hymettus	Kynigos-1 Mine	Modern	Goeth, Cer	Marble	6.301	1.024	18.4321

HYM-04	Hymettus	Hymittos-2 (kamini)	Modern	Goeth, Cer	Marble	0.715	0.259	18.4040
PE-01	Pelion	Gourounotrypa	Ancient	Goeth, cer	Marble	8.193	0.369	18.8707
PE-02	Pelion	Gourounotrypa	Ancient	Goeth, cer	Marble	13.018	1.397	18.8701
PE-03A	Pelion	Souvria	Ancient	Goeth, cer	Marble	2.947	0.061	18.8796
PE-03B	Pelion	Souvria	Ancient	Goeth, cer	Marble	11.004	0.059	18.8785
PE-04	Pelion	Souvria	Ancient	Goeth, cer	Marble	10.871	0.342	18.8696
LES-01	Lesbos	Argenos	Modern	Gal	Andesite	154.536	37.982	18.6284
SAM-01	Samothrace	Pachia Ammos	Modern	Gal	Granite	471.108	58.564	18.3785
MP-01A	Chalkidiki	Mavres Petres	Modern	Gal	Marble	2825.600	82.768	18.7966
MP-01B	Chalkidiki	Mavres Petres	Modern	Gal	Marble	2879.577	82.366	18.8045
MP-01C	Chalkidiki	Mavres Petres	Modern	Gal	Marble	2708.115	72.417	18.8076
OL-01A	Chalkidiki	Olympiada	Modern	Gal	Marble	1536.102	55.023	18.7805
OL-01B	Chalkidiki	Olympiada	Modern	Gal	Marble	1574.803	52.449	18.7801
OL-02A	Chalkidiki	Olympiada	Ancient	Cer, Fe-Mn	Marble	291.414	0.025	18.7878
OL-02B	Chalkidiki	Olympiada	Ancient	Goeth, Cer, Pyrol	Marble	674.232	0.032	18.7928
C-01A	Chalkidiki	Stratoni	Modern	Gal, Cer	Marble	14.247	0.195	18.8121
C-01B	Chalkidiki	Stratoni	Modern	Gal, Cer	Marble	18.475	0.190	18.8147
C-02	Chalkidiki	Fterouda	Ancient	Goeth, Cer	Marble	39.459	3.217	18.7061
T-01	Thasos	Acropolis Mine	Ancient	Gal, Cer	Marble	50.818	0.097	18.6928
T-02	Thasos	Rachoni Mine	Ancient	Goeth, Cer	Marble	44.933	2.798	18.8502
T-03	Thasos	Sotiros Mine	Ancient	Goeth, Cer	Marble	8.485	1.711	18.7992
T-04	Thasos	Koumaria	Ancient	Goeth, Cer	Marble	2.788	0.002	18.8010
T-06	Thasos	Rachoni Mine	Ancient	Goeth, Cer	Marble	5.967	1.779	18.8468
T-07	Thasos	Vouves	Modern	Smith, Cer	Marble	13.848	0.008	18.7902
T-08	Thasos	Vouves	Modern	Goeth, Cer	Marble	0.233	0.164	18.7820
T-10	Thasos	Acropolis Mine	Ancient	Goeth, Cer	Marble	101.642	0.048	18.6901
T-11	Thasos	Acropolis Mine	Ancient	Goeth, Cer	Marble	2.243	0.061	18.6886
T-12	Thasos	Acropolis Mine	Ancient	Goeth, Cer	Marble	945.059	0.040	18.6921
D-01	Kroussia	Kerkini	Ancient	Cer	Marble	23.655	0.912	18.7909
D-02	Kroussia	Agios Markos	Modern	Gal	Gneiss	1364.079	13.735	18.8251
D-03	Kroussia	Agios Markos	Modern	Gal	Gneiss	214.609	13.558	18.8260
D-04	Kroussia	Koulachli Mine	Ancient	Cer	Gneiss	8.930	0.752	18.8077
D-05	Kroussia	Koulachli Mine	Ancient	Cer	Gneiss	4.733	0.095	18.8133
D-06	Kroussia	Koulachli Mine	Ancient	Cer	Gneiss	18.802	0.160	18.8224
D-07	Kroussia	Vathi Ancient Mine	Ancient	Cer	Rhyolite	0.000	0.082	18.8632
D-10	Kroussia	Myriophyto outcrop	Modern Quarry	Goeth, Cer	Marble	0.700	0.021	18.3296
LE-01	Angistron	Lechovo	Ancient-Modern	Cer	Marble	11.350	4.490	18.7211
LE-02	Angistron	Lechovo	Ancient-Modern	Cer	Marble	182.462	8.018	18.7250
LE-03	Angistron	Lechovo	Ancient-Modern	Cer	Marble	11.793	3.839	18.7299
LE-04	Angistron	Lechovo	Ancient-Modern	Cer	Marble	176.214	8.466	18.7283
PA-01	Pangaeon	Nerostria	Modern-Ancient	Goeth, Cer	Granodiorite	1.324	0.008	18.7317
PA-02	Pangaeon	Asimotrypes	Ancient-Modern	Pyr, Apy, Gal. Spha, Cpy	Marble	9697.459	22.400	18.7013
PA-02B	Pangaeon	Asimotrypes	Ancient-Modern	Pyr, Apy, Gal. Spha, Cpy	Marble	9906.324	20.114	18.7044
PA-03	Pangaeon	Agia Triada-1	Ancient	Goeth, Mal, Cer	Marble	124.429	0.302	18.7075
PA-04A	Pangaeon	Asimotrypes	Ancient-Modern	Pyr, Apy, Gal. Spha, Cpy	Marble	5439.100	11.364	18.7012
PA-04B	Pangaeon	Asimotrypes	Ancient-Modern	Pyr, Apy, Gal. Spha, Cpy	Marble	5042.224	10.575	18.6974
PA-05	Pangaeon	Avgo peak	Ancient-Modern	Goeth, Cer	Marble	86.924	1.851	18.7013
PA-06	Pangaeon	Avgo peak	Ancient-Modern	Goeth, Cer	Marble	145.377	5.704	18.6948
PA-07A	Pangaeon	Ofrynio-2	Ancient	Goeth, Cer	Marble	20.220	1.253	18.7919
PA-07B	Pangaeon	Ofrynio-2	Ancient	Goeth, Cer	Marble	23.808	1.089	18.7906
PA-11	Pangaeon	Asimotrypes	Ancient-Modern	Cer, Goeth	Marble	31.146	0.082	18.7051
PA-15	Pangaeon	Asimotrypes	Ancient-Modern	Gal	Marble	7726.971	20.137	18.6936
SY-04	Pangaeon	Kokkinochoma-1 Symvolon	Ancient	Goeth, Cer	Marble	10.061	0.007	18.7062
PK-01	Palaea Kavala	Agia Eleni Mine	Ancient	Cer, Goeth, Hem	Marble	114.442	4.582	18.7606
PK-02	Palaea Kavala	Agia Eleni Mine	Ancient	Cer, Goeth, Hem	Marble	147.384	3.908	18.7666
PK-03	Palaea Kavala	Agia Eleni Mine	Ancient	Cer, Goeth, Hem	Marble	140.134	5.517	18.7675
PK-04	Palaea Kavala	Agia Eleni Mine	Ancient	Cer, Goeth, Hem	Marble	57.137	5.250	18.7680
PK-06	Palaea Kavala	Mavri Trypa Mine	Ancient	Cer	Marble	95.320	0.910	18.7565
PK-07	Palaea Kavala	Lazaros-1 Mine	Ancient	Cer	Marble	213.268	4.684	18.7643
PK-08	Palaea Kavala	Lazaros-1 Mine	Ancient	Cer	Marble	147.120	0.177	18.7570
PK-09	Palaea Kavala	Peristerionas Mine	Ancient	Cer	Marble	80.467	13.026	18.7652
PK-11	Palaea Kavala	Kel-Tepe	Ancient	Goeth, Cer	Marble	58.591	9.665	18.7595
THE-01	Thermes	Loutra	Modern	Gal	Marble	13.933	0.010	18.6328
THE-02	Thermes	Razul	Modern	Gal	Marble	52.245	19.075	18.7138
THE-03	Thermes	Razul	Modern	Gal	Marble	3.735	0.004	18.7146
KIR-01	Kirki	Saint-Philippos	Modern	Gal	Andesite	949.152	1.998	18.7177
KIR-02	Kirki	Saint-Philippos	Modern	Gal-Cpy	Andesite	97.448	0.538	18.7155
KIR-03	Kirki	Saint-Philippos	Modern	Gal-Cpy	Andesite	1044.842	0.328	18.7170
KIR-04	Kirki	Saint-Philippos	Modern	Gal-Cpy	Andesite	371.873	19.810	18.7146
SAP-01	Sappes	Sappes	Modern	Gal	Diorite	0.396	0.040	18.7549
SAP-02	Sappes	Sappes	Modern	Gal	Diorite	0.000	0.009	18.8143
AIS-01	Aisymi	Aisymi	Modern	Gal	Marble	66.164	2.040	18.7430
NED-01	Neda	Neda	Modern	Gal	Marble	38.667	19.581	18.7527
NED-02	Neda	Neda	Modern	Gal	Marble	45.473	29.177	18.7482

NED-03	Neda	Neda	Modern	Gal	Marble	17.677	7.502	18.7443
PEF-02	Pefkos	Pefkos	Modern	Gal	Rhyolite	1.300	0.112	18.7472

2SD	$^{207}Pb/^{204}Pb$	2SD	$^{208}Pb/^{204}Pb$	2SD	$^{204}Pb/^{206}Pb$	2SD	$^{207}Pb/^{206}Pb$	2SD	$^{208}Pb/^{206}Pb$	2SD	x	y
0.0007	15.6852	0.0006	38.820	0.002	0.0531	0.0007	0.83254	0.00001	2.06048	0.00003	37° 42' 57.7866" N	24° 00' 49.5334" E
0.0010	15.6938	0.0011	38.939	0.003	0.0530	0.0010	0.83216	0.00001	2.06471	0.00008	37° 47' 27.5781" N	24° 04' 55.6097" E
0.0008	15.6939	0.0008	38.938	0.003	0.0530	0.0008	0.83216	0.00001	2.06471	0.00005	37° 47' 27.5781" N	24° 04' 55.6097" E
0.0011	15.6936	0.0008	38.884	0.002	0.0530	0.0011	0.83194	0.00003	2.06127	0.00008	37° 45' 42.8612" N	23° 59' 28.2221" E
0.0008	15.6925	0.0009	38.865	0.003	0.0530	0.0008	0.83165	0.00001	2.05975	0.00009	37° 43' 34.3682" N	24° 01' 58.0272" E
0.0009	15.6916	0.0011	38.884	0.004	0.0530	0.0009	0.83136	0.00002	2.06013	0.00010	37° 45' 11.1933" N	24° 00' 06.0348" E
0.0008	15.6837	0.0009	38.825	0.003	0.0530	0.0008	0.83158	0.00001	2.05856	0.00007	37° 43' 42.7689" N	24° 00' 38.2815" E
0.0007	15.6872	0.0007	38.824	0.002	0.0530	0.0007	0.83175	0.00001	2.05845	0.00005	37° 43' 34.3682" N	24° 01' 58.0272" E
0.0032	15.7093	0.0026	38.938	0.006	0.0529	0.0032	0.83160	0.00001	2.06122	0.00006	37° 45' 36.1342" N	24° 01' 59.6156" E
0.0019	15.7034	0.0016	38.923	0.003	0.0530	0.0019	0.83155	0.00001	2.06112	0.00005	37° 45' 35.8797" N	24° 01' 57.0971" E
0.0007	15.6921	0.0006	38.878	0.002	0.0530	0.0007	0.83141	0.00001	2.05984	0.00008	37° 45' 11.1933" N	24° 00' 06.0347" E
0.0008	15.6918	0.0007	38.893	0.002	0.0530	0.0008	0.83131	0.00001	2.06040	0.00005	37° 45' 35.5808" N	24° 02' 01.0620" E
0.0007	15.6901	0.0006	38.838	0.002	0.0530	0.0007	0.83171	0.00001	2.05874	0.00004	37° 43' 34.1947" N	24° 02' 01.7645" E
0.0012	15.6905	0.0011	38.837	0.003	0.0530	0.0012	0.83164	0.00001	2.05850	0.00006	37° 43' 34.1947" N	24° 02' 01.7645" E
0.0010	15.6845	0.0010	38.857	0.003	0.0530	0.0010	0.83166	0.00001	2.06033	0.00009	37° 43' 34.4729" N	24° 02' 01.3349" E
0.0006	15.6865	0.0005	38.860	0.001	0.0530	0.0006	0.83163	0.00001	2.06021	0.00002	37° 43' 34.4729" N	24° 02' 01.3349" E
0.0007	15.6795	0.0007	38.858	0.002	0.0531	0.0007	0.83305	0.00001	2.06450	0.00006	37° 43' 13.2700" N	24° 00' 41.5551" E
0.0009	15.6941	0.0010	38.913	0.003	0.0530	0.0009	0.83142	0.00002	2.06148	0.00010	37° 40' 51.8589" N	24° 04' 03.8284" E
0.0005	15.6925	0.0004	38.882	0.001	0.0531	0.0005	0.83367	0.00001	2.06561	0.00003	37° 40' 51.6458" N	24° 01' 02.4408" E
0.0007	15.6850	0.0006	38.874	0.002	0.0530	0.0007	0.83202	0.00001	2.06207	0.00002	37° 42' 41.4758" N	24° 01' 27.2640" E
0.0025	15.6861	0.0031	38.860	0.010	0.0530	0.0025	0.83154	0.00005	2.06003	0.00023	37° 45' 11.1933" N	24° 00' 06.0347" E
0.0006	15.6995	0.0006	38.889	0.002	0.0530	0.0006	0.83240	0.00001	2.06195	0.00004	37° 41' 58.1481" N	24° 00' 38.6262" E
0.0009	15.6946	0.0008	38.886	0.003	0.0530	0.0009	0.83256	0.00001	2.06280	0.00007	37° 41' 37.6138" N	24° 01' 36.2949" E
0.0015	15.6840	0.0014	38.830	0.004	0.0530	0.0015	0.83143	0.00002	2.05841	0.00010	37° 44' 02.4144" N	24° 01' 10.9848" E
0.0007	15.6896	0.0006	38.858	0.002	0.0530	0.0007	0.83105	0.00001	2.05827	0.00003	37° 46' 10.1912" N	23° 59' 53.8461" E
0.0009	15.6942	0.0007	38.921	0.002	0.0530	0.0009	0.83159	0.00001	2.06231	0.00005	37° 44' 17.0548" N	24° 03' 15.7263" E
0.0006	15.6977	0.0005	38.908	0.001	0.0535	0.0006	0.84006	0.00001	2.08217	0.00003	38° 06' 49.4600" N	24° 30' 47.7804" E
0.0006	15.6957	0.0005	38.912	0.002	0.0535	0.0006	0.83963	0.00001	2.08156	0.00003	38° 06' 48.7526" N	24° 30' 40.3656" E
0.0006	15.7009	0.0005	38.927	0.002	0.0535	0.0006	0.83952	0.00001	2.08141	0.00003	38° 06' 48.7526" N	24° 30' 40.3656" E
0.0007	15.7011	0.0006	38.916	0.002	0.0535	0.0007	0.84012	0.00001	2.08230	0.00004	38° 06' 15.6060" N	24° 30' 38.9232" E
0.0006	15.6994	0.0005	38.913	0.002	0.0535	0.0006	0.84013	0.00001	2.08242	0.00005	38° 06' 17.2800" N	24° 30' 39.5208" E
0.0008	15.6943	0.0007	38.947	0.002	0.0534	0.0008	0.83802	0.00001	2.07966	0.00005	38° 08' 32.1909" N	24° 32' 14.6206" E
0.0006	15.6958	0.0005	38.669	0.001	0.0536	0.0006	0.84063	0.00001	2.07105	0.00004	38° 08' 32.1909" N	24° 32' 14.6206" E
0.0009	15.6977	0.0008	38.675	0.002	0.0535	0.0009	0.84061	0.00001	2.07107	0.00004	38° 08' 38.4173" N	24° 26' 52.0365" E
0.0007	15.6915	0.0007	38.941	0.002	0.0534	0.0007	0.83801	0.00001	2.07963	0.00006	38° 08' 38.4173" N	24° 26' 52.0365" E
0.0010	15.7059	0.0009	38.933	0.003	0.0532	0.0010	0.83549	0.00001	2.07112	0.00004	38° 15' 00.9759" N	24° 10' 14.4010" E
0.0011	15.7004	0.0010	38.912	0.003	0.0532	0.0011	0.83600	0.00001	2.07202	0.00005	38° 15' 11.1816" N	24° 10' 15.4272" E
0.0007	15.7048	0.0007	38.930	0.002	0.0532	0.0007	0.83569	0.00001	2.07155	0.00005	38° 15' 19.3932" N	24° 10' 30.7668" E
0.0009	15.7141	0.0010	38.960	0.003	0.0534	0.0009	0.83869	0.00001	2.07940	0.00011	37° 00' 48.9132" N	24° 42' 49.2732" E
0.0006	15.7045	0.0005	38.954	0.002	0.0534	0.0006	0.83851	0.00001	2.07985	0.00002	37° 00' 45.6151" N	24° 42' 49.0187" E
0.0005	15.7040	0.0004	38.951	0.001	0.0534	0.0005	0.83817	0.00001	2.07894	0.00002	37° 00' 22.4271" N	24° 42' 23.6622" E
0.0005	15.7048	0.0004	38.955	0.001	0.0534	0.0005	0.83850	0.00001	2.07987	0.00002	36° 58' 32.6352" N	24° 41' 21.3432" E
0.0005	15.7018	0.0005	38.950	0.002	0.0534	0.0005	0.83843	0.00001	2.07987	0.00003	36° 58' 50.7396" N	24° 41' 25.9548" E
0.0006	15.7058	0.0006	38.961	0.002	0.0534	0.0006	0.83833	0.00001	2.07964	0.00004	37° 00' 48.9132" N	24° 42' 49.2732" E
0.0007	15.7009	0.0007	38.946	0.002	0.0534	0.0007	0.83846	0.00001	2.07974	0.00006	36° 58' 32.6352" N	24° 41' 21.3432" E
0.0008	15.7010	0.0008	39.009	0.003	0.0529	0.0008	0.83076	0.00001	2.06400	0.00006	37° 11' 12.1704" N	24° 30' 06.5340" E
0.0008	15.7030	0.0007	39.014	0.003	0.0529	0.0008	0.83075	0.00001	2.06394	0.00007	37° 11' 12.1704" N	24° 30' 06.5340" E
0.0006	15.6892	0.0006	39.007	0.002	0.0530	0.0006	0.83188	0.00001	2.06829	0.00003	36° 42' 23.5944" N	24° 20' 47.9112" E
0.0007	15.6896	0.0008	39.008	0.002	0.0530	0.0007	0.83181	0.00001	2.06810	0.00005	36° 42' 23.5944" N	24° 20' 47.9112" E
0.0006	15.6935	0.0006	38.971	0.002	0.0531	0.0006	0.83387	0.00001	2.07071	0.00004	36° 43' 58.2240" N	24° 22' 02.5392" E
0.0005	15.6954	0.0005	38.973	0.001	0.0531	0.0005	0.83398	0.00001	2.07082	0.00004	36° 43' 58.2240" N	24° 22' 02.5392" E
0.0016	15.7186	0.0012	39.103	0.003	0.0531	0.0016	0.83431	0.00002	2.07551	0.00005	37° 24' 50.1300" N	24° 57' 50.3700" E
0.0007	15.7099	0.0007	39.045	0.002	0.0531	0.0007	0.83486	0.00001	2.07495	0.00004	37° 22' 29.9928" N	24° 54' 15.0552" E
0.0010	15.7141	0.0009	39.054	0.006	0.0531	0.0010	0.83455	0.00001	2.07419	0.00018	37° 22' 28.8372" N	24° 54' 16.1100" E
0.0016	15.7114	0.0014	39.056	0.003	0.0531	0.0016	0.83479	0.00002	2.07514	0.00005	37° 22' 29.9928" N	24° 54' 15.0552" E
0.0019	15.7140	0.0009	39.064	0.004	0.0531	0.0019	0.83494	0.00001	2.07559	0.00004	37° 22' 29.9928" N	24° 54' 15.0552" E
0.0010	15.7196	0.0011	39.086	0.003	0.0531	0.0010	0.83450	0.00002	2.07494	0.00008	37° 22' 29.9928" N	24° 54' 15.0552" E
0.0010	15.7013	0.0009	39.025	0.003	0.0528	0.0010	0.82913	0.00001	2.06074	0.00005	37° 18' 07.3233" N	24° 21' 51.8554" E
0.0007	15.7018	0.0006	39.024	0.002	0.0528	0.0007	0.82980	0.00001	2.06227	0.00004	37° 18' 03.8231" N	24° 21' 57.7715" E
0.0007	15.7024	0.0007	39.008	0.002	0.0531	0.0007	0.83367	0.00001	2.07098	0.00003	37° 22' 53.2584" N	24° 25' 47.5470" E
0.0016	15.7009	0.0015	39.008	0.005	0.0529	0.0016	0.83050	0.00002	2.06330	0.00010	37° 21' 29.9736" N	24° 23' 22.3764" E
0.0009	15.7196	0.0007	39.123	0.002	0.0531	0.0009	0.83494	0.00001	2.07805	0.00003	37° 22' 44.6990" N	24° 27' 21.9268" E
0.0006	15.7258	0.0005	39.170	0.001	0.0531	0.0006	0.83475	0.00001	2.07920	0.00003	37° 00' 10.7244" N	25° 02' 00.1500" E
0.0008	15.7259	0.0008	39.173	0.002	0.0531	0.0008	0.83466	0.00001	2.07911	0.00006	36° 59' 41.0712" N	25° 03' 21.9744" E
0.0007	15.7190	0.0006	39.118	0.002	0.0531	0.0007	0.83506	0.00001	2.07816	0.00003	36° 59' 07.6596" N	25° 01' 49.6668" E
0.0007	15.7181	0.0006	39.117	0.002	0.0531	0.0007	0.83505	0.00001	2.07820	0.00006	36° 59' 07.6596" N	25° 01' 49.6668" E
0.0006	15.6974	0.0006	39.015	0.001	0.0530	0.0006	0.83156	0.00001	2.06680	0.00003	36° 47' 07.8527" N	24° 36' 43.7007" E
0.0009	15.6924	0.0011	39.003	0.004	0.0530	0.0009	0.83149	0.00002	2.06658	0.00012	36° 47' 07.6344" N	24° 36' 43.7904" E
0.0009	15.6974	0.0008	39.017	0.002	0.0530	0.0009	0.83152	0.00001	2.06677	0.00004	36° 47' 07.8527" N	24° 36' 43.7007" E
0.0011	15.7009	0.0014	39.031	0.004	0.0529	0.0011	0.83098	0.00002	2.06566	0.00011	36° 21' 59.5620" N	25° 45' 45.8244" E
0.0015	15.6851	0.0013	38.597	0.004	0.0543	0.0015	0.85105	0.00001	2.09420	0.00005	37° 59' 58.5700" N	23° 50' 12.4600" E
0.0007	15.6876	0.0007	38.575	0.002	0.0543	0.0007	0.85233	0.00001	2.09587	0.00004	37° 58' 58.6619" N	23° 50' 28.0622" E
0.0006	15.6858	0.0005	38.597	0.001	0.0543	0.0006	0.85100	0.00001	2.09404	0.00003	37° 59' 58.5700" N	23° 50' 12.4600" E

0.0006	15.6854	0.0006	38.574	0.001	0.0543	0.0006	0.85227	0.00001	2.09599	0.00003	37° 58' 58.3285" N	23° 50' 27.7016" E
0.0007	15.7090	0.0006	39.046	0.001	0.0530	0.0007	0.83246	0.00001	2.06912	0.00003	39° 21' 29.9987" N	23° 11' 03.9587" E
0.0006	15.7090	0.0006	39.048	0.002	0.0530	0.0006	0.83248	0.00001	2.06935	0.00003	39° 21' 29.9987" N	23° 11' 03.9587" E
0.0008	15.7127	0.0007	39.067	0.002	0.0530	0.0008	0.83225	0.00001	2.06930	0.00003	39° 23' 53.2373" N	23° 10' 13.2839" E
0.0006	15.7134	0.0005	39.070	0.001	0.0530	0.0006	0.83234	0.00001	2.06955	0.00002	39° 23' 53.2373" N	23° 10' 13.2839" E
0.0007	15.7112	0.0005	39.058	0.002	0.0530	0.0007	0.83262	0.00001	2.06993	0.00002	39° 23' 53.2373" N	23° 10' 13.2839" E
0.0008	15.6922	0.0007	39.010	0.002	0.0537	0.0008	0.84237	0.00001	2.09412	0.00004	39° 22' 38.7120" N	26° 15' 04.8636" E
0.0007	15.6730	0.0006	38.538	0.002	0.0544	0.0007	0.85278	0.00001	2.09688	0.00003	40° 23' 46.0527" N	25° 33' 38.9740" E
0.0007	15.6656	0.0007	38.889	0.002	0.0532	0.0007	0.83343	0.00001	2.06895	0.00003	40° 31' 01.2847" N	23° 42' 29.5980" E
0.0007	15.6684	0.0006	38.900	0.002	0.0532	0.0007	0.83323	0.00001	2.06867	0.00003	40° 31' 01.2847" N	23° 42' 29.5980" E
0.0007	15.6707	0.0007	38.903	0.002	0.0532	0.0007	0.83322	0.00001	2.06855	0.00004	40° 31' 01.2847" N	23° 42' 29.5980" E
0.0008	15.6760	0.0008	38.877	0.003	0.0532	0.0008	0.83472	0.00001	2.07005	0.00007	40° 35' 11.0020" N	23° 45' 00.6924" E
0.0006	15.6751	0.0007	38.872	0.002	0.0532	0.0006	0.83467	0.00001	2.06986	0.00004	40° 35' 11.0020" N	23° 45' 00.6924" E
0.0005	15.6790	0.0004	38.887	0.001	0.0532	0.0005	0.83453	0.00001	2.06978	0.00002	40° 35' 51.5256" N	23° 44' 50.0640" E
0.0007	15.6836	0.0006	38.897	0.002	0.0532	0.0007	0.83456	0.00001	2.06979	0.00003	40° 35' 51.5256" N	23° 44' 50.0640" E
0.0013	15.6755	0.0011	38.920	0.003	0.0532	0.0013	0.83326	0.00001	2.06883	0.00004	40° 31' 46.8264" N	23° 46' 10.0920" E
0.0006	15.6733	0.0005	38.920	0.002	0.0532	0.0006	0.83303	0.00001	2.06860	0.00003	40° 31' 46.8264" N	23° 46' 10.0920" E
0.0009	15.6712	0.0009	38.835	0.003	0.0535	0.0009	0.83777	0.00001	2.07602	0.00006	40° 31' 46.8264" N	23° 46' 10.0920" E
0.0005	15.6842	0.0005	38.869	0.001	0.0535	0.0005	0.83905	0.00001	2.07935	0.00003	40° 46' 32.4552" N	24° 43' 04.8144" E
0.0006	15.6898	0.0006	38.991	0.002	0.0530	0.0006	0.83235	0.00001	2.06848	0.00003	40° 47' 02.0371" N	24° 37' 19.6057" E
0.0007	15.6841	0.0006	38.937	0.002	0.0532	0.0007	0.83429	0.00001	2.07121	0.00003	40° 43' 16.8707" N	24° 34' 17.5007" E
0.0007	15.6853	0.0007	38.932	0.002	0.0532	0.0007	0.83428	0.00001	2.07072	0.00003	40° 39' 54.1540" N	24° 34' 09.6350" E
0.0007	15.6870	0.0006	38.984	0.002	0.0531	0.0007	0.83233	0.00001	2.06848	0.00003	40° 47' 02.0371" N	24° 37' 19.6057" E
0.0006	15.6838	0.0006	38.929	0.002	0.0532	0.0006	0.83467	0.00001	2.07173	0.00005	40° 38' 05.3052" N	24° 35' 40.6320" E
0.0009	15.6845	0.0008	38.923	0.002	0.0532	0.0009	0.83506	0.00001	2.07235	0.00004	40° 38' 05.3052" N	24° 35' 40.6320" E
0.0010	15.6848	0.0011	38.869	0.003	0.0535	0.0010	0.83919	0.00002	2.07958	0.00008	40° 46' 32.4552" N	24° 43' 04.8144" E
0.0005	15.6802	0.0005	38.858	0.001	0.0535	0.0005	0.83902	0.00001	2.07923	0.00004	40° 46' 32.4552" N	24° 43' 04.8144" E
0.0008	15.6836	0.0007	38.871	0.002	0.0535	0.0008	0.83905	0.00001	2.07953	0.00003	40° 46' 32.4552" N	24° 43' 04.8144" E
0.0007	15.6608	0.0006	38.854	0.001	0.0532	0.0007	0.83341	0.00001	2.06767	0.00003	41° 09' 34.8722" N	23° 10' 07.6496" E
0.0006	15.6698	0.0006	38.932	0.002	0.0531	0.0006	0.83239	0.00001	2.06807	0.00003	41° 08' 14.1108" N	23° 04' 10.9271" E
0.0006	15.6686	0.0006	38.923	0.002	0.0531	0.0006	0.83228	0.00001	2.06751	0.00004	41° 08' 14.1108" N	23° 04' 10.9271" E
0.0005	15.6612	0.0005	38.905	0.001	0.0532	0.0005	0.83272	0.00001	2.06858	0.00004	41° 09' 02.6280" N	23° 06' 59.0255" E
0.0010	15.6665	0.0008	38.923	0.002	0.0532	0.0010	0.83274	0.00001	2.06894	0.00003	41° 09' 02.6280" N	23° 06' 59.0255" E
0.0008	15.6677	0.0007	38.926	0.002	0.0531	0.0008	0.83241	0.00001	2.06809	0.00004	41° 09' 02.6280" N	23° 06' 59.0255" E
0.0006	15.6808	0.0005	38.970	0.001	0.0530	0.0006	0.83130	0.00001	2.06599	0.00004	41° 08' 47.1732" N	22° 58' 06.3695" E
0.0006	15.6443	0.0006	38.428	0.001	0.0546	0.0006	0.85350	0.00001	2.09648	0.00002	41° 12' 21.0816" N	22° 49' 59.8978" E
0.0006	15.6713	0.0004	38.827	0.001	0.0534	0.0006	0.83708	0.00001	2.07393	0.00003	41° 22' 27.0300" N	23° 29' 16.1016" E
0.0006	15.6721	0.0006	38.827	0.002	0.0534	0.0006	0.83696	0.00001	2.07351	0.00003	41° 22' 27.0300" N	23° 29' 16.1016" E
0.0007	15.6725	0.0005	38.837	0.002	0.0534	0.0007	0.83677	0.00001	2.07351	0.00002	41° 22' 27.0300" N	23° 29' 16.1016" E
0.0008	15.6710	0.0008	38.832	0.002	0.0534	0.0008	0.83675	0.00001	2.07342	0.00005	41° 22' 27.0300" N	23° 29' 16.1016" E
0.0005	15.6827	0.0005	38.841	0.001	0.0534	0.0005	0.83723	0.00001	2.07349	0.00002	40° 55' 34.9248" N	24° 07' 15.4128" E
0.0008	15.6805	0.0007	38.819	0.002	0.0535	0.0008	0.83846	0.00001	2.07571	0.00003	40° 54' 56.0765" N	24° 06' 37.9461" E
0.0006	15.6827	0.0006	38.826	0.002	0.0535	0.0006	0.83845	0.00001	2.07575	0.00003	40° 54' 56.0765" N	24° 06' 37.9461" E
0.0005	15.6841	0.0007	38.862	0.002	0.0535	0.0005	0.83839	0.00001	2.07733	0.00002	40° 55' 12.7038" N	24° 12' 43.2706" E
0.0010	15.6835	0.0010	38.823	0.003	0.0535	0.0010	0.83864	0.00001	2.07599	0.00006	40° 54' 56.0765" N	24° 06' 37.9461" E
0.0008	15.6798	0.0009	38.812	0.002	0.0535	0.0008	0.83861	0.00001	2.07580	0.00005	40° 54' 56.0765" N	24° 06' 37.9461" E
0.0007	15.6819	0.0009	38.828	0.002	0.0535	0.0007	0.83855	0.00001	2.07623	0.00005	40° 54' 30.6504" N	24° 06' 26.9100" E
0.0007	15.6820	0.0006	38.826	0.002	0.0535	0.0007	0.83884	0.00001	2.07685	0.00004	40° 54' 30.6504" N	24° 06' 26.9100" E
0.0006	15.6844	0.0005	38.917	0.001	0.0532	0.0006	0.83462	0.00001	2.07091	0.00002	40° 49' 01.4746" N	23° 54' 29.9437" E
0.0007	15.6836	0.0006	38.914	0.002	0.0532	0.0007	0.83464	0.00001	2.07092	0.00003	40° 49' 01.4746" N	23° 54' 29.9437" E
0.0006	15.6835	0.0005	38.831	0.002	0.0535	0.0006	0.83846	0.00001	2.07595	0.00004	40° 54' 56.0765" N	24° 06' 37.9461" E
0.0009	15.6772	0.0008	38.807	0.002	0.0535	0.0009	0.83862	0.00001	2.07596	0.00004	40° 54' 56.0765" N	24° 06' 37.9461" E
0.0006	15.6914	0.0005	38.937	0.002	0.0535	0.0006	0.83882	0.00001	2.08151	0.00004	40° 55' 24.6557" N	24° 18' 58.6504" E
0.0009	15.6817	0.0007	38.841	0.002	0.0533	0.0009	0.83589	0.00001	2.07039	0.00006	41° 01' 06.9872" N	24° 23' 41.6675" E
0.0006	15.6874	0.0004	38.869	0.001	0.0533	0.0006	0.83590	0.00001	2.07120	0.00003	41° 01' 06.9872" N	24° 23' 41.6675" E
0.0007	15.6882	0.0007	38.870	0.002	0.0533	0.0007	0.83593	0.00001	2.07116	0.00004	41° 01' 06.9872" N	24° 23' 41.6675" E
0.0008	15.6887	0.0007	38.872	0.002	0.0533	0.0008	0.83593	0.00001	2.07118	0.00004	41° 01' 06.9872" N	24° 23' 41.6675" E
0.0006	15.6838	0.0005	38.856	0.001	0.0533	0.0006	0.83617	0.00001	2.07162	0.00002	41° 01' 14.2529" N	24° 23' 35.2166" E
0.0008	15.6904	0.0007	38.881	0.002	0.0533	0.0008	0.83617	0.00001	2.07208	0.00002	41° 01' 57.9359" N	24° 23' 37.8996" E
0.0007	15.6868	0.0006	38.870	0.002	0.0533	0.0007	0.83633	0.00001	2.07230	0.00002	41° 01' 57.9359" N	24° 23' 37.8996" E
0.0007	15.6863	0.0006	38.867	0.001	0.0533	0.0007	0.83593	0.00001	2.07120	0.00002	41° 02' 06.8675" N	24° 23' 52.8720" E
0.0008	15.6893	0.0010	38.883	0.003	0.0533	0.0008	0.83631	0.00001	2.07271	0.00005	41° 01' 47.8883" N	24° 24' 19.5587" E
0.0008	15.6669	0.0007	38.815	0.002	0.0537	0.0008	0.84082	0.00001	2.08312	0.00003	41° 22' 44.8599" N	24° 56' 00.5299" E
0.0008	15.6749	0.0007	38.949	0.002	0.0534	0.0008	0.83760	0.00001	2.08125	0.00003	41° 22' 44.8599" N	24° 56' 00.5299" E
0.0006	15.6747	0.0005	38.935	0.001	0.0534	0.0006	0.83757	0.00001	2.08045	0.00004	41° 20' 56.9417" N	25° 00' 09.1599" E
0.0006	15.6727	0.0006	38.886	0.002	0.0534	0.0006	0.83731	0.00001	2.07754	0.00006	41° 01' 16.1292" N	25° 49' 03.5579" E
0.0006	15.6696	0.0006	38.881	0.002	0.0534	0.0006	0.83726	0.00001	2.07747	0.00003	41° 01' 16.1292" N	25° 49' 03.5579" E
0.0009	15.6691	0.0008	38.878	0.002	0.0534	0.0009	0.83716	0.00001	2.07718	0.00004	41° 01' 16.1292" N	25° 49' 03.5579" E
0.0007	15.6695	0.0005	38.880	0.001	0.0534	0.0007	0.83728	0.00001	2.07752	0.00003	41° 01' 16.1292" N	25° 49' 03.5579" E
0.0007	15.6715	0.0006	38.849	0.002	0.0533	0.0007	0.83559	0.00001	2.07139	0.00003	41° 00' 39.7079" N	25° 44' 40.8443" E
0.0006	15.7137	0.0005	39.086	0.001	0.0532	0.0006	0.83521	0.00001	2.07747	0.00003	41° 00' 46.5444" N	25° 44' 31.1711" E
0.0006	15.6644	0.0005	38.819	0.001	0.0534	0.0006	0.83574	0.00001	2.07109	0.00003	41° 02' 05.6658" N	25° 59' 00.0348" E
0.0011	15.6730	0.0010	38.845	0.003	0.0533	0.0011	0.83575	0.00002	2.07141	0.00008	41° 03' 26.5571" N	25° 49' 11.7299" E
0.0013	15.6687	0.0013	38.835	0.004	0.0533	0.0013	0.83575	0.00002	2.07139	0.00008	41° 03' 26.5571" N	25° 49' 11.7299" E

0.0013	15.6669	0.0012	38.830	0.003	0.0533	0.0013	0.83582	0.00001	2.07156	0.00005	41° 03' 26.5571" N	25° 49' 11.7299" E
0.0008	15.6745	0.0007	38.875	0.002	0.0533	0.0008	0.83608	0.00001	2.07361	0.00003	40° 54' 32.0399" N	26° 02' 14.8559" E

Tmod	μ	k
43	9.855	3.858
46	9.885	3.908
46	9.885	3.908
43	9.883	3.878
36	9.878	3.865
31	9.873	3.870
26	9.846	3.848
32	9.859	3.848
54	9.938	3.893
46	9.917	3.888
32	9.875	3.868
30	9.874	3.874
35	9.869	3.853
34	9.870	3.852
28	9.849	3.864
46	9.837	3.886
34	9.883	3.884
29	9.856	3.864
70	9.886	3.902
34	9.852	3.877
28	9.854	3.863
57	9.906	3.885
54	9.889	3.887
23	9.846	3.848
23	9.865	3.854
37	9.884	3.891
181	9.933	4.005
172	9.924	4.002
176	9.943	4.005
186	9.946	4.009
184	9.940	4.008
144	9.912	3.996
189	9.929	3.892
190	9.936	3.894
141	9.902	3.994
115	9.943	3.948
118	9.925	3.947
117	9.940	3.949
176	9.987	4.004
163	9.951	4.003
157	9.948	3.996
163	9.952	4.003
159	9.941	4.001
161	9.955	4.003
158	9.938	3.999
30	9.905	3.919
32	9.912	3.921
36	9.867	3.939
36	9.868	3.939
74	9.891	3.948
79	9.898	3.950
109	9.984	4.010
108	9.954	3.993
108	9.969	3.991
109	9.960	3.997
114	9.970	4.002
113	9.988	4.004
3	9.899	3.904
15	9.904	3.913
26	9.903	3.916
81	9.922	3.960
120	9.990	4.029
123	10.012	4.047
122	10.012	4.047
121	9.988	4.029
120	9.985	4.028
40	9.895	3.936
33	9.877	3.931
39	9.895	3.936
34	9.905	3.919
345	9.942	4.010
367	9.958	4.016
345	9.944	4.009

364	9.950	4.015
68	9.941	3.959
68	9.941	3.960
68	9.953	3.965
71	9.956	3.967
73	9.950	3.967
213	9.924	4.078
360	9.906	4.009
37	9.788	3.913
37	9.797	3.914
39	9.805	3.915
70	9.831	3.921
68	9.828	3.918
70	9.841	3.922
75	9.858	3.926
45	9.823	3.922
39	9.814	3.919
115	9.826	3.946
151	9.880	3.976
45	9.871	3.938
72	9.858	3.942
73	9.863	3.938
42	9.861	3.936
78	9.859	3.943
85	9.863	3.946
154	9.883	3.978
146	9.865	3.972
150	9.877	3.977
32	9.771	3.897
24	9.799	3.917
21	9.794	3.912
20	9.769	3.912
26	9.788	3.919
22	9.791	3.915
17	9.834	3.916
343	9.804	3.973
104	9.824	3.932
103	9.826	3.930
100	9.827	3.932
99	9.821	3.930
119	9.866	3.936
137	9.863	3.944
139	9.871	3.946
140	9.876	3.963
143	9.875	3.947
139	9.862	3.943
140	9.869	3.949
145	9.871	3.952
78	9.861	3.936
77	9.858	3.936
140	9.875	3.949
136	9.852	3.942
155	9.905	4.005
96	9.856	3.918
102	9.877	3.930
103	9.880	3.930
104	9.882	3.931
103	9.866	3.929
110	9.889	3.938
108	9.877	3.936
101	9.874	3.929
111	9.886	3.942
162	9.825	3.982
117	9.839	4.000
116	9.839	3.992
110	9.830	3.965
105	9.819	3.962
103	9.816	3.960
106	9.818	3.962
80	9.818	3.921
118	9.970	4.017
75	9.793	3.911
84	9.824	3.921
79	9.809	3.918

78	9.802	3.917
92	9.831	3.941

Table 3

Click here to access/download;Table;TABLE 3. LIA Greek mineralizations Revised 17-8-2021.xlsx

Sample	District	Mine	Ancient Mining	Collected by
388	Lavrion	Esperanza	Yes	
389	Lavrion	Esperanza	Yes	
390	Lavrion	Esperanza	Yes	
396	Lavrion	Kamareza	Yes	
397	Lavrion	Kamareza	Yes	
398	Lavrion	Kamareza	Yes	
399	Lavrion	Kamareza	Yes	
D1	Lavrion	Kamareza	Yes	Dayton
TG60A-3	Lavrion	Kamareza	Yes	NHG/Gentner/Wagner
TG60A-2	Lavrion	Kamareza	Yes	NHG/Gentner/Wagner
383	Lavrion	Plaka	No	V. Avdis
384	Lavrion	Plaka	No	V. Avdis
22252/91	Lavrion	Plaka	No	S. Papastavrou
Filon 80	Lavrion	Plaka	No	S. Papastavrou
PL1/90	Lavrion	Plaka	No	NHG&ZSG
PL2	Lavrion	Plaka	No	NHG&ZSG
385	Lavrion	Plaka 33	No	V. Avdis
386	Lavrion	Plaka 33	No	V. Avdis
387	Lavrion	Plaka 33	No	V. Avdis
391	Lavrion	Plaka-80	No	V. Avdis
392	Lavrion	Plaka-80	No	V. Avdis
393	Lavrion	Plaka-80	No	V. Avdis
394	Lavrion	Plaka-80	No	V. Avdis
A6	Lavrion	Plaka N.	No	NHG&ZSG
A5	Lavrion	Plaka N.	No	NHG&ZSG
A5B	Lavrion	Plaka N.	No	NHG&ZSG
C3	Lavrion	Plaka S.	No	NHG&ZSG
395	Lavrion	Plaka, Filon Sklives	No	V. Avdis
B2	Lavrion	Plaka	No	Dayton
B5	Lavrion	Plaka	No	Dayton
S12 published	Lavrion	Sounio	Yes	NHG&ZSG
SOUL 7a	Lavrion	Soureza	Yes	NHG&ZSG
22364B	Makronisos	Central mines	Yes	S. Papastavrou
22354 KAM 354	Lavrion	Kamareza	Yes	S. Papastavrou
KAM 102	Lavrion	Kamareza	Yes	NHG&ZSG
22221 MP 221	Lavrion	Megala Pevka	Yes	S. Papastavrou
22235 PL 235	Lavrion	Plaka	No	S. Papastavrou
22251 PL 251	Lavrion	Plaka	No	S. Papastavrou
22252a PL 252A	Lavrion	Plaka	No	S. Papastavrou
22345 PL 345	Lavrion	Plaka	No	S. Papastavrou
PL 11	Lavrion	Plaka	No	NHG&ZSG
PL 16	Lavrion	Plaka Christiana	Yes	NHG&ZSG
PL 17	Lavrion	Plaka Christiana	Yes	NHG&ZSG
PL 13	Lavrion	Plaka-80	No	NHG&ZSG
PL 14	Lavrion	Plaka-80	No	NHG&ZSG
PL 15	Lavrion	Plaka-80	No	NHG&ZSG
PL F85	Lavrion	Plaka-80	No	NHG&ZSG
KALL 1	Euboea	Kallianou	Yes	NHG/ZSG
KALL 2 (TG59)	Euboea	Kallianou	Yes	NHG/ZSG
KALL3 (TG59)	Euboea	Kallianou	Yes	NHG/ZSG
KALL3 (TG59)	Euboea	Kallianou, Saliza mine	No	NHG/ZSG
TG-56A	Euboea	Almyropotamos	Yes	
TG-56B	Euboea	Almyropotamos	Yes	
AVE 1 (TG56)	Euboea	Almyropotamos	Yes	NHG/ZSG
AVE2 (TG56)	Euboea	Almyropotamos	Yes	NHG/ZSG
TG43/9	Siphnos	Ay. Sostis Dump	Yes	Gale
TG43/10	Siphnos	Ay. Sostis	Yes	Gale
TG43/10	Siphnos	Ay. Sostis	Yes	Gale

TG54-4/2	Siphnos	Voreini	Yes	
TG55A-13	Siphnos	Kapsalos-Tsingoura	Yes	
TG55A-14	Siphnos	Kapsalos-Tsingoura	Yes	
TG55A-15	Siphnos	Kapsalos-Tsingoura	Yes	
TG55A-16	Siphnos	Kapsalos-Tsingoura	Yes	
TG55A-17	Siphnos	Kapsalos-Tsingoura	Yes	
TG55A-18	Siphnos	Kapsalos-Tsingoura	Yes	
TG55A-19	Siphnos	Kapsalos-Tsingoura	Yes	
TG55A-20	Siphnos	Kapsalos-Tsingoura	Yes	
TG55A-21	Siphnos	Kapsalos-Tsingoura	Yes	
TG69-6	Siphnos	Xero Xylo	Yes	
SER21/TG52a2	Seriphos	Moutoula	Yes	NHG
SER1/96	Seriphos	Moutoula	Yes	ZSG/NHG
SER10/2	Seriphos	Moutoula	Yes	ZSG/NHG
SER2/2	Seriphos	Moutoula	Yes	ZSG/NHG
SER25/TG52b5	Seriphos	Moutoula	Yes	Gale
SER26/TG52b6	Seriphos	Moutoula	Yes	Gale
SER27/TG52b7	Seriphos	Moutoula	Yes	Gale
SER28/TG52 B8	Seriphos	Moutoula	Yes	Gale
SER29	Seriphos	Moutoula	Yes	Gale
SER31	Seriphos	Moutoula	Yes	Gale
SER33	Seriphos	Moutoula	Yes	Gale
SER34	Seriphos	Moutoula	Yes	Gale
SER35	Seriphos	Moutoula	Yes	Gale
SER36	Seriphos	Moutoula	Yes	Gale
SER37	Seriphos	Moutoula	Yes	Gale
SER39	Seriphos	Moutoula	Yes	Gale
SER40	Seriphos	Moutoula	Yes	Gale
SER41	Seriphos	Moutoula	Yes	Gale
SER42	Seriphos	Moutoula	Yes	Gale
SER45	Seriphos	Moutoula	Yes	Gale
SER7/4	Seriphos	Moutoula	Yes	Gale
SER8/2	Seriphos	Moutoula	Yes	Gale
SER9/2	Seriphos	Moutoula	Yes	Gale
SER 20	Seriphos	Moutoula	Yes	ZSG/NHG
SER14/2	Seriphos	Moutoula	Yes	NHG
SER18/2	Seriphos	Moutoula	Yes	NHG
SER20	Seriphos	Moutoula	Yes	NHG
TG 52 A2	Seriphos	Moutoula	Yes	Gale
TG 52 A4	Seriphos	Moutoula	Yes	Gale
TG 52 A5	Seriphos	Moutoula	Yes	Gale
SER1	Seriphos	Moutoula	Yes	ZSG/NHG
SER10/1	Seriphos	Moutoula	Yes	ZSG/NHG
SER12/1	Seriphos	Moutoula	Yes	ZSG/NHG
SER12/2	Seriphos	Moutoula	Yes	ZSG/NHG
SER13/2	Seriphos	Moutoula	Yes	ZSG/NHG
SER14/1	Seriphos	Moutoula	Yes	ZSG/NHG
SER15/1	Seriphos	Moutoula	Yes	ZSG/NHG
SER16/2	Seriphos	Moutoula	Yes	ZSG/NHG
SER17/1	Seriphos	Moutoula	Yes	ZSG/NHG
SER17/2	Seriphos	Moutoula	Yes	ZSG/NHG
SER18/1	Seriphos	Moutoula	Yes	ZSG/NHG
SER19	Seriphos	Moutoula	Yes	ZSG/NHG
SER2/95 (TG52A)	Seriphos	Moutoula	Yes	Gale
SER3 (TG52B)	Seriphos	Moutoula	Yes	Gale
SER15/2	Seriphos	Moutoula	Yes	Gale
SER23/TG52b3	Seriphos	Moutoula	Yes	Gale

SER5/2	Seriphos	Moutoula	Yes	Gale
SER6/1	Seriphos	Moutoula	Yes	Gale
SER6/2	Seriphos	Moutoula	Yes	Gale
SER7/1	Seriphos	Moutoula	Yes	Gale
SER8/1	Seriphos	Moutoula	Yes	Gale
SER9/1	Seriphos	Moutoula	Yes	Gale
TG 52 B1	Seriphos	Moutoula	Yes	Gale
TG 52 B2/1	Seriphos	Moutoula	Yes	Gale
TG 52 B2/2	Seriphos	Moutoula	Yes	Gale
TG 52 B3	Seriphos	Moutoula	Yes	Gale
TG 52 B6	Seriphos	Moutoula	Yes	Gale
TG 52 B7	Seriphos	Moutoula	Yes	Gale
MIL1	Milos	Pilonisi		IGME
IGMRII	Milos			
SYR 17A-1	Syros	Komito	No	ZSG/NHG
SYR 17A-2	Syros	Komito	No	ZSG/NHG
SYR 18A-1	Syros	Komito	No	ZSG/NHG
SYR 18A-2	Syros	Komito	No	ZSG/NHG
SYR 3A-1	Syros	Rozos	Yes	ZSG/NHG
SYR 3A-2	Syros	Rozos	Yes	ZSG/NHG
SYR 3A-3	Syros	Rozos	Yes	ZSG/NHG
SYR 3A-4	Syros	Rozos	Yes	ZSG/NHG
SYR 3B	Syros	Rozos	Yes	ZSG/NHG
SYR 3C-2	Syros	Rozos	Yes	ZSG/NHG
SYR 3C-3	Syros	Rozos	Yes	ZSG/NHG
SYR 2B	Syros	Rozos	Yes	ZSG/NHG
SYR 2C	Syros	Rozos	Yes	ZSG/NHG
SYR 2D-1	Syros	Rozos	Yes	ZSG/NHG
SYR 2D-2	Syros	Rozos	Yes	ZSG/NHG
SYR 2D-3	Syros	Rozos	Yes	ZSG/NHG
JK 5	Kythnos	Agios Dimitrios	Yes	Jansen, Utrecht
JK 4	Kythnos	Agios Dimitrios	Yes	Jansen, Utrecht
KYTG9	Kythnos	Agios Dimitrios	Yes	Jansen, Utrecht
KYTG10	Kythnos	Agios Dimitrios	Yes	Jansen, Utrecht
ANTI 5	Antiparos	Agios Georgios	No	Gale
ANTI 6	Antiparos	Agios Georgios	No	Gale
ANTI 7	Antiparos	Agios Georgios	No	Gale
ANTI 8	Antiparos	Agios Georgios	No	Gale
ANTI 9	Antiparos	Agios Georgios	No	Gale
ANTI 10	Antiparos	Agios Georgios	No	Gale
ANTI 11	Antiparos	Agios Georgios	No	Gale
ANTI 12	Antiparos	Agios Georgios	No	Gale
ANTI 13	Antiparos	Agios Georgios	No	Gale
ANTI 14	Antiparos	Agios Georgios	No	Gale
AP1/95	Antiparos	Agios Georgios	No	Gale
AP4/95	Antiparos	Agios Georgios	No	Gale
AP8	Antiparos	Agios Georgios	No	Gale
AP9	Antiparos	Agios Georgios	No	Gale
TG45D	Polyaigos	Tris Panagies	No	Gale/Gentner
TG45E	Polyaigos	Tris Panagies	No	Gale/Gentner
SN 12 B	Thera	Athinios	No	Gale/Bassiakos
SN 12 C/1	Thera	Athinios	No	Gale/Bassiakos
SN 17 B	Thera	Athinios	No	Gale/Bassiakos
SN 20 A	Thera	Athinios	No	Gale/Bassiakos
SN 20 B	Thera	Athinios	No	Gale/Bassiakos
SN 21 A	Thera	Athinios	No	Gale/Bassiakos
SN 21 C	Thera	Athinios	No	Gale/Bassiakos
SN 21 D	Thera	Athinios	No	Gale/Bassiakos
SN 21 E	Thera	Athinios	No	Gale/Bassiakos

360B/2	Thera	Cape Athinios	No	Karlsruhe
PH30o/2	Thera	Cape Athinios	No	Karlsruhe
ANAPHI1	Anaphi	Doumbaria	No	NHG&ZSG
ANA1/95	Anaphi	Stavros	No	NHG&ZSG
ANA11a	Anaphi	Stavros	No	NHG&ZSG
ANA11b	Anaphi	Stavros	No	NHG&ZSG
ANA13	Anaphi	Stavros	No	NHG&ZSG
ANA14	Anaphi	Stavros	No	NHG&ZSG
ANA15	Anaphi	Stavros	No	NHG&ZSG
ANA16	Anaphi	Stavros	No	NHG&ZSG
ANA17	Anaphi	Stavros	No	NHG&ZSG
ANA18	Anaphi	Stavros	No	NHG&ZSG
ANA4	Anaphi	Stavros	No	NHG&ZSG
ANA5	Anaphi	Stavros	No	NHG&ZSG
ANA6	Anaphi	Stavros	No	NHG&ZSG
ANA7	Anaphi	Stavros	No	NHG&ZSG
TG49	Samos	Ampelos (Nenedes)	No	Gentner
TG50B	Samos	Dhrakaioi, W. shore,Kalives	No	Gentner
TG50A	Samos	Dhrakaioi, W. shore, Mili	No	Gentner
TG47 published	Samos	Sikia, south shore	No	Gentner
TG46	Samos	Spatharaioi, galleries	No	Gentner
TG48	Samos	Zestos, N. Shore	No	Gentner
27711	Tinos	Apigania	No	Papastavrou
27798	Tinos	Apigania	No	Papastavrou
27708/2	Tinos	Apigania	No	Papastavrou
Ti1	Tinos	Apigania	No	Papastavrou
Ti2	Tinos	Apigania	No	Papastavrou
Ti27711	Tinos	Apigania	No	Papastavrou
Ti3	Tinos	Apigania	No	Papastavrou
Kea MEN 1	Kea	Schoinos	No	Mendoni
Kea MEN 4	Kea	Schoinos	No	Mendoni
F 1W/1	Kea	Faros	No	ZSG/NHG
F 1X/1 (TG 123B)	Kea	Faros	No	ZSG/NHG
F 1X/2 (TG 123B)	Kea	Faros	No	ZSG/NHG
FAR 1/3	Kea	Faros	No	ZSG/NHG
FAR 2/1	Kea	Faros	No	ZSG/NHG
FAR 5/1	Kea	Faros	No	ZSG/NHG
PET5	Kea	Faros	No	ZSG/NHG
PET6	Kea	Faros	No	ZSG/NHG
PET7	Kea	Faros	No	ZSG/NHG
KGP1	Kea	Faros	No	Jack Davis
KGP1	Kea	Faros	No	Jack Davis
KJD1A	Kea	Faros	No	Jack Davis
KJD1B	Kea	Faros	No	Jack Davis
KJD1C	Kea	Faros	No	Jack Davis
N 1W/1	Kea	Nikoleri	No	ZSG/NHG
N 1W/2	Kea	Nikoleri	No	ZSG/NHG
N 2C	Kea	Nikoleri	No	ZSG/NHG
N 2W	Kea	Nikoleri	No	ZSG/NHG
N 2W	Kea	Nikoleri	No	ZSG/NHG
NI X	Kea	Nikoleri	No	ZSG/NHG
NIK 1C	Kea	Nikoleri	No	ZSG/NHG
PET10	Kea	Petroussa	No	ZSG/NHG
PET11	Kea	Petroussa	No	ZSG/NHG
PET12	Kea	Petroussa	No	ZSG/NHG
PET16	Kea	Petroussa	No	ZSG/NHG
PET19	Kea	Petroussa	No	ZSG/NHG
PET20	Kea	Petroussa	No	ZSG/NHG
PW 1	Kea	Petroussa	No	ZSG/NHG

PY 1	Kea	Petroussa	No	ZSG/NHG
PY 2	Kea	Petroussa	No	ZSG/NHG
D6a	Kea	Schoinos	No	Mendoni
G3	Kea	Schoinos	No	Mendoni
Kea MEN 2	Kea	Schoinos	No	Mendoni
Kea MEN 3	Kea	Schoinos	No	Mendoni
KG2	Kea	Spasmata	No	Photos
AT-1d	SW Peloponnisos	Ano Tiros	No	NHG/ZSG
AT-1e	SW Peloponnisos	Ano Tiros	No	NHG/ZSG
AT-1f	SW Peloponnisos	Ano Tiros	No	NHG/ZSG
AT-1j	SW Peloponnisos	Ano Tiros	No	NHG/ZSG
AT-1m	SW Peloponnisos	Ano Tiros	No	NHG/ZSG
4541	SW Peloponnisos	Molai	No	IGME
4550	SW Peloponnisos	Molai	No	IGME
4543/94	SW Peloponnisos	Molai	No	IGME
MOL 11c	SW Peloponnisos	Molai	No	NHG/ZSG
MOL 11d	SW Peloponnisos	Molai	No	NHG/ZSG
MOL 11f	SW Peloponnisos	Molai	No	NHG/ZSG
MOL 11f	SW Peloponnisos	Molai	No	NHG/ZSG
4546	SW Peloponnisos	Molai	No	IGME
MOL 11b	SW Peloponnisos	Molai	No	NHG/ZSG
CH12	Chios		No	Papastavrou
CHI1	Chios	Agrelopos	No	Papastavrou
CHI3	Chios	Rosoja	No	Papastavrou
PIN 1A	Pelion	Agios Konstantinos	Yes	NHG/ZSG
PIN 5A	Pelion	Agios Konstantinos	Yes	NHG/ZSG
PIN 5A4	Pelion	Agios Konstantinos	Yes	NHG/ZSG
PIN 5A6	Pelion	Agios Konstantinos	Yes	NHG/ZSG
PIN 3A1	Pelion	Agios Konstantinos	Yes	NHG/ZSG
PIN 3A2	Pelion	Agios Konstantinos	Yes	NHG/ZSG
PIN 2A	Pelion	Agios Konstantinos	Yes	NHG/ZSG
PIN 5A2	Pelion	Agios Konstantinos	Yes	NHG/ZSG
PVORE-3	Pelion	Ksourichti	Yes	Vaxevanopoulos
TG51	Lesbos	Argenos	Yes	Gentner
ML-A	Chalkidiki	Madem Lakkos	Yes	
ML-A	Chalkidiki	Madem Lakkos	Yes	
ML-A	Chalkidiki	Madem Lakkos	Yes	
ML-A	Chalkidiki	Madem Lakkos	Yes	
ML-B	Chalkidiki	Madem Lakkos	Yes	
ML-B	Chalkidiki	Madem Lakkos	Yes	
ML-B	Chalkidiki	Madem Lakkos	Yes	
ML-B	Chalkidiki	Madem Lakkos	Yes	
ML-Nr.3	Chalkidiki	Madem Lakkos	Yes	
ML-Nr.5a	Chalkidiki	Madem Lakkos	Yes	
ML-Nr.5b	Chalkidiki	Madem Lakkos	Yes	
ML-Nr.5	Chalkidiki	Madem Lakkos	Yes	
B-97	Chalkidiki	Madem Lakkos	Yes	
E-5	Chalkidiki	Madem Lakkos	Yes	
E-27	Chalkidiki	Madem Lakkos	Yes	
E-28	Chalkidiki	Madem Lakkos	Yes	
E-37	Chalkidiki	Madem Lakkos	Yes	
E-40	Chalkidiki	Madem Lakkos	Yes	
7~1~5	Chalkidiki	Madem Lakkos	Yes	
8~2~1	Chalkidiki	Madem Lakkos	Yes	
7~10~1	Chalkidiki	Madem Lakkos	Yes	
7~29~1	Chalkidiki	Madem Lakkos	Yes	
AVE1	Chalkidiki	Madem Lakkos	Yes	
GRL1	Chalkidiki	Madem Lakkos	Yes	
GRL3	Chalkidiki	Madem Lakkos	Yes	

38 A-8	Chalkidiki	Mavres Petres	Yes	
GRL4	Chalkidiki	Mavres Petres	Yes	
GRL5	Chalkidiki	Mavres Petres	Yes	
PBS	Chalkidiki	Olympiada	Yes	
AVE4	Chalkidiki	Olympiada	Yes	
GRL6	Chalkidiki	Olympiada	Yes	
GRL7	Chalkidiki	Olympiada	Yes	
GRL8	Chalkidiki	Olympiada	Yes	
ST-12a	Chalkidiki	Stratoni	Yes	
ST-12b	Chalkidiki	Stratoni	Yes	
TG25	Thasos	Agios Eleftherios	Yes	NHG/ZSG
KM3	Thasos	Koumaria	Yes	NHG/ZSG
KM2	Thasos	Koumaria	Yes	NHG/ZSG
KM1	Thasos	Koumaria	Yes	NHG/ZSG
MR1	Thasos	Marlou	Yes	IGME
IGME 49	Thasos	Sotiros	Yes	IGME
TG28 Sotir	Thasos	Sotiros	Yes	Gale
IGME15	Pangaeon	Nikisiani Valley	Yes	NHG/ZSG
PS13	Rhodope	Kirki	No	Papastavrou
PS5 (GAMMA)	Rhodope	Kirki	No	Papastavrou
PS8 (GAMMA)	Rhodope	Kirki	No	Papastavrou
PS9	Rhodope	Kirki	No	Papastavrou
PS12 (KA 1)/871	Rhodope	Kirki	No	Papastavrou
PS2 (SP 2)	Rhodope	Kirki	No	Papastavrou
18	Rhodope	Kalotycho	No	
1	Rhodope	Saint Philippos	No	
PS-2	Rhodope	Saint Philippos	No	
PS-3	Rhodope	Saint Philippos	No	
PS-9	Rhodope	Saint Philippos	No	
PS-12	Rhodope	Saint Philippos	No	
PS-13	Rhodope	Saint Philippos	No	
2	Rhodope	Saint Philippos	No	
KA-1	Rhodope	King Arthur	No	
7	Rhodope	Distrato	No	
8	Rhodope	Distrato	No	
9	Rhodope	Distrato	No	
11	Rhodope	Distrato	No	
KA1	Rhodope	Thermes	No	
MI/2	Rhodope	Thermes	No	
RA/5	Rhodope	Thermes	No	
MI/10	Rhodope	Thermes	No	
MI/11	Rhodope	Thermes	No	
MY-4B	Rhodope	Thermes	No	
MY-1	Rhodope	Thermes	No	
MY-2A	Rhodope	Thermes	No	
MY-12	Rhodope	Thermes	No	
MY-2	Rhodope	Thermes	No	
MY/13B	Rhodope	Thermes	No	
MY-2A	Rhodope	Thermes	No	
MY/14B	Rhodope	Thermes	No	
MY-1E	Rhodope	Thermes	No	
MY-3	Rhodope	Thermes	No	
KI/8	Rhodope	Thermes	No	
3	Rhodope	Kirki Tris Vryses	No	
MP-41	Rhodope	Boukates Tris Vryses	No	
MP-44	Rhodope	Boukates Tris Vryses	No	
V-129	Rhodope	Virini	No	
21	Rhodope	Aisymi	No	
23	Rhodope	Aisymi	No	

4	Rhodope	Aisymi	No
5	Rhodope	Aisymi	No
6	Rhodope	Aisymi	No
ГА-328А	Rhodope	Aisymi	No
ES-27	Rhodope	Aisymi	No
NK-17	Rhodope	Aisymi	No
BB/15	Rhodope	Thermes	No

Main minerals	$^{206}Pb/^{204}Pb$	$^{207}Pb/^{204}Pb$	$^{208}Pb/^{204}Pb$	$^{204}Pb/^{206}Pb$	$^{207}Pb/^{206}Pb$	$^{208}Pb/^{206}Pb$
Gal	18.83300	15.67094	38.81670	0.05310	0.83210	2.06110
Gal	18.84600	15.67026	38.82276	0.05306	0.83149	2.06000
Gal	18.85100	15.67046	38.84437	0.05305	0.83128	2.06060
Gal	18.82200	15.66329	38.76014	0.05313	0.83218	2.05930
Gal	18.84200	15.66995	38.80321	0.05307	0.83165	2.05940
Gal	18.87500	15.69834	38.84475	0.05298	0.83170	2.05800
Gal	18.86400	15.67278	38.82023	0.05301	0.83083	2.05790
Gal	18.85100	15.68667	38.80610	0.05305	0.83214	2.05857
Gal/Cer?	18.83000	15.65922	38.75685	0.05311	0.83161	2.05825
Cer	18.89500	15.70250	38.89933	0.05292	0.83104	2.05871
Gal	18.86600	15.68274	38.86396	0.05301	0.83127	2.06000
Gal	18.83100	15.65666	38.79939	0.05310	0.83143	2.06040
Gal	18.92300	15.73693	38.99254	0.05285	0.83163	2.06059
Gal	18.91588	15.72670	38.97301	0.05287	0.83140	2.06033
Gal	18.90600	15.71826	38.96886	0.05289	0.83139	2.06119
Gal	18.88600	15.70692	38.93991	0.05295	0.83167	2.06184
Gal	18.83100	15.66268	38.80128	0.05310	0.83175	2.06050
Gal	18.82000	15.65749	38.77296	0.05313	0.83196	2.06020
Gal	18.83200	15.66841	38.86360	0.05310	0.83201	2.06370
Gal	18.85700	15.67394	38.83788	0.05303	0.83120	2.05960
Gal	18.87400	15.67372	38.86345	0.05298	0.83044	2.05910
Gal	18.87700	15.68641	38.88284	0.05298	0.83098	2.05980
Gal	18.84900	15.68312	38.85533	0.05305	0.83204	2.06140
Gal	18.84600	15.69325	38.89343	0.05306	0.83271	2.06375
Gal	18.88600	15.71372	38.95936	0.05295	0.83203	2.06287
Gal	18.89700	15.70756	38.95617	0.05292	0.83122	2.06150
Gal	18.91100	15.70426	38.93813	0.05288	0.83043	2.05902
Gal	18.84900	15.68312	38.85533	0.05305	0.83204	2.06140
Gal	18.88200	15.69415	38.83574	0.05296	0.83117	2.05676
Gal	18.85700	15.67526	38.83618	0.05303	0.83127	2.05951
Gal	18.91000	15.70797	38.97540	0.05288	0.83067	2.06110
Gal in lim	18.86810	15.69892	38.88885	0.05300	0.83204	2.06109
Gal	18.82200	15.64447	38.71704	0.05313	0.83118	2.05701
Gal	18.86800	15.68704	38.86242	0.05300	0.83141	2.05970
Gal	18.87200	15.69037	38.87575	0.05299	0.83141	2.05997
Gal	18.85400	15.69068	38.84678	0.05304	0.83222	2.06040
Gal	18.86300	15.68194	38.84212	0.05301	0.83136	2.05917
Gal	18.84300	15.67945	38.82977	0.05307	0.83211	2.06070
Gal	18.84800	15.68135	38.83197	0.05306	0.83199	2.06027
Gal	18.85000	15.69677	38.84476	0.05305	0.83272	2.06073
Gal	18.88500	15.69513	38.89120	0.05295	0.83109	2.05937
Gal	18.85600	15.68291	38.84430	0.05303	0.83172	2.06005
Gal	18.85600	15.67744	38.84393	0.05303	0.83143	2.06003
Gal	18.88400	15.68127	38.82362	0.05295	0.83040	2.05590
Gal	18.86800	15.68403	38.84016	0.05300	0.83125	2.05852
Gal	18.88200	15.68603	38.82328	0.05296	0.83074	2.05610
Gal	18.87800	15.68403	38.84149	0.05297	0.83081	2.05750
Gal	18.66600	15.67141	38.80531	0.05357	0.83957	2.07893
Gal	18.65500	15.68214	38.85146	0.05360	0.84064	2.08263
Gal	18.66800	15.66936	38.78818	0.05357	0.83937	2.07779
Gal	18.66700	15.67487	38.83744	0.05357	0.83971	2.08054
Gal	18.82000	15.70000	38.98000	0.05313	0.83422	2.07120
Gal	18.85000	15.72000	38.92000	0.05305	0.83395	2.06472
Galena	18.82700	15.70774	38.92896	0.05312	0.83432	2.06772
Galena	18.83500	15.71762	38.91951	0.05309	0.83449	2.06634
Gal	18.71400	15.68813	38.91483	0.05344	0.83831	2.07945
Cerussite	18.73100	15.71587	38.98633	0.05339	0.83903	2.08138
Cerussite	18.73100	15.71587	38.98633	0.05339	0.83903	2.08138

Jar, Lim	18.72000	15.68923	38.90952	0.05342	0.83810	2.07850
	18.74100	15.71414	38.97716	0.05336	0.83849	2.07978
	18.72300	15.69530	38.93822	0.05341	0.83829	2.07970
	18.74300	15.71582	38.98413	0.05335	0.83849	2.07993
	18.73500	15.69937	38.92327	0.05338	0.83797	2.07757
	18.76200	15.73100	39.06961	0.05330	0.83845	2.08238
	18.75700	15.72343	39.00368	0.05331	0.83827	2.08238
	18.77500	15.74303	39.06327	0.05326	0.83851	2.07942
	18.75200	15.71924	39.03923	0.05333	0.83827	2.08060
	18.76300	15.73052	38.98764	0.05330	0.83838	2.08187
Jar	18.73000	15.69012	38.65760	0.05339	0.83770	2.07790
Gal	18.91966	15.71751	39.04904	0.05286	0.83075	2.06394
Gal	18.90038	15.69771	38.96861	0.05291	0.83055	2.06179
Gal	18.90270	15.70436	38.98871	0.05290	0.83080	2.06260
Gal	18.90208	15.70196	38.98252	0.05290	0.83070	2.06234
Gal	18.89985	15.69481	38.96053	0.05291	0.83042	2.06142
Gal	18.89989	15.69598	38.96420	0.05291	0.83048	2.06161
Gal	18.90150	15.69770	38.97168	0.05291	0.83050	2.06183
Gal	18.90088	15.69548	38.96605	0.05291	0.83041	2.06160
Gal	18.89630	15.69187	38.95151	0.05292	0.83042	2.06133
Gal	18.89941	15.69672	38.96718	0.05291	0.83054	2.06182
Gal	18.90103	15.69882	38.97071	0.05291	0.83058	2.06183
Gal	18.89477	15.69267	38.94911	0.05292	0.83053	2.06137
Gal	18.91158	15.71401	39.02386	0.05288	0.83092	2.06349
Gal	18.89356	15.69129	38.94605	0.05293	0.83051	2.06134
Gal	18.89610	15.69038	38.94297	0.05292	0.83035	2.06090
Gal	18.89650	15.69430	38.95438	0.05292	0.83054	2.06146
Gal	18.89580	15.69069	38.94065	0.05292	0.83038	2.06081
Gal	18.89770	15.69397	38.95232	0.05292	0.83047	2.06122
Gal	18.89386	15.68965	38.94119	0.05293	0.83041	2.06105
Gal	18.89970	15.69507	38.96230	0.05291	0.83044	2.06153
Gal	18.89366	15.69402	39.01050	0.05293	0.83065	2.06474
Gal	18.89760	15.70088	39.03167	0.05292	0.83084	2.06543
Gal	18.89457	15.69704	39.01785	0.05293	0.83077	2.06503
Gal	18.87900	15.67580	38.93095	0.05297	0.83033	2.06213
Gal	18.90160	15.70080	38.97869	0.05291	0.83066	2.06219
Gal	18.89860	15.71135	39.01087	0.05291	0.83135	2.06422
Gal	18.89460	15.69197	38.95008	0.05293	0.83050	2.06144
Gal	18.91900	15.71242	39.04876	0.05286	0.83051	2.06400
Gal	18.89200	15.68584	38.95568	0.05293	0.83029	2.06202
Gal	18.88500	15.67946	38.94805	0.05295	0.83026	2.06238
Gal	18.94200	15.73967	39.08568	0.05279	0.83094	2.06344
Gal	18.88770	15.68982	38.97987	0.05294	0.83069	2.06377
Gal	18.90060	15.70394	39.01689	0.05291	0.83087	2.06432
Gal	18.89623	15.69804	38.96762	0.05292	0.83075	2.06219
Gal	18.90148	15.70014	38.97788	0.05291	0.83063	2.06216
Gal	18.89300	15.69366	38.98948	0.05293	0.83066	2.06370
Gal	18.89885	15.70116	39.01497	0.05291	0.83080	2.06441
Gal	18.89650	15.70072	39.00255	0.05292	0.83088	2.06401
Gal	18.93788	15.74457	39.15994	0.05280	0.83138	2.06781
Gal	18.87880	15.68356	38.96282	0.05297	0.83075	2.06384
Gal	18.90900	15.71226	39.05085	0.05288	0.83094	2.06520
Gal	18.89460	15.69442	38.98712	0.05293	0.83063	2.06340
Gal	18.92000	15.71476	39.05788	0.05285	0.83059	2.06437
Gal	18.89300	15.69196	38.96776	0.05293	0.83057	2.06255
Gal	18.90399	15.69863	38.97681	0.05290	0.83044	2.06183
Gal	18.90091	15.69683	38.96725	0.05291	0.83048	2.06166

Gal	18.89600	15.69426	39.00890	0.05292	0.83056	2.06440
Gal	18.90090	15.69172	38.98046	0.05291	0.83021	2.06236
Gal	18.90862	15.71155	39.00073	0.05289	0.83092	2.06259
Gal	18.92300	15.73315	39.11971	0.05285	0.83143	2.06731
Gal	18.90640	15.70763	39.04398	0.05289	0.83081	2.06512
Gal	18.90376	15.70751	39.03418	0.05290	0.83092	2.06489
Gal	18.89000	15.68437	38.96629	0.05294	0.83030	2.06280
Gal	18.92740	15.72280	39.08773	0.05283	0.83069	2.06514
Gal	18.85600	15.64388	38.82620	0.05303	0.82965	2.05909
Gal	18.86100	15.64897	38.84178	0.05302	0.82970	2.05937
Gal	18.91560	15.71987	39.08303	0.05287	0.83105	2.06618
Gal	18.89870	15.70085	39.01712	0.05291	0.83079	2.06454
Gal	18.85200	15.66733	38.90148	0.05304	0.83107	2.06352
	18.88200	15.70095	39.06138	0.05296	0.83153	2.06871
Gal	18.79800	15.66776	38.93611	0.05320	0.83348	2.07129
Gal	18.80000	15.67450	38.95398	0.05319	0.83375	2.07202
Gal	18.80000	15.67807	38.95266	0.05319	0.83394	2.07195
Gal	18.85400	15.72254	39.12375	0.05304	0.83391	2.07509
Gal	18.78500	15.66876	38.92308	0.05323	0.83411	2.07203
Gal	18.78000	15.66421	38.90333	0.05325	0.83409	2.07153
Gal	18.80300	15.69186	38.99441	0.05318	0.83454	2.07384
Gal	18.80700	15.69670	39.02208	0.05317	0.83462	2.07487
Gal	18.78100	15.66429	38.90879	0.05325	0.83405	2.07171
Gal	18.80200	15.69121	38.99610	0.05319	0.83455	2.07404
Gal	18.78800	15.67295	38.93024	0.05323	0.83420	2.07208
Gal	18.81800	15.70419	39.03568	0.05314	0.83453	2.07438
Gal	18.80600	15.68345	38.97562	0.05317	0.83396	2.07251
Gal	18.80300	15.68076	38.95718	0.05318	0.83395	2.07186
Gal	18.84200	15.70933	39.08113	0.05307	0.83374	2.07415
Gal	18.80500	15.69653	39.00627	0.05318	0.83470	2.07425
Gal	18.93700	15.69593	39.00151	0.05281	0.82885	2.05954
Gal	18.94000	15.69804	39.01337	0.05280	0.82883	2.05984
Gal	18.92700	15.67212	38.93587	0.05283	0.82803	2.05716
Gal	18.98700	15.74649	39.17967	0.05267	0.82933	2.06350
Gal	18.81700	15.72593	39.14670	0.05314	0.83573	2.08039
Gal	18.82200	15.71468	39.08934	0.05313	0.83491	2.07679
Gal	18.81535	15.70988	39.08456	0.05315	0.83495	2.07727
Gal	18.80900	15.71097	39.08585	0.05317	0.83529	2.07804
Gal	18.82007	15.72774	39.15196	0.05313	0.83569	2.08033
Gal	18.81500	15.71598	39.10321	0.05315	0.83529	2.07830
Gal	18.82000	15.71602	39.10570	0.05313	0.83507	2.07788
Gal	18.81550	15.72298	39.13492	0.05315	0.83564	2.07993
Gal	18.81400	15.71477	39.11619	0.05315	0.83527	2.07910
Gal	18.81500	15.70714	39.08289	0.05315	0.83482	2.07722
Gal	18.81800	15.71341	39.09327	0.05314	0.83502	2.07744
Gal	18.81250	15.71201	39.09125	0.05316	0.83519	2.07794
Gal	18.83200	15.73395	39.16227	0.05310	0.83549	2.07956
Gal	18.82700	15.72958	39.13456	0.05312	0.83548	2.07864
Gal	18.91400	15.73153	39.14177	0.05287	0.83174	2.06946
Gal	18.91700	15.73819	39.16311	0.05286	0.83196	2.07026
Gal	18.98300	15.72381	39.14352	0.05268	0.82831	2.06203
Gal	18.99500	15.73318	39.16579	0.05265	0.82828	2.06190
Gal	18.94601	15.66702	38.94693	0.05278	0.82693	2.05568
Gal	18.96200	15.68954	39.01962	0.05274	0.82742	2.05778
Gal	18.97400	15.70231	39.06595	0.05270	0.82757	2.05892
Gal	18.97500	15.70618	39.07617	0.05270	0.82773	2.05935
Gal	18.97000	15.69843	39.05373	0.05271	0.82754	2.05871
Gal	18.96820	15.68765	39.01892	0.05272	0.82705	2.05707
Gal	18.97200	15.70161	39.06126	0.05271	0.82762	2.05889

Gal	18.99210	15.70894	39.08836	0.05265	0.82713	2.05814
Gal	18.98770	15.70985	39.09112	0.05267	0.82737	2.05876
Gal	18.88300	15.70745	39.04683	0.05296	0.83183	2.06783
Gal	18.90300	15.70083	39.02619	0.05290	0.83060	2.06455
Gal	18.89900	15.69600	39.00999	0.05291	0.83052	2.06413
Gal	18.91260	15.71185	39.06848	0.05287	0.83076	2.06574
Gal	18.89350	15.70554	39.05371	0.05293	0.83127	2.06705
Gal	18.89902	15.70603	39.09877	0.05291	0.83105	2.06883
Gal	18.94620	15.74391	39.18151	0.05278	0.83098	2.06804
Gal	18.93200	15.72706	39.12752	0.05282	0.83071	2.06674
Gal	18.89633	15.69306	39.00921	0.05292	0.83048	2.06438
Gal	18.90430	15.69378	39.01545	0.05290	0.83017	2.06384
Gal	18.91605	15.70732	39.05483	0.05287	0.83037	2.06464
Gal	18.94170	15.74211	39.18147	0.05279	0.83108	2.06853
Gal	18.91300	15.70422	39.05221	0.05287	0.83034	2.06483
Gal	18.91170	15.70389	39.04517	0.05288	0.83038	2.06460
Gal	18.90200	15.68620	38.89559	0.05290	0.82987	2.05775
Gal	18.85300	15.69361	38.97669	0.05304	0.83242	2.06740
Gal	18.86700	15.69300	38.99884	0.05300	0.83177	2.06704
Gal	17.83300	15.61083	37.87480	0.05608	0.87539	2.12386
Gal	17.85800	15.61986	37.98164	0.05600	0.87467	2.12687
Gal	18.87200	15.67961	38.86839	0.05299	0.83084	2.05958
Gal	18.79900	15.68325	38.94871	0.05319	0.83426	2.07185
Gal	18.81100	15.70004	38.99859	0.05316	0.83462	2.07318
Gal	18.80000	15.68597	38.94721	0.05319	0.83436	2.07166
Gal	18.83100	15.72163	39.07941	0.05310	0.83488	2.07527
Gal	18.84700	15.72688	39.09999	0.05306	0.83445	2.07460
Gal	18.82700	15.71132	39.03854	0.05312	0.83451	2.07354
Gal	18.83900	15.72378	39.08395	0.05308	0.83464	2.07463
Gal	18.87070	15.69217	38.96994	0.05299	0.83156	2.06510
Gal	18.86830	15.68573	38.94851	0.05300	0.83133	2.06423
Gal	18.90500	15.74106	39.13751	0.05290	0.83264	2.07022
Gal	18.88100	15.71579	39.05610	0.05296	0.83236	2.06854
Gal	18.86040	15.69166	38.97803	0.05302	0.83199	2.06666
Gal	18.87060	15.69770	39.00610	0.05299	0.83186	2.06703
Gal	18.86800	15.69063	38.97242	0.05300	0.83160	2.06553
Gal	18.85590	15.67340	38.91537	0.05303	0.83122	2.06383
Gal	18.86100	15.68896	38.91741	0.05302	0.83182	2.06338
Gal	18.86400	15.68919	38.94680	0.05301	0.83170	2.06461
Gal	18.86100	15.68443	38.92722	0.05302	0.83158	2.06390
Gal	18.83900	15.66745	38.87202	0.05308	0.83165	2.06338
Gal	18.85800	15.69118	38.95007	0.05303	0.83207	2.06544
Gal	18.86400	15.68315	38.94586	0.05301	0.83138	2.06456
Gal	18.88300	15.70688	39.02399	0.05296	0.83180	2.06662
Gal	18.85400	15.67182	38.86809	0.05304	0.83122	2.06153
Gal	18.89300	15.72710	39.09321	0.05293	0.83243	2.06919
Gal	18.87400	15.70260	39.01482	0.05298	0.83197	2.06712
Gal	18.87340	15.70399	39.01509	0.05298	0.83207	2.06720
Gal	18.92000	15.75393	39.18086	0.05285	0.83266	2.07087
Gal	18.87300	15.69611	38.99539	0.05299	0.83167	2.06620
Gal	18.88600	15.71107	39.04189	0.05295	0.83189	2.06724
Gal	18.90500	15.72537	39.09081	0.05290	0.83181	2.06775
Gal	18.86760	15.69181	38.97650	0.05300	0.83168	2.06579
Gal	18.87200	15.69716	38.99408	0.05299	0.83177	2.06624
Gal	18.86800	15.69346	38.98261	0.05300	0.83175	2.06607
Gal	18.87500	15.70174	39.01161	0.05298	0.83188	2.06684
Gal	18.87200	15.69848	38.99823	0.05299	0.83184	2.06646
Gal	18.88100	15.70616	39.02136	0.05296	0.83185	2.06670
Gal	18.89000	15.71535	39.05640	0.05294	0.83194	2.06757

Gal	18.89200	15.71833	39.06563	0.05293	0.83201	2.06784
Gal	18.86500	15.69002	38.97452	0.05301	0.83170	2.06597
Gal	18.86350	15.70526	38.99280	0.05301	0.83257	2.06710
Gal	18.87520	15.70907	39.02466	0.05298	0.83226	2.06751
Gal	18.89640	15.72275	39.07152	0.05292	0.83205	2.06767
Gal	18.87640	15.69373	38.97826	0.05298	0.83139	2.06492
Gal	18.87230	15.70024	38.99489	0.05299	0.83192	2.06625
Cpy /Gal	18.42368	15.71899	38.68335	0.05428	0.85319	2.09965
Cpy /Gal	18.40022	15.68807	38.58194	0.05435	0.85260	2.09682
Cpy /Gal	18.43211	15.72742	38.71496	0.05425	0.85326	2.10041
Cpy /Gal	18.43145	15.72592	38.71176	0.05426	0.85321	2.10031
Cpy /Gal	18.42808	15.72204	38.70098	0.05427	0.85316	2.10011
Gal	18.40000	15.69097	38.53714	0.05435	0.85277	2.09441
Gal	18.41300	15.70758	38.58776	0.05431	0.85307	2.09568
Gal	18.40408	15.69621	38.61029	0.05434	0.85287	2.09792
Gal	18.39978	15.67459	38.53499	0.05435	0.85189	2.09432
Gal	18.42058	15.69804	38.61344	0.05429	0.85220	2.09621
Gal	18.42629	15.70502	38.63517	0.05427	0.85232	2.09674
Gal	18.42629	15.70502	38.63517	0.05427	0.85232	2.09674
Gal	18.39600	15.67946	38.50485	0.05436	0.85233	2.09311
Gal	18.44337	15.72703	38.70826	0.05422	0.85272	2.09876
Gal	18.21100	15.61648	38.29628	0.05491	0.85753	2.10292
Gal	18.23300	15.64391	38.38539	0.05485	0.85800	2.10527
Gal	18.23200	15.64233	38.35174	0.05485	0.85796	2.10354
Gal	18.79900	15.68983	38.95754	0.05319	0.83461	2.07232
Gal	18.79890	15.69558	38.97181	0.05319	0.83492	2.07309
Gal	18.80288	15.69514	38.97367	0.05318	0.83472	2.07275
Gal	18.81050	15.70620	39.01824	0.05316	0.83497	2.07428
Gal	18.81830	15.71385	39.03405	0.05314	0.83503	2.07426
Gal	18.79506	15.68955	38.95671	0.05321	0.83477	2.07271
Gal	18.80120	15.69693	38.97884	0.05319	0.83489	2.07321
Gal	18.82165	15.72041	39.05586	0.05313	0.83523	2.07505
goeth, cer	18.86698	15.70443	39.02521	0.05300	0.83238	2.06840
Gal	18.60100	15.67023	38.97709	0.05376	0.84244	2.09543
Gal	18.82300	15.68900	38.98900	0.05313	0.83350	2.07135
Gal	18.82500	15.69400	38.99100	0.05312	0.83368	2.07124
Gal	18.79000	15.68100	38.95900	0.05322	0.83454	2.07339
Gal	18.82000	15.68700	38.96600	0.05313	0.83353	2.07046
Gal	18.85500	15.73100	39.11300	0.05304	0.83431	2.07441
Gal	18.84900	15.72100	39.07300	0.05305	0.83405	2.07295
Gal	18.82300	15.72500	39.10600	0.05313	0.83541	2.07756
Gal	18.85500	15.73000	39.11500	0.05304	0.83426	2.07452
Gal	18.77900	15.66900	38.91300	0.05325	0.83439	2.07216
Gal	18.77800	15.66400	38.86100	0.05325	0.83417	2.06950
Gal	18.72700	15.65900	38.88100	0.05340	0.83617	2.07620
Gal	18.79800	15.66400	38.89400	0.05320	0.83328	2.06905
Gal	18.77600	15.65700	38.87500	0.05326	0.83388	2.07046
Gal	18.76800	15.65400	38.87100	0.05328	0.83408	2.07113
Gal	18.77700	15.66700	38.90800	0.05326	0.83437	2.07211
Gal	18.77300	15.66900	38.91400	0.05327	0.83466	2.07287
Gal	18.81800	15.70300	39.04500	0.05314	0.83447	2.07488
Gal	18.78200	15.66900	38.91400	0.05324	0.83426	2.07188
Gal	18.78000	15.67000	38.91000	0.05325	0.83440	2.07188
Gal	18.78000	15.66500	38.87600	0.05325	0.83413	2.07007
Gal	18.81000	15.67000	38.88000	0.05316	0.83307	2.06699
Gal	18.79500	15.67400	38.88900	0.05321	0.83395	2.06911
Gal	18.78000	15.65900	38.86800	0.05325	0.83381	2.06965
Gal	18.78000	15.66000	38.88000	0.05325	0.83387	2.07029
Gal	18.78000	15.66000	38.91000	0.05325	0.83387	2.07188

Gal	18.76000	15.62000	38.77000	0.05330	0.83262	2.06663
Gal	18.81000	15.67000	38.90000	0.05316	0.83307	2.06805
Gal	18.81000	15.66000	38.90000	0.05316	0.83254	2.06805
Gal	18.77100	15.66200	38.84000	0.05327	0.83437	2.06915
Gal	18.78000	15.67100	38.84400	0.05325	0.83445	2.06837
Gal	18.78000	15.68000	38.90000	0.05325	0.83493	2.07135
Gal	18.79000	15.68000	38.91000	0.05322	0.83449	2.07078
Gal	18.78000	15.67000	38.89000	0.05325	0.83440	2.07082
Gal	18.77600	15.65700	38.86200	0.05326	0.83388	2.06977
Gal	18.78500	15.66600	38.88600	0.05323	0.83396	2.07006
Gal	18.75100	15.64133	38.78719	0.05333	0.83416	2.06854
Gal	18.77400	15.67028	38.87870	0.05327	0.83468	2.07088
Gal	18.78100	15.68251	38.89883	0.05325	0.83502	2.07118
Gal	18.76400	15.66062	38.82384	0.05329	0.83461	2.06906
Gal	18.78000	15.66365	38.82314	0.05325	0.83406	2.06726
Gal	18.78200	15.66588	38.84906	0.05324	0.83409	2.06842
Gal	18.77800	15.65916	38.86558	0.05325	0.83391	2.06974
Gal	18.70700	15.68096	38.80992	0.05346	0.83824	2.07462
Gal	18.72900	15.64995	38.76959	0.05339	0.83560	2.07003
Gal	18.69600	15.65827	38.81682	0.05349	0.83752	2.07621
Gal	18.68600	15.63981	38.75420	0.05352	0.83698	2.07397
Gal	18.68600	15.63869	38.76672	0.05352	0.83692	2.07464
Gal	18.72800	15.64893	38.74711	0.05340	0.83559	2.06894
Gal	18.69000	15.63923	38.76437	0.05350	0.83677	2.07407
Gal	18.64500	15.69400	38.91800	0.05363	0.84173	2.08732
Gal	18.72100	15.67600	38.92200	0.05342	0.83735	2.07906
Gal	18.70100	15.65000	38.80600	0.05347	0.83685	2.07508
Gal	18.70400	15.65700	38.83400	0.05346	0.83709	2.07624
Gal	18.68600	15.63900	38.76700	0.05352	0.83694	2.07465
Gal	18.73000	15.64800	38.75300	0.05339	0.83545	2.06903
Gal	18.72900	15.64900	38.76900	0.05339	0.83555	2.07000
Gal	18.73000	15.65300	38.77200	0.05339	0.83572	2.07005
Gal	18.76900	15.65000	38.76900	0.05328	0.83382	2.06559
Gal	18.68800	15.65900	38.91500	0.05351	0.83792	2.08235
Gal	18.71600	15.67700	38.97600	0.05343	0.83763	2.08250
Gal	18.71200	15.69000	39.01700	0.05344	0.83850	2.08513
Gal	18.75400	15.74000	39.18500	0.05332	0.83929	2.08942
Gal	18.69800	15.65900	38.91500	0.05348	0.83747	2.08124
Gal	18.69500	15.66100	38.93400	0.05349	0.83771	2.08259
Gal	18.69900	15.66000	38.87900	0.05348	0.83748	2.07920
Gal	18.69800	15.66000	38.92100	0.05348	0.83752	2.08156
Gal	18.69800	15.66600	38.92600	0.05348	0.83784	2.08183
Gal	18.68800	15.66000	38.91400	0.05351	0.83797	2.08230
Gal	18.69500	15.66500	38.90900	0.05349	0.83792	2.08125
Gal	18.69000	15.66000	38.90700	0.05350	0.83788	2.08170
Gal	18.68900	15.66200	38.90900	0.05351	0.83803	2.08192
Gal	18.68900	15.66000	38.91300	0.05351	0.83793	2.08213
Gal	18.69600	15.67000	38.94900	0.05349	0.83815	2.08328
Gal	18.69800	15.66900	38.93400	0.05348	0.83800	2.08225
Gal	18.68600	15.66400	38.91200	0.05352	0.83827	2.08241
Gal	18.68900	15.66300	38.91300	0.05351	0.83809	2.08213
Gal	18.68600	15.66100	38.91400	0.05352	0.83811	2.08252
Gal	18.70400	15.66900	38.96400	0.05346	0.83774	2.08319
Gal	18.70600	15.66000	38.86800	0.05346	0.83716	2.07784
Gal	18.73100	15.66200	38.76600	0.05339	0.83615	2.06962
Gal	18.70300	15.63400	38.67900	0.05347	0.83591	2.06806
Gal	18.71300	15.63500	38.69000	0.05344	0.83552	2.06755
Gal	18.73500	15.65900	38.79200	0.05338	0.83582	2.07056
Gal	18.72500	15.64500	38.76800	0.05340	0.83551	2.07039

Gal	18.76600	15.69500	38.91200	0.05329	0.83635	2.07354
Gal	18.73800	15.66800	38.80000	0.05337	0.83616	2.07066
Gal	18.77300	15.69200	38.93200	0.05327	0.83588	2.07383
Gal	18.73600	15.66000	38.81100	0.05337	0.83582	2.07147
Gal	18.73800	15.66100	38.78700	0.05337	0.83579	2.06996
Gal	18.74000	15.66400	38.80400	0.05336	0.83586	2.07065
Gal	18.70700	15.66200	38.91300	0.05346	0.83723	2.08013

Reference

Barnes et al, 1975
Barnes et al, 1975
Barnes et al, 1975
Barnes et al, 1975
Barnes et al, 1975
Barnes et al, 1975
Barnes et al, 1975
Stos-Gale et al, 1996
Stos-Gale et al, 1996
Stos-Gale et al, 1996
Barnes et al, 1975
Barnes et al, 1975
OXALID unpublished data
OXALID unpublished data
Stos-Gale et al, 1996
Stos-Gale et al, 1996
Barnes et al, 1974
Barnes et al, 1975
Barnes et al, 1975
Barnes et al, 1975
Barnes et al, 1975
Barnes et al, 1975
Barnes et al, 1976
Stos-Gale et al, 1996
Stos-Gale et al, 1996
Stos-Gale et al, 1996
Stos-Gale et al, 1996
Barnes et al, 1975
Stos-Gale et al, 1996
Stos-Gale et al, 1996
Stos-Gale et al, 1996
OXALID unpublished data
OXALID unpublished data
OXALID unpublished data
OXALID unpublished data
OXALID unpublished data
OXALID unpublished data
OXALID unpublished data
OXALID unpublished data
OXALID unpublished data
OXALID unpublished data
OXALID unpublished data
OXALID unpublished data
OXALID unpublished data
OXALID unpublished data
OXALID unpublished data
OXALID unpublished data
OXALID unpublished data
OXALID unpublished data
OXALID unpublished data
Wagner and Weisgerber, 1985
Wagner and Weisgerber, 1985
OXALID unpublished data
OXALID unpublished data
Wagner and Weisgerber, 1985
Wagner and Weisgerber, 1985
Wagner and Weisgerber, 1985

Wagner and Weisgerber, 1985
Wagner and Weisgerber, 1985
Wagner and Weisgerber, 1985
Wagner and Weisgerber, 1985
Wagner and Weisgerber, 1985
Wagner and Weisgerber, 1985
Wagner and Weisgerber, 1985
Wagner and Weisgerber, 1985
Wagner and Weisgerber, 1985
Wagner and Weisgerber, 1985
Wagner and Weisgerber, 1985
OXALID unpublished data
OXALID unpublished data
OXALID unpublished data
OXALID unpublished data
OXALID unpublished data
OXALID unpublished data
OXALID unpublished data
OXALID unpublished data
OXALID unpublished data
OXALID unpublished data
OXALID unpublished data
OXALID unpublished data
OXALID unpublished data
OXALID unpublished data
OXALID unpublished data
OXALID unpublished data
OXALID unpublished data
OXALID unpublished data
OXALID unpublished data
OXALID unpublished data
OXALID unpublished data
OXALID unpublished data
OXALID unpublished data
OXALID unpublished data
OXALID unpublished data
OXALID unpublished data
OXALID unpublished data
OXALID unpublished data
Gale, 1998
Gale, 1998
Gale and Stos-Gale, 1981
Stos-Gale et al, 1996
Stos-Gale et al, 1996
OXALID unpublished data
OXALID unpublished data
OXALID unpublished data
Gale, 1998
Stos-Gale et al, 1996
Gale, 1998
Stos-Gale et al, 1996
Stos-Gale et al, 1996
Gale, 1998
Stos-Gale et al, 1996
Gale and Stos-Gale, 1981
OXALID unpublished data
OXALID unpublished data

OXALID unpublished data
OXALID unpublished data
OXALID unpublished data
Stos-Gale et al, 1996
OXALID unpublished data
Gale, 1998
Gale, 1998
OXALID unpublished data
OXALID unpublished data
OXALID unpublished data
Stos-Gale et al, 1996
Gale, 1998
IGME
Gale and Stos-Gale, 1981
Stos-Gale et al, 1996
Stos-Gale et al, 1996
Stos-Gale et al, 1996
Stos-Gale et al, 1996
Stos-Gale et al, 1996
Stos-Gale et al, 1996
Stos-Gale et al, 1996
Stos-Gale et al, 1996
Stos-Gale et al, 1996
Stos-Gale et al, 1996
Stos-Gale et al, 1996
Stos-Gale et al, 1996
Stos-Gale et al, 1996
Stos-Gale et al, 1996
Stos-Gale et al, 1996
Stos-Gale et al, 1996
Stos-Gale et al, 1996
OXALID unpublished data
OXALID unpublished data
OXALID unpublished data
OXALID unpublished data
Stos-Gale et al, 1996
Stos-Gale et al, 1996
Stos-Gale et al, 1996
Stos-Gale et al, 1996
Stos-Gale et al, 1996
Stos-Gale et al, 1996
Stos-Gale et al, 1996
Stos-Gale et al, 1996
Stos-Gale et al, 1996
Stos-Gale et al, 1996
Stos-Gale et al, 1996
Stos-Gale et al, 1996
Stos-Gale et al, 1996
Gale and Stos-Gale, 1981
Gale and Stos-Gale, 1981
Stos-Gale et al, 1996
Stos-Gale et al, 1996
Stos-Gale et al, 1996
Stos-Gale et al, 1996
Stos-Gale et al, 1996
OXALID unpublished data
Stos-Gale et al, 1996
Stos-Gale et al, 1996
Stos-Gale et al, 1996
Stos-Gale et al, 1996
OXALID unpublished data

Stos-Gale et al, 1996
Stos-Gale et al, 1996
OXALID unpublished data
OXALID unpublished data
OXALID unpublished data
OXALID unpublished data
OXALID unpublished data
OXALID unpublished data
OXALID unpublished data
OXALID unpublished data
OXALID unpublished data
OXALID unpublished data
OXALID unpublished data
OXALID unpublished data
OXALID unpublished data
OXALID unpublished data
OXALID unpublished data
OXALID unpublished data
OXALID unpublished data
OXALID unpublished data
OXALID unpublished data
OXALID unpublished data
OXALID unpublished data
OXALID unpublished data
OXALID unpublished data
OXALID unpublished data
OXALID unpublished data
OXALID unpublished data
OXALID unpublished data
Gale, 1998
Gale, 1998
OXALID unpublished data
OXALID unpublished data
OXALID unpublished data
OXALID unpublished data
OXALID unpublished data
OXALID unpublished data
OXALID unpublished data
Gale, 1998
Gale, 1998
OXALID unpublished data
OXALID unpublished data
OXALID unpublished data
OXALID unpublished data
OXALID unpublished data
OXALID unpublished data
OXALID unpublished data
OXALID unpublished data
OXALID unpublished data
OXALID unpublished data
OXALID unpublished data
OXALID unpublished data
OXALID unpublished data
OXALID unpublished data
OXALID unpublished data
OXALID unpublished data
OXALID unpublished data
OXALID unpublished data
OXALID unpublished data
OXALID unpublished data
OXALID unpublished data
OXALID unpublished data
OXALID unpublished data

OXALID unpublished data
OXALID unpublished data
Gale, 1998
Gale, 1998
Gale, 1998
Gale, 1998
Gale, 1998
OXALID unpublished data
OXALID unpublished data
OXALID unpublished data
OXALID unpublished data
OXALID unpublished data
OXALID unpublished data
OXALID unpublished data
OXALID unpublished data
OXALID unpublished data
OXALID unpublished data
OXALID unpublished data
OXALID unpublished data
OXALID unpublished data
OXALID unpublished data
OXALID unpublished data
OXALID unpublished data
OXALID unpublished data
OXALID unpublished data
OXALID unpublished data
OXALID unpublished data
OXALID unpublished data
OXALID unpublished data
OXALID unpublished data
OXALID unpublished data
Asderaki et al, 2017
OXALID unpublished data
Frei, 1992
Frei, 1992
Frei, 1992
Frei, 1992
Frei, 1992
Frei, 1992
Frei, 1992
Frei, 1992
Frei, 1992
Frei, 1992
Frei, 1992
Frei, 1992
Frei, 1992
Frei, 1992
Frei, 1992
Frei, 1992
Frei, 1992
Frei, 1992
Frei, 1992
Nebel et al, 1991
Nebel et al, 1991
Nebel et al, 1991
Nebel et al, 1991
Kalogeropoulos et al, 1989
Wagner et al, 1986
Wagner et al, 1986

Vavelidis, 1985
Wagner et al, 1986
Wagner et al, 1986
Frei, 1992
Kalogeropoulos et al,1989
Wagner et al, 1986
Wagner et al, 1986
Wagner et al, 1986
Frei, 1992
Frei, 1992
Stos-Gale et al, 1996
Stos-Gale et al, 1996
Stos-Gale et al, 1996
Stos-Gale et al, 1996
Stos-Gale et al, 1996
Stos-Gale et al, 1996
Stos-Gale et al, 1996
OXALID unpublished data
Stos-Gale et al, 1996
Stos-Gale et al, 1996
Stos-Gale et al, 1996
Stos-Gale et al, 1996
Stos-Gale et al, 1996
Stos-Gale et al, 1996
Frei, 1992
Frei, 1992
IGME Xanthi department
IGME Xanthi department
IGME Xanthi department
IGME Xanthi department
IGME Xanthi department
Frei, 1992
IGME Xanthi department
Frei, 1992
Frei, 1992
Frei, 1992
Frei, 1992
Frei, 1992
Frei, 1992
Frei, 1992
IGME Xanthi department
IGME Xanthi department
IGME Xanthi department
IGME Xanthi department
IGME Xanthi department
IGME Xanthi department
IGME Xanthi department
IGME Xanthi department
IGME Xanthi department
IGME Xanthi department
IGME Xanthi department
Frei, 1992
IGME Xanthi department
IGME Xanthi department
IGME Xanthi department
Frei, 1992
Frei, 1992

Frei, 1992
Frei, 1992
Frei, 1992
IGME Xanthi department
IGME Xanthi department
IGME Xanthi department
IGME Xanthi department

Table 4

Click here to access/download;Table;TABLE 4. Mining districts Sampled.xlsx

	Mining Area	Subdistricts	Mining Activity	Dating of surface observed findings	Metallurgy
1	Lavrion	Ari-Dimoliaki-Manoutsos	Over 100 ancient shafts and adits	Prehistoric, Archaic, Classical, Hellenistic, Roman, Byzantine period	Numerous metallurgical establishments with washeries, grinding stones, furnace remains and slag heaps
		Plaka	Over 14 modern shafts and adits		
		Kamariza-Soureza	Over 130 ancient shafts and adits		
		Botsari-Noria-Agrileza	Over 40 ancient shafts and adits		
		Spitharopoussi-Megala Pefka	Over 50 ancient shafts and adits		
		Sounion	Over 30 ancient shafts and adits		
2	South Euboea	Gialpides	2 ancient adits	Classical period	Two metallurgical areas with grinding stones, furnace remains and slag heaps.
		Kallianou Valley	11 modern and 2 ancient adits		
		Schinodavli	3 Ancient adits		
3	Central Euboea	Almyropotamos	3 Modern shafts and 2 adits with ancient horizontal parts		No metallurgical remains
4	Siphnos	Ayios Sostis	Ancient and modern shafts and adits	Prehistoric, Archaic, Roman, Byzantine period	Three metallurgical areas with grinding stones, furnace remains and slag heaps.
		Agios Silvestros	Ancient and modern adits		
		Voreini	Ancient and modern adits		
		Kapsalos-Frase	Ancient and modern adits		
		Xero Xylo	Ancient and modern shafts and adits		
		Aspros Pyrgos	Modern adits and trenches		
5	Seriphos	Moutoula	9 modern adits with ancient parts		No metallurgical remains
6	Melos	Triades	2 ancient open works	Prehistoric, Roman period	No metallurgical remains
		Katsimouti	1 ancient adit		
7	Syros	Rozos	1 ancient adit and 1 modern shaft	Prehistoric times	No metallurgical remains
8	Kythnos	Agios Dimitrios	1 ancient adit and 1 modern shaft		Slags and furnace remains from copper smelting
9	Antiparos	Agios Georgios	2 modern adits and 1 modern shaft		No metallurgical remains
		Prassovounia	4 modern adits		
		Monastiria	Modern adits with ancient parts		
10	Polyaigos	Tris Panagies	Modern adits		No metallurgical remains
11	Anaphi	Kandakospilia/ Doumbaria/Lagada	Modern adits		No metallurgical remains
12	Hymettus	Agios Ioannis	3 modern adits and 1 modern shaft		No metallurgical remains
		Kamini	2 modern adits		
13	Pelion	Agios Konstantinos	5 modern adits and 1 ancient adit	Roman period	No metallurgical remains
		Xourichti	Ancient adit		
14	Lesbos	Argenos (Megala Therma)	Modern adits		No metallurgical remains
15	Samothrace	Megalo Akrotiri	2 modern adits		No metallurgical remains
16	NE Chalkidiki	Olympias	Over 20 ancient shafts and 2 adits	Prehistoric, Hellenistic, Roman, Byzantine, Ottoman period	Metallurgical areas with grinding stones, furnace remains and slag heaps.
		Madem Lakkos	1 ancient adit		
		Mavres Petres	2 ancient adits		
		Piavitsa	1 ancient adit		
17	Thasos	Akropoli	1 ancient adit with modern parts	Prehistoric, Archaic, Hellenistic, Roman period	Metallurgical areas with grinding stones, furnace remains and slag heaps.
		Vouves	Modern adits		
		Kourlou	1 ancient adit		
		Sotiros	Modern adits and 1 ancient adit		
		Marlou	Modern adits with ancient parts		
		Koulachli	2 ancient adits		Two metallurgical areas with

18	Kroussia	Agios Markos	Modern shaft		Two metallurgical areas with grinding stones, furnace remains and slag heaps.
		Vathi	6 ancient adits		
19	Angistron	Agios Konstantinos	Modern and ancient adits and shafts	Hellenistic period	Two metallurgical areas with grinding stones, furnace remains and slag heaps.
20	Pangaeon	Agia Triada	3 ancient adits	Hellenistic, Byzantine, Ottoman period	Nine metallurgical areas with grinding stones, furnace remains and slag heaps.
		Nikisiani	5 ancient and 3 modern adits		
		Trikorfo-Avgo-Mavrokorfi	6 ancient adits		
		Ofrynio	3 ancient adits		
21	Palaea Kavala	Kryoneri-Zygos	7 ancient adits and 2 shafts	Roman period	Slags and furnace remains
		Garizo Lofos	4 ancient adits		
		Mandra Kari	3 ancient adits		
		Kokkala	2 ancient adits		
		Giolia	1 ancient adit		
		Chalkero	2 ancient adit		
		Lefki	1 ancient adit		
		Petropigi	1 ancient adit		
22	Thermes		3 modern adits		No metallurgical remains
23	Sappes		Modern adits		No metallurgical remains
24	Kirki		Modern adits		No metallurgical remains
25	Aisymi		2 modern adits		No metallurgical remains
26	Neda		1 modern adit and 1 of unidentified age		No metallurgical remains
27	Pefka		1 adit of unidentified age		No metallurgical remains

Table 5

Event		T_{mod} (Ma)	*s*	μ	*s*	κ
Aegean galenas (this study)						
	1	35	9	9.85	0.04	3.88
	2	97	34	9.89	0.06	3.94
	3	154	12	9.92	0.04	3.97
	4	190	13	9.94	0.01	3.97
	5	354	10	9.92	0.05	3.99
Aegean galenas (all data)						
	1	31	27	9.89	0.06	3.89
	2	77	39	9.8	0.02	3.95
	3	107	39	9.89	0.07	3.95
	4	198	12	9.91	0.04	3.98
	5	403	76	9.95	0.11	4.01
Iberian galenas (Millot *et al.* , in press)						
	1	90	34	9.85	0.06	3.96
	2	185	26	9.78	0.23	3.95
	3	313	41	9.92	0.12	4.04
	4	395	40	9.77	0.12	3.98
	5	613	42	9.89	0.2	4.04

s	*N*
0.03	42
0.04	79
0.03	22
0.07	7
0.01	6
0.04	220
0.04	32
0.04	163
0.1	4
0.03	25
0.05	80
0.07	29
0.06	44
0.05	237
0.07	74

Figure 1

Click here to access/download;Figure;FIG. 01.jpg

Figure 2

Click here to access/download;Figure;FIG. 02 Revised 17-8-2021.jpg

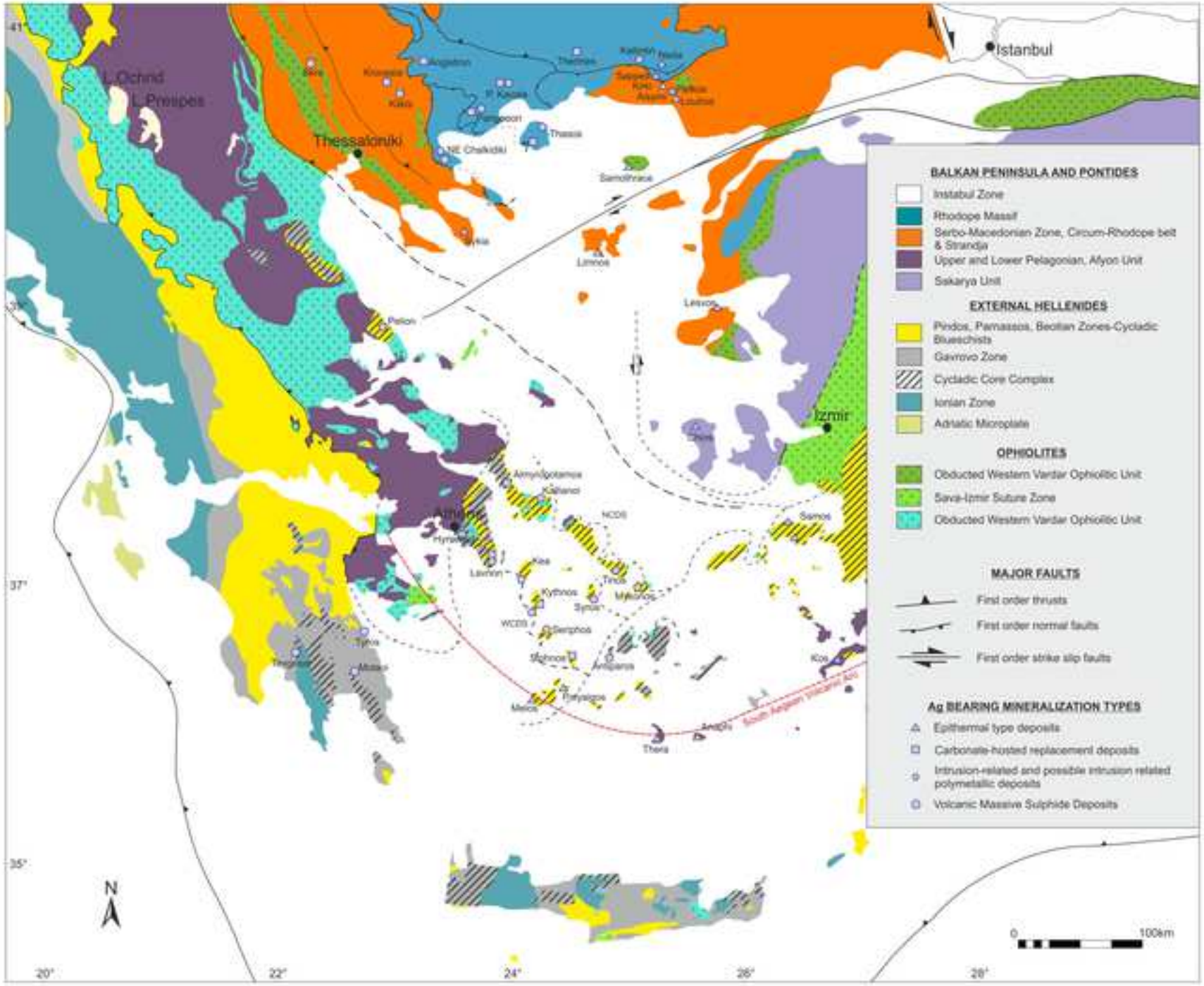

Figure 3

Click here to access/download;Figure;FIG. 3 mines.jpg

Figure 4a

Click here to access/download;Figure;Fig4a Revised 17-8-2021.tif

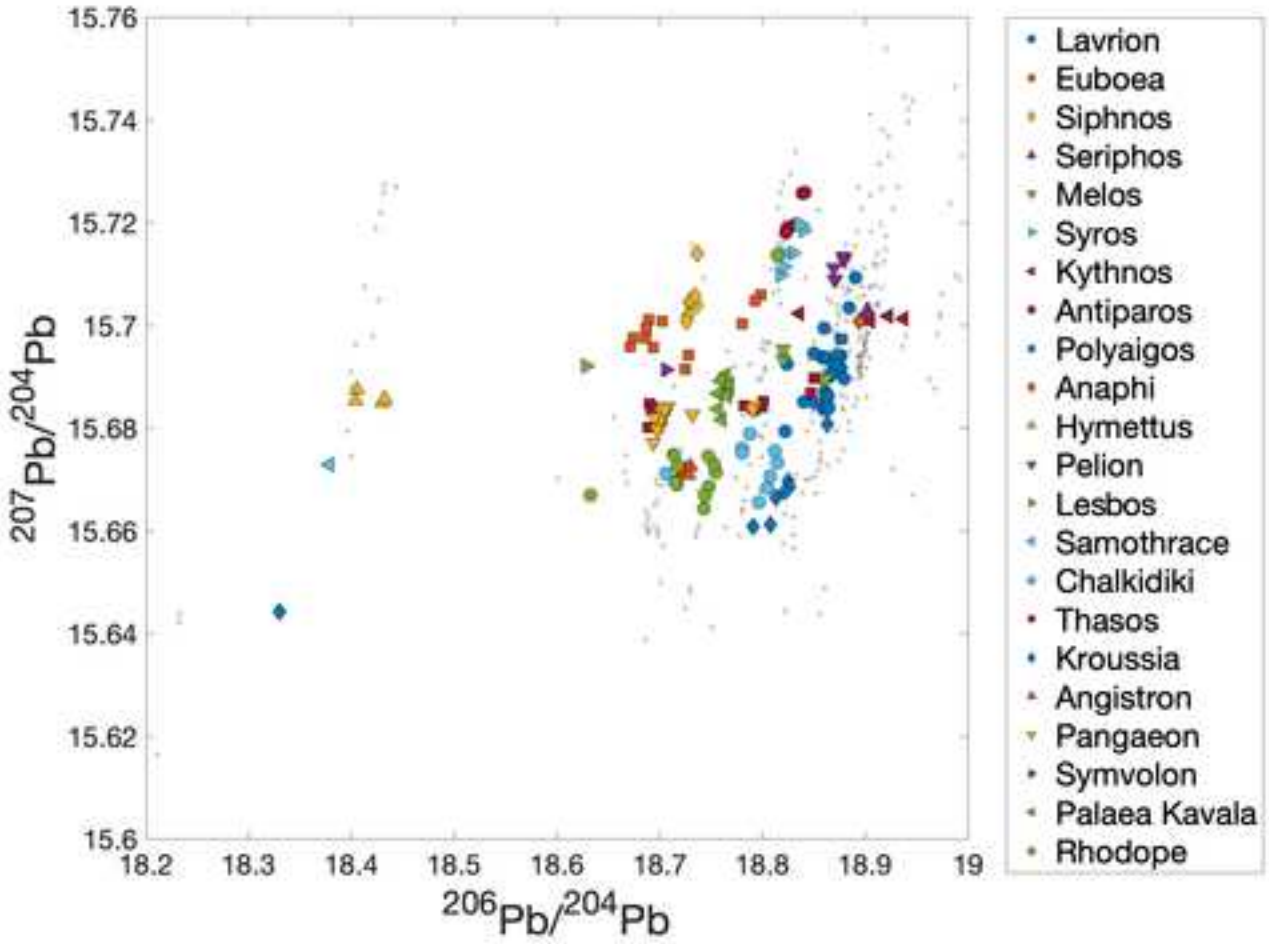

Figure 4b

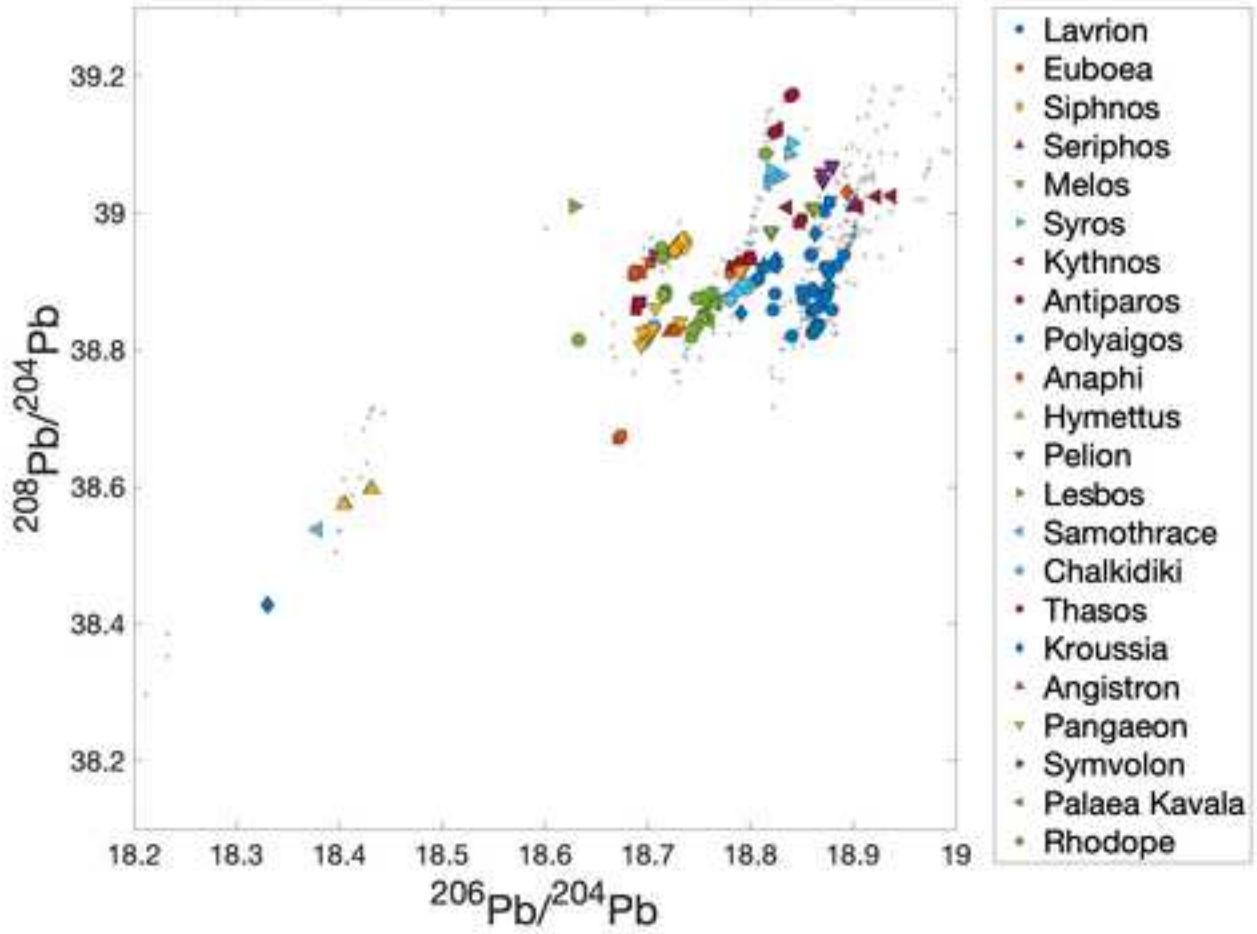

Figure 4c

Click here to access/download;Figure;Fig4c Revised 17-8-2021.tif

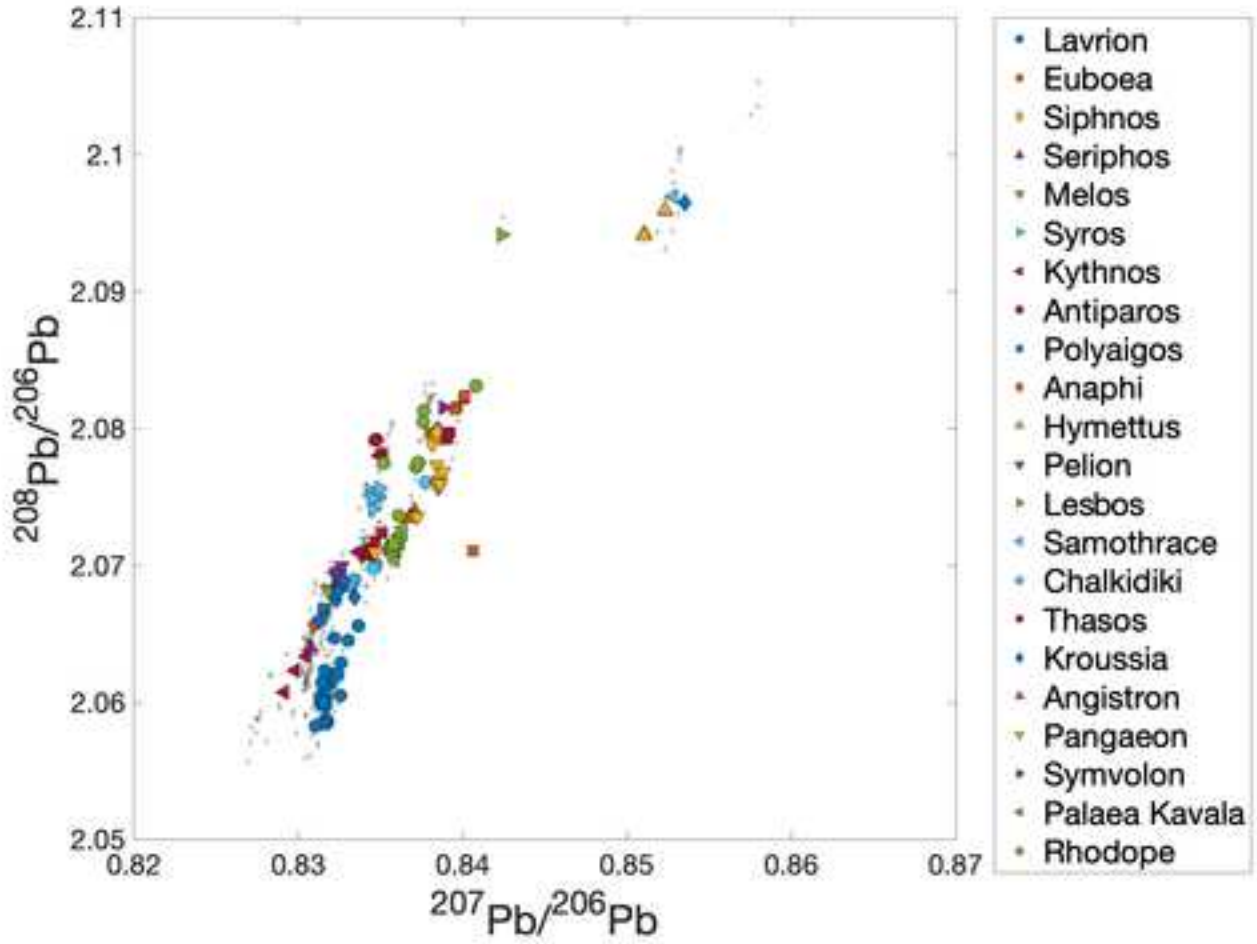

Figure 4d

Click here to access/download;Figure;Fig4d Revised 17-8-2021.tif

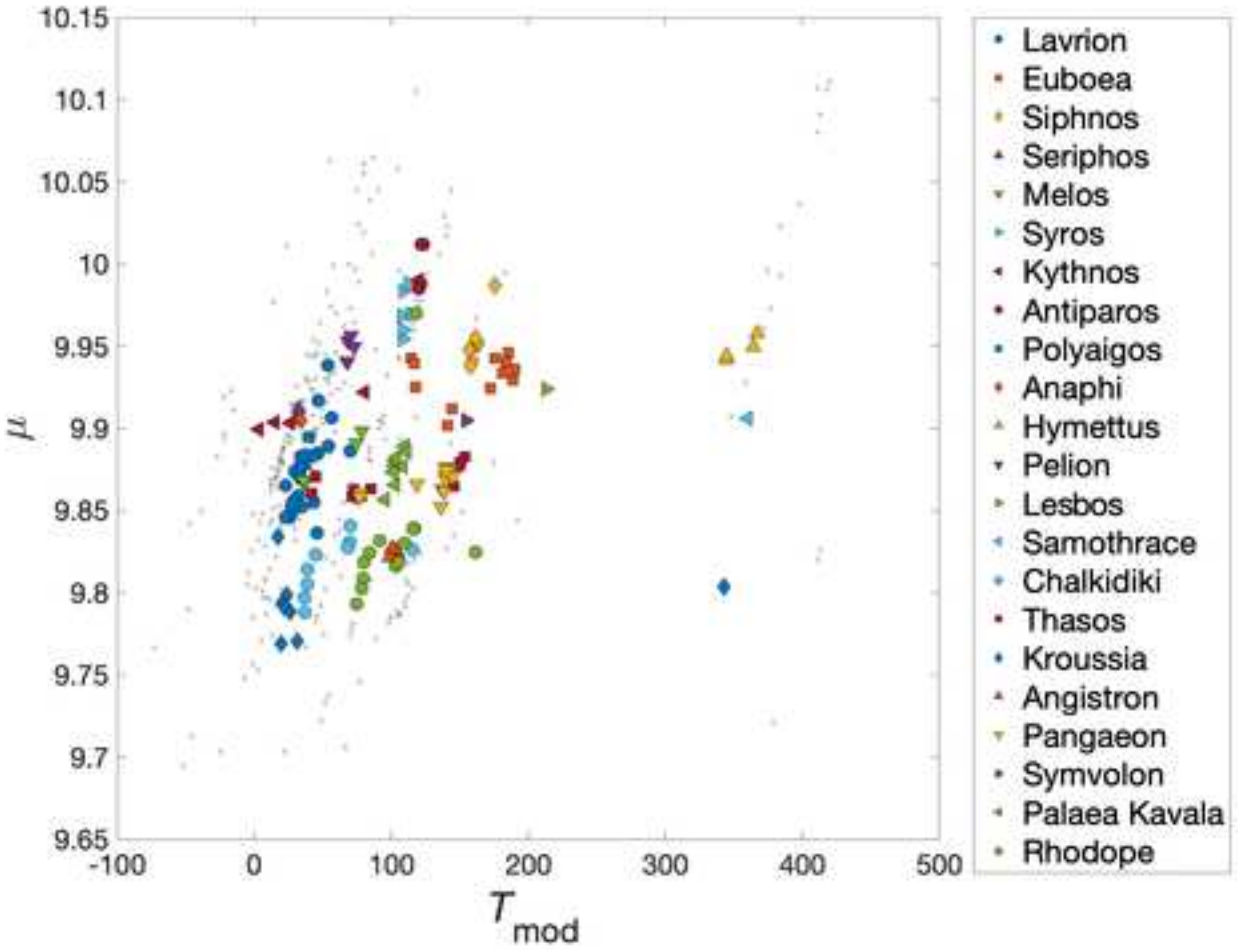

Figure 4e

Click here to access/download;Figure;Fig4e Revised 17-8-2021.tif

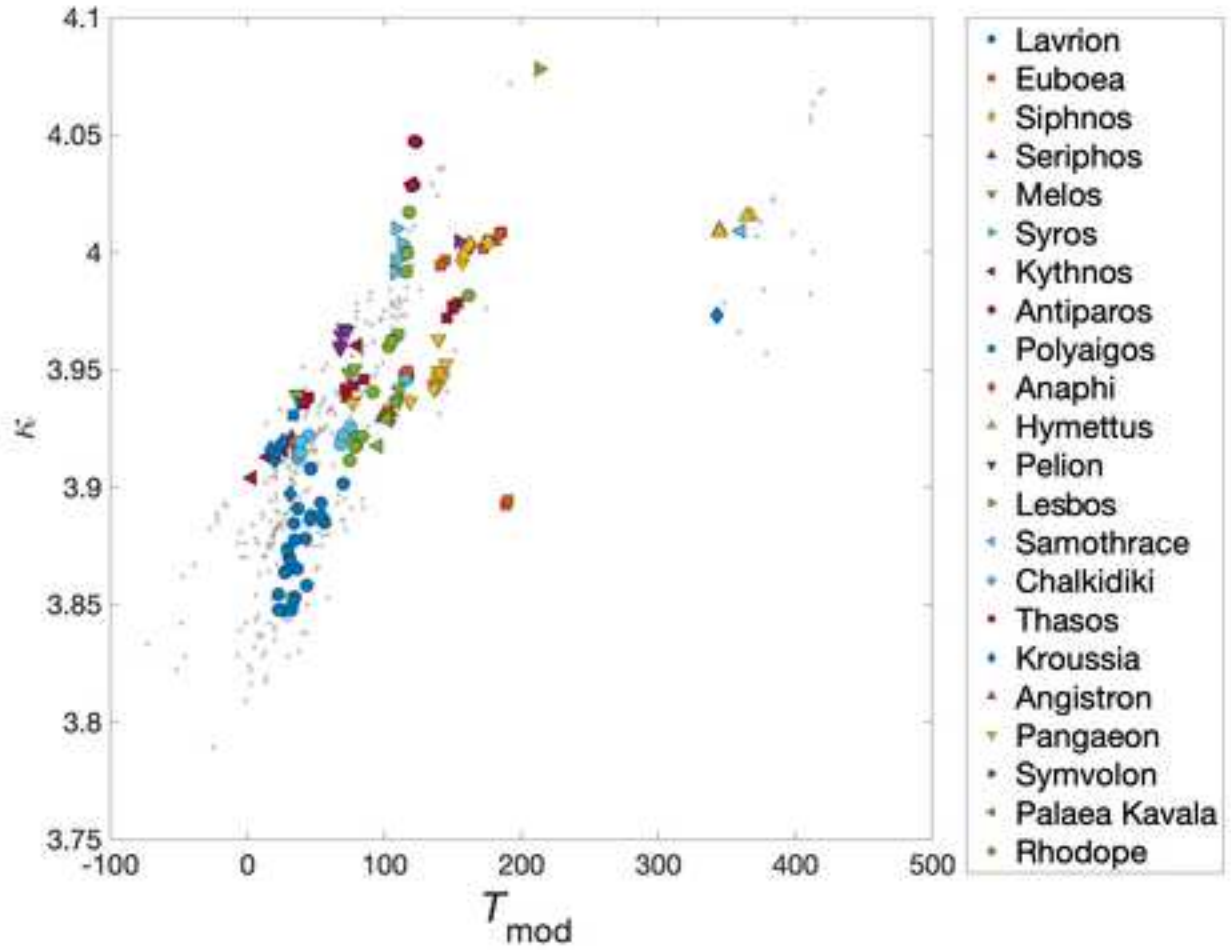

Figure 5

Click here to access/download;Figure;FIG. 5 geographic distribution.jpg

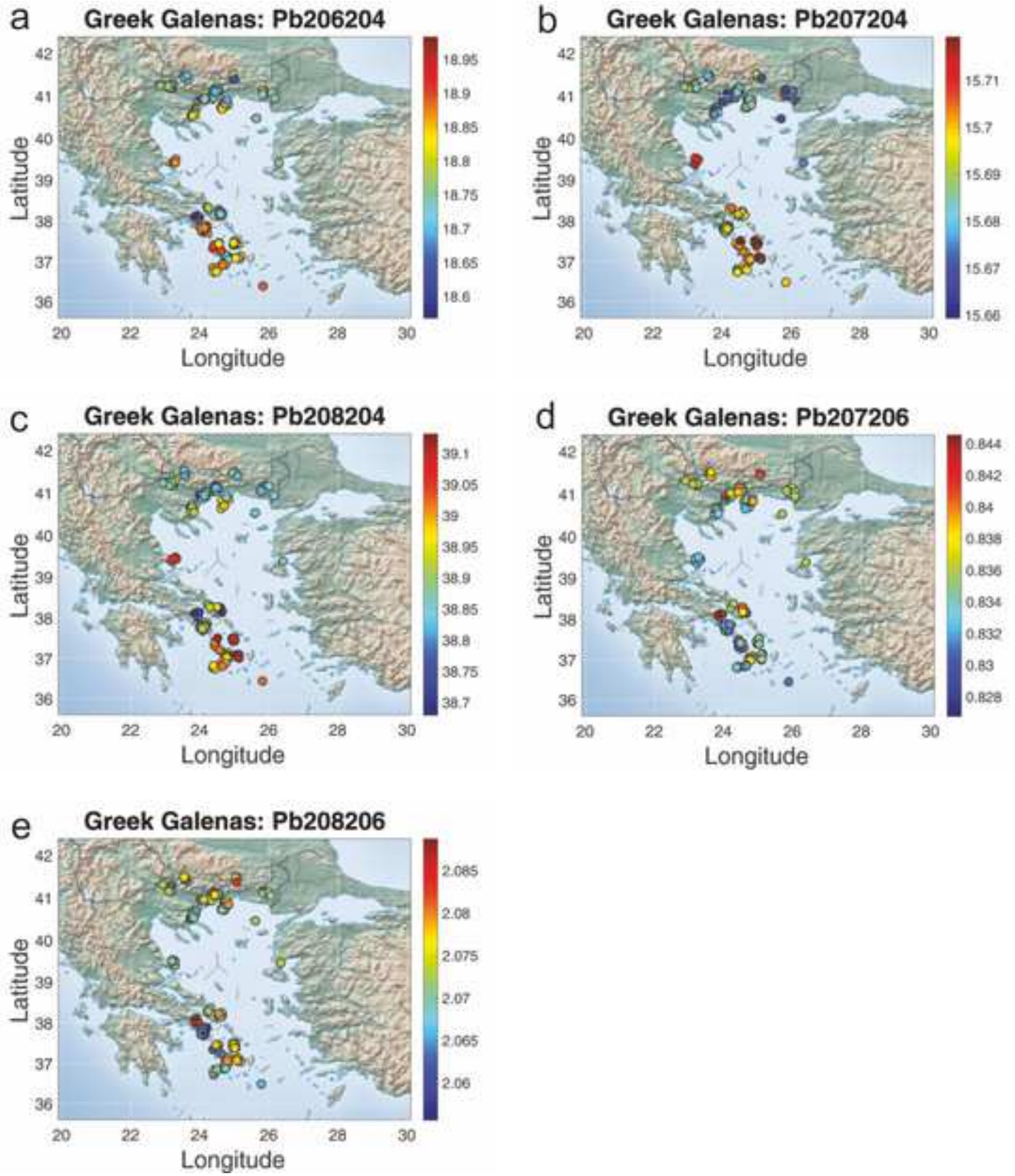

Figure 6

Click here to access/download;Figure;renamed_14518.jpg

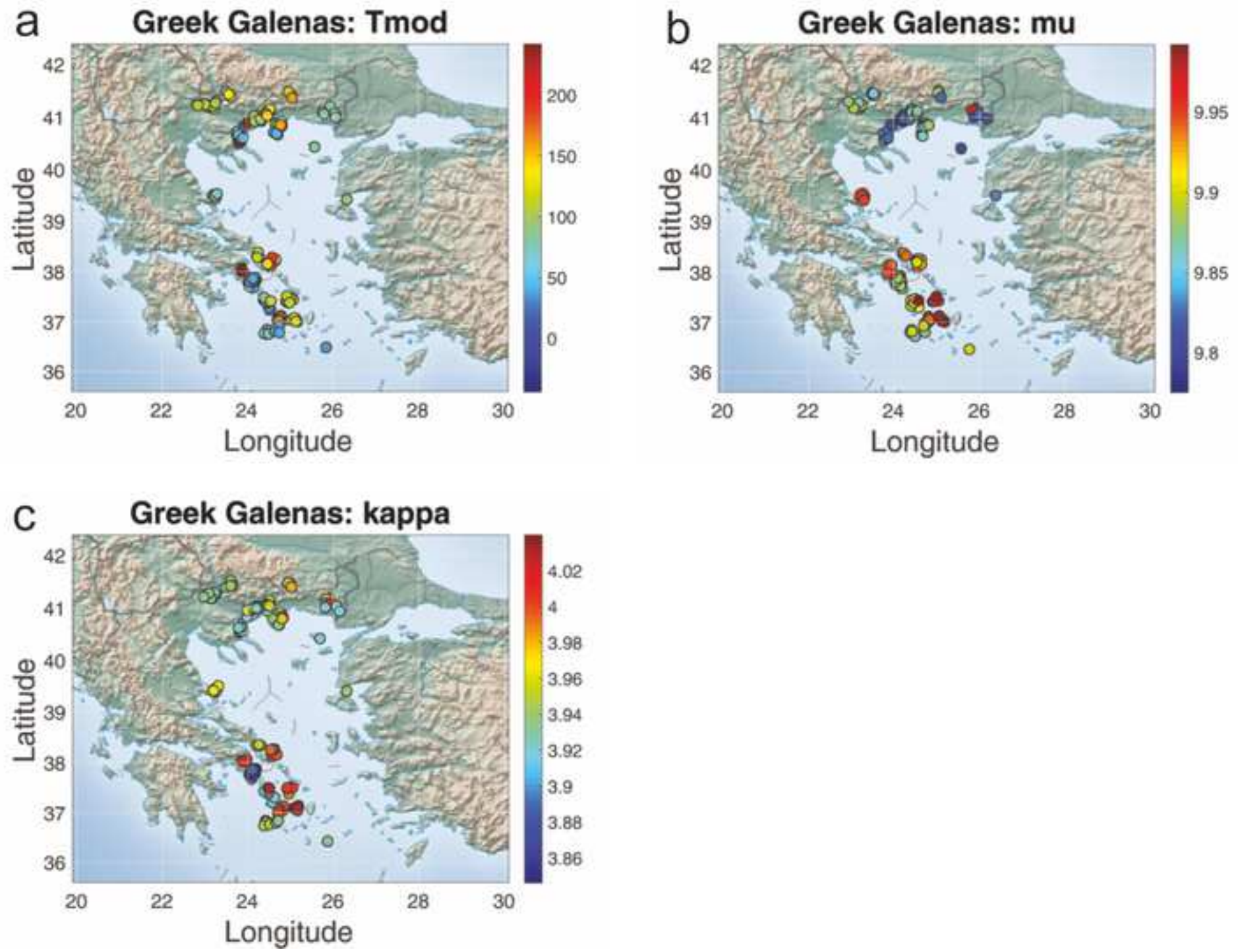

Figure 7

Click here to access/download;Figure;FIG. 7 anoxic events diagram.jpg